ENGINEERING FIRE-RESILIENT FORESTS: APPLICATIONS OF REMOTE SENSING TO ASSESS ASPEN'S DISTRIBUTION AND POTENTIAL TO REDUCE FIRE HAZARD

by

MAXWELL C. COOK

B.S., Colorado State University, 2016

M.A., University of Colorado-Boulder, 2021

A thesis submitted to the
Faculty of the Graduate School of the
University of Colorado in partial fulfillment
Of the requirements for the degree of
Doctor of Philosophy
Department of Geography
2025

Committee Members:

Jennifer K Balch, Chair

William R. Travis

Stefan Leyk

Sarah J. Hart

Teresa B. Chapman

Cook, Maxwell Cody (Ph.D., Geography)

Engineering fire-resilient forests: Applications of satellite remote sensing to assess aspen's distribution and potential to reduce fire hazard

Thesis directed by Dr. Jennifer K. Balch

ABSTRACT

Across the United States and globally, wildfire impacts to the built environment and ecosystems are driving increasing costs to society. There is no "one-size-fits-all" solution to reducing wildfire hazard for communities. The convergence of climate- and human-driven changes in wildfire activity requires collective action, innovative science and technology, and intentional management to mitigate the fire hazard. Addressing where and how we build, increasing wildland fire use and prescribed burning, and targeted fuels mitigation in hazard hotspots all play a significant role. However, traditional fuel treatments such as thinning or clear cutting often require revisitation to maintain positive benefits, creating persistent management challenges for communities. The expansion of "fire-resistant" species, such as quaking aspen (*Populus tremuloides Michx.*), has been proposed as one potential solution (or another "tool in the toolbox") to reducing fire hazard in some regions, particularly in the Southern Rockies. Beyond the potential for aspen to reduce fire hazard, its ability to respond readily in post-disturbance landscapes provides critical forest resilience at a time when that has become more challenging due to compound disturbance interactions, a more fire-conducive climate, and increased area burned at high severity. However, more information is needed to understand where, how, and when aspen might moderate fire behavior, especially in the context of recent extreme fire activity. The growing widespread availability of remote sensing and geospatial data before, during, and after wildfires offers a promising avenue for elucidating answers to these questions and informing management decisions for this important forest species.

In this dissertation, I present a series of studies which leverage remote sensing and geospatial analysis, environmental data science, statistical and machine learning and ecological principles to explore one potentially novel solution to wildfire hazard: the management of quaking aspen as a *living fire break*. To this end, we first developed new reproducible methods for mapping aspen at a higher spatial resolution than existing products, identifying an average patch size of 0.53 ha in the Southern Rockies. These new maps have major implications for management decision-making, as small patches may be disproportionally important for both maintaining and expanding existing aspen stands. Next, we demonstrate a novel application of satellite-derive fire radiative power (FRP) harmonized with burn severity, national wall-to-wall forest inventory, and geographic setting to elucidate the relationship between aspen forest composition and structure on fire intensity and severity in the Southern Rockies. We found that the proportion of forested area that is made up of aspen has a significant influence on both intensity and severity, with a -8.1% reduction for every unit increase in proportional aspen area. Further, we found that the influence of aspen dominance diminishes greatly under more extreme fire weather but may still offer a buffering effect where it co-occurs with other forest types, especially lodgepole. This demonstrates the capacity for aspen forests, especially in greater proportions, to reduce extreme fire behavior in some settings. Finally, we harmonized a suite of environmental data to map and prioritize firesheds in the Southern Rockies based on archetypes of aspen management now and into the future. This exercise identified 93 (5.4%) firesheds where aspen management for fire hazard reduction may be advantageous and successful and provides a rich database geared towards management prioritization and planning. Beyond this, we highlight other firesheds with different management scenarios. This overall effort contributes new data and ecological understanding of aspen's distribution and potential to reduce fire hazard.

ACKNOWLEDGEMENTS

Throughout my doctoral journey, I've had the immense pleasure of working on a wide variety of projects with amazing collaborators, mentors, and friends. None of this would have been possible without the true dedication of my advisor, Dr. Jennifer Balch, for providing these opportunities and ensuring I had the funding and resources to accomplish my goals. Working with Jennifer has been an absolute joy, and I've grown much as a scientist, researcher, and team player under her guidance and support. Through this relationship, I have been able to make strong connections with the incredible teams at the Earth Lab, NC CASC, and ESIIL. While there are too many names to list, you know who you are, and thank you all for your support. One of the more impactful aspects of my journey has been the connections I've made with tribal partners through my involvement with ESIIL. As a member of the *Observing Unci Maka* working group, I have the great privilege to work alongside amazing tribal scientists, students, and representatives to leverage remote sensing for environmental justice issues on tribal lands. As I continue in my journey, these connections and this work will be a primary focus, and I have Jennifer and ESIIL to thank for putting me on that path.

I also would like to thank my amazing committee members for their dedication and indefatigable efforts to promoting my work and helping me dial in this research. I've learned a great deal from each of them. It was such a blessing to have a committee who provided critical feedback in a way that felt productive, supportive, and genuine. I hope to pay this forward in the future by helping and mentoring younger students in the same ways.

I've also been lucky to have a network of mentors and colleagues from CSU, CU, and The Nature Conservancy who have always been my biggest supporters. From CSU, Sophia – your mentorship and guidance through the years has played a major role in getting me to where I am. From TNC – Brian, Teresa, and Catherine (among others) – where to even begin? Thank you for your support, friendship and mentorship over the years. A special thank you to Teresa for always supporting me and pushing me to be a better scientist. You helped me navigate the professional world right out of undergrad, pushed me apply for graduate school, and then served on my PhD committee. I would not be achieving this goal without the incredible mentors I've been lucky to have.

Of course, none of this would have been possible without the love and support from my family – my parents, Suzanne and Howard, and my sisters, Sophie and Hanna. They have seen me through the hard times and the joyous ones, and I am constantly inspired by their own stories. Thanks for always having my back. To my friends as well, who have suffered through my excited rants about my research, supported me through feast and famine, and always showed up when I needed them. I am a better person for having my friends and family around me, thank you for everything.

This work was funded by the Joint Fire Science Program Project ID: 21-2-02-29.

CONTENTS

INTRODUCTION **1**

INFORMATION NEED 1
BACKGROUND 5
Quaking aspen ecology and management *5*
Aspen as a "living fire break" *8*
Remote sensing applications in fire ecology *10*
RESEARCH AIMS 12

1 CHAPTER ONE **14**

GOLD IN THE HILLS: MAPPING QUAKING ASPEN USING SEASONAL MULTISPECTRAL AND RADAR IMAGERY IN THE SOUTHERN ROCKIES, USA 14
1.1. INTRODUCTION 14
1.2. MATERIALS AND METHODS 19
1.2.1. Study Area *19*
1.2.2. Image Reference Data *22*
1.2.3. Satellite Imagery *25*
1.2.4. Seasonal Sentinel-2 Composites *28*
1.2.5. Topographic Data *29*
1.2.6. Image Classification *30*
1.2.7. Agreement with Existing Products *32*
1.2.8. Case Study: Landscape Patch Dynamics *33*
1.3. RESULTS 33
1.3.1. Annual Spectral Response of Quaking Aspen Forests *33*
1.3.2. Model Selection and Accuracy Assessment *34*
1.3.3. Agreement with Reference Datasets *38*
1.3.4. Landscape and Patch Dynamics *41*
1.4. DISCUSSION 42
1.5. CONCLUSION 47

2 CHAPTER TWO **49**

QUAKING ASPEN'S INFLUENCE ON FIRE INTENSITY AND SEVERITY IS MODERATED BY FOREST COMPOSITION, STRUCTURE, AND FIRE WEATHER IN THE SOUTHERN ROCKIES 49
2.1. INTRODUCTION 49
2.2. MATERIALS AND METHODS 53
2.2.1. Study System and Wildfire Census *53*
2.2.2. Active fire detections and fire radiative power (FRP) *55*
2.2.3. Composite Burn Index (CBI) *57*
2.2.4. Forest Composition and Structure *58*
2.2.5. Climate and Topography *60*
2.2.6. Statistical analysis *60*
2.2.7. Model parameters and assessment *62*
2.2.8. Spatial mesh grid *63*
2.3. RESULTS 64
2.3.1. Differences between dominant forest types relative to aspen *65*
2.3.2. Effect of composition and structure *66*
2.3.3. Topography and fire weather *68*
2.3.4. Aspen co-dominance and fire weather mediation *69*
2.3.5. Spatial patterns in FRP and CBI *71*
2.4. DISCUSSION 73
2.4.1. Aspen turns down the heat during recent wildfires *73*
2.4.2. Forest composition and structure effects align with expected fire regime characteristics *75*
2.4.3. Opportunities, limitations and future directions *77*

2.5. CONCLUSION ... 78

3 CHAPTER THREE ... 80

THE FIERY FUTURE OF QUAKING ASPEN: MANAGEMENT OPPORTUNITIES FOR WILDFIRE HAZARD REDUCTION IN THE SOUTHERN ROCKIES ... 80
3.1. INTRODUCTION ... 80
3.2. MATERIALS AND METHODS ... 84
3.2.1. Aspen habitat suitability ... 85
3.2.2. Projected future wildfire activity ... 86
3.1.1. Contemporary fire hazard and risk ... 87
3.1.2. Historic wildfire activity ... 88
3.2.3. Built Environment and Wildland Urban Interface ... 89
3.2.4. Contemporary aspen canopy, patch size, and existing vegetation ... 90
3.2.5. Statistical Analysis ... 91
3.3. RESULTS ... 94
3.3.1. Alignment of future fire and aspen habitat suitability ... 94
3.3.2. Priority firesheds for aspen management ... 97
3.4. DISCUSSION ... 101
3.5. CONCLUSION ... 104

SUMMARY AND CONCLUSIONS ... 106

STATEMENT OF IMPORTANCE ... 106
SUMMARY OF WORK ... 106
METHODOLOGICAL CONTRIBUTIONS ... 111
MANAGEMENT IMPLICATIONS ... 114

LITERACTURE CITED ... 118

APPENDIX A: CHAPTER ONE ... 134

APPENDIX B: CHAPTER TWO ... 139

TABLES

Table 1-1 Distribution of background samples across all spatial blocks with at least 100 aspen presence points. 24
Table 1-2 Original Sentinel-1 and Sentinel-2 bands with abbreviations, names, center wavelengths, and seasonal windows. 26
Table 1-3 Spectral vegetation indices and radar textural features. The formula and associated reference to calculate each index is provide where relevant. Indices and textural features were calculated for each seasonal window 27
Table 1-4 Precision, recall, and F1-score for aspen test data across the three reference datasets and for the Sentinel-based map. 39
Table 1-5 Landscape patch dynamics summarized across spatial blocks for the Southern Rockies. We report the total area, number of patches, average patch density, average patch size, and average perimeter to area ratio. 42
Table 2-1 Model fit statistics and effective number of parameters. Spatial models with random effects for fire event and day-of-burn were far more complex (greater number of effective parameters) and performed significantly better based on WAIC and CPO. 66
Table 3-1 Variables considered for input to SOM analysis including their respective “category”, name, abbreviation, fireshed aggregation method (if relevant), and data source. 92
Table 3-2 Descriptive statistics of bivariate classes showing the mean wildfire hazard potential, trend in burned area, change in aspen suitability, and contemporary aspen cover sorted by wildfire hazard potential 96
Table 3-3 Distribution of clusters within bivariate classes. Bold values signify the majority bivariate class for each cluster. Rows represent bivariate class, and columns represent cluster numbers (denoted with “C#”) 100
Table 3-4 Summary statistics within SOM-based clusters showing aspen area, patch size (average), building footprints, population, wildfire hazard potential (unitless), and housing unit impact (unitless) 101

FIGURES

Figure 1.1 Map of the Southern Rockies study area with spatial blocks, case study landscape, aspen reference data and forest canopy cover. Inset map showing aspen photo points overlain with National Agricultural Imagery Program (NAIP, ca. 2019). 22
Figure 1.2 Annual (A-B) and seasonal (C-D) spectral response of aspen presence data (c. 2019). Grey shading defines the temporal windows. (A) Median bi-weekly surface reflectance values for S2 bands; (B) Median weekly response of derived spectral indices; (C) Seasonal differences in S2 bands from image composites (summer and autumn); (D) Seasonal difference in spectral indices....................34
Figure 1.3 Results from the classification scenarios. We report the average and standard error F1-score across folds for each scenario. Topographic data (elevation, slope, and aspect) were included in all scenarios. 35
Figure 1.4 Feature importance for the top 10 features across folds for the final model measured as the sum of decrease in Gini impurity index. Color shade indicates the seasonality. 36
Figure 1.5 Map of quaking aspen canopy cover with reference location (Hahns Peak, Steamboat Lake State Park, Routt County, CO). (A) Aspen canopy probability (0-100%); (B) NAIP image for the reference; (C) Aspen canopy cover probability (0-100%) for the reference location; (D) Aspen classification based on the optimum threshold of the probability (0.42). 38
Figure 1.6 Distribution of pixel-based precision, recall, and F1-score of existing products compared to the Sentinel-based map across spatial blocks within the Southern Rockies. Diamonds indicate the values for the targeted geography (White River NF). 41
Figure 1.7 Comparison of patch metrics for the Southern Rockies and the White River NF for the Sentinel-based map and the three existing products. The White River NF is dominated by large, often pure stands of quaking aspen which is highlighted in the much larger average patch density and patch size when compared to the Southern Rockies. 42
Figure 2.1 Study region and wildfire census data (2017-2023). (**A**) Map of the Southern Rockies and fire census. Size of points represents burned area; color represents the proportion of forested area that is aspen; (**B**) Annual area burned; (**C**) Fire size distribution....................54
Figure 2.2 Distribution of major forest types within burned areas in the fire census. Hatching indicates the proportion of area where that forest type was the gridcell majority (>50% of forested proportion)....................55
Figure 2.3 Aggregation of VIIRS active fire detections (AFD) onto a regular grid for the Williams Fork Fire (2020). (**A**) Pixel centers of AFD from both satellites (S-NPP and JPSS-1); (**B**) Pixel ground area based on swath position (relative nadir position); (**C**) Maximum FRP based on fractional overlap aggregation. 57
Figure 2.4 Southern Rockies study region with spatial mesh grid and inset for the Williams Fork Fire, CO (2020). (**A**) Full spatial mesh with all fire census in red. The mesh is designed to capture within-fire variability while relaxing the intra-fire spatial dependence as seen by the wider triangular mesh between fire events. (**B**) Spatial mesh for the Williams Fork Fire, CO (2020) showing the within-fire spatial dependence with smaller triangles. (**C**) Predominant forest type aggregated to gridcells, defined by the pixel count majority from TreeMap FORTYPCD. (**D**) Aggregated cumulative FRP (W/km^2). Where gridcells remain gray, there were no daytime observations. (**E**) 90th percentile CBIbc. 64
Figure 2.5 Posterior distributions of effects of predominant forest types on FRPc and CBIbc relative to aspen as the baseline. Lodgepole, Douglas-fir, white fir, ponderosa pine, and spruce-fir forest types had significant positive effects on both FRPc and CBIbc. Gambel oak and pinon-juniper forests showed a lower FRPc though credible intervals pass zero for Gambel oak and credible intervals are wide. Pinon-juniper relative to aspen but a higher CBIbc. Except for Gambel oak, all forest types showed significant positive effects on CBIbc relative to aspen. 66
Figure 2.6 Posterior distribution of effects for forest type-specific composition and structure metrics on (**A**) FRPc, and (**B**) CBIbc. We assessed the percent cover of the gridcell majority forest type, forest-specific stand density index (SDI), average live basal area, and height-diameter ratio (HDR). Posterior distributions which overlap zero are uncertain/insignificant. 68

Figure 2.7 Posterior distribution of effects on (**A**) FRPc, and (**B**) 90th percentile CBIbc, for the influence of quaking aspen dominance relative to co-occurring major forest types with and without VPD mediation. Light orange ridges represent the VPD-mediated effect which was modeled as an interaction term (forest type:aspen dominance * VPD). For both models, terms were included to account for other fire weather, topography, fire-dependent random effects, day-of-burn temporal random effects, VIIRS aggregation information and spatial effects (see Section 2.7). 71
Figure 2.8 Results from the spatial model (SPDE); (**A**) Spatial mesh grid covering the Southern Rockies; (**B**) Cumulative FRP (FRPc); (**C**) Spatial effect of FRPc; (**D**) Uncertainty in the spatial effect of FRPc; (**E**) 90th percentile CBIbc; (**F**) Spatial effect of CBIbc; and (**G**) Uncertainty in the spatial effect of CBIbc. 72
Figure 3.1 Aspen habitat suitability summarized at the fireshed scale. (**A**) Historic (1981-2010) climatic and topographic aspen habitat suitability; (**B**) Change in future quaking aspen suitability based on the SSP585 scenario and difference between historic (1981-2010) and future (2041-2070). Warm colors represent areas of expected decreased suitability. Aspen habitat suitability is likely to decrease significantly in parts of the western slope of the Southern Rockies, particularly at lower elevation and drier sites. Conversely, higher elevation forests may see an increase in aspen suitability under future climate scenarios (represented in cool colors). 86
Figure 3.2 Trends in projected future (2023-2060) fire counts (**A**) and area burned (**B**) across Southern Rockies firesheds. All trends were significant ($|p|<0.05$). Many low-elevation regions are expected to increase in fire activity substantially, though all regions demonstrate a positive and significant trend. 87
Figure 3.3 Southern Rockies annual area burned by ignition cause (natural, human, or undetermined) between 1992-2023. Fire data from 1992-2020 is from the FPA-FOD and 2021-2023 from the ICS209-PLUS. Human-caused ignitions accounted for 55.1% of all fires in this database, 33.8% were natural, and 11.1%. 89
Figure 3.4 Built environment characteristics summarized by firesheds in the Southern Rockies; (**A**) Total wildland urban interface/intermix (grassland and forested) percent cover; (**B**) Total combustible mass of the built environment (COMBUST; units). 90
Figure 3.5 Aspen patch metrics including the number of patches, average patch size, patch density, and largest patch index (the proportion of the landscape of the largest patch). 91
Figure 3.6 Intersection of the trend in future fire occurrence and change in future aspen habitat suitability under the more severe climate scenario (SSP585). (**A**) Bivariate map of the Southern Rockies showing firesheds where future fire and aspen suitability intersect or diverge; (**B**) Total land area (hectares) in each bivariate mapping classes. 96
Figure 3.7 Results from SOM analysis. (**A**) Map of cluster assignments by firesheds in the Southern Rockies; (**B**) Radar plots showing the contributions of variables to SOM cluster definitions. 99
Figure 3.8 Distribution of input variables by cluster. Variables were centered and scaled before analysis. 100

INTRODUCTION

Information need

Global fire activity and hazards to communities and the built environment are increasing (Bowman et al., 2009, 2020). Driven by the confluence of rapid housing development in flammable landscapes (Iglesias et al., 2021; Radeloff et al., 2018, 2023), an increasingly fire-conducive climate (Abatzoglou & Williams, 2016; Parks & Abatzoglou, 2020), and exclusion of fire as a fundamental ecological process (Bowman et al., 2020; Marlon et al., 2012), communities world-wide have experienced a growing fire hazard. This has manifested in recent years across the western U.S. in particular, with a 256% increase in wildfire-related structure loss in the most recent decade compared to the previous (Higuera et al., 2023). Much of this increased loss can be attributed to unintentional human ignitions, which start 84% of fires that threaten homes (Balch et al., 2017) and cause four times the number of large wildfires than lightning ignitions (Nagy et al., 2018). These fires often start during dry, windy periods, fueling increasingly common fast-moving fires and extreme single-day spread events into communities and resulting in dire evacuation scenarios and losses (Balch et al., 2024; Coop et al., 2022).

There is no “one-size-fits-all” solution to reducing this hazard. On one hand, addressing risk to the built environment will require changes in how we build (e.g., where and with what materials) and modifications to existing buildings through home-hardening practices (K. Barrett & Quarles, 2024; Mahmoud, 2024), improving evacuation and scenario planning (Cova et al., 2021), and leveraging new technology for early detection, response, and prediction (Stavros et al., 2023). On the other hand, improving our capacity to use fire to our benefit, through prescribed burning and wildland fire use, alongside targeted fuels management through mechanical treatments, will be crucial for building fire-resilient communities and ecosystems (Hessburg et al., 2021; Prichard et al., 2021). In this, we have a great deal to learn from Indigenous fire stewardship, knowledge which has been applied for millennia to maintain ecosystem functioning and limit the build-up of fuels, moderating fire-climate relationships that lead to extreme fire behavior (Kimmerer & Lake, 2001; Lake et al., 2017; Roos et al., 2022). Disruption of Indigenous burning practices, introduction of intensive livestock grazing, and now over a century of aggressive fire suppression in the U.S. and other regions of the world has fundamentally changed fuel availability and condition and has led to fire-starved landscapes which readily burn at higher severity when conditions align (Parks et al., 2025). For example, in the western U.S., wildfires have become more severe in recent decades (1984-2022) compared to reference periods (1600-1875), threatening the persistence of dry conifer forests (Parks et al., 2023). Despite this recognition, the use of fire to fight fire is limited by policy restrictions, public support, and a shortening window of appropriate weather conditions for burning (Schultz et al., 2019; Swain et al., 2023). Furthermore, fuels management activities, such as thinning or clear-cutting, may offer only short-term gains and require revisitation with subsequent treatments or prescribed / cultural burning to maintain positive benefit (Keane, 2015; Prichard et al., 2021). This results in persistent management concerns for communities and can be costly from both a financial and personnel time perspective. Despite these costs, fuels treatments are a necessary component to reducing hazard for communities and providing crucial forest resilience following wildfire (Hessburg et al., 2021). However, and given the complexity of the wildfire hazard, particularly in western North America, varied and intentional solutions are needed to augment current fuels treatments and improve both forest and community resilience to wildfire.

The expansion of “fire-resistant” species, such as quaking aspen (*Populus tremuloides* Michx.), has been proposed as one potential solution (or another “tool in the toolbox”) for reducing fire hazard in some regions. This concept was perhaps first introduced by Fechner and Barrows (1976), though colloquially aspen has long been considered fire-resistant, often referred to as “asbestos forests” (DeByle et al., 1987; Nesbit et al., 2023). Aspen is often considered less flammable than co-occurring forest species, particularly conifer types, due to higher litter and canopy moisture content, higher canopy base height, and potential chemical differences in flammability at the leaf level, among other possible pathways (Nesbit et al., 2023). Managing aspen for fire hazard reduction may also garner far more support and interest from local communities and has the potential to reduce extreme fire hazard without clearing all the trees, as is currently done in high elevation lodgepole or spruce-fir forest types. Local, state, and federal land management agencies and non-governmental organizations have expressed interest in the expansion of aspen in strategic areas as a way of reducing extreme fire intensity and severity. For example, the Town of Breckenridge, CO, in partnership with The Nature Conservancy and Summit County Open Space has planted aspen seedlings inside prior clearcuts with the purpose of creating *living fire breaks*. Similarly, Rocky Mountain National Park has expressed interest in expanding existing aspen stands at the boundary of the Park to buffer fire spread to adjacent communities. For the past few years, stakeholders from a variety of agencies, universities and local non-profits have gathered for the Colorado Aspen Summit – a venue to discuss the challenges and opportunities for aspen management in Colorado and neighboring regions. One consistent conversation in these annual gatherings has been when how and where can aspen be leveraged to reduce fire risk. This interest extends being the Southern Rockies in other regions of the southwest and intermountain west where aspen is the dominant deciduous forest type.

Despite this growing interest, there is a dearth of academic studies quantifying the relationship between aspen forests and fire behavior (Nesbit et al., 2023), especially in the context of recent extreme fire years and increasing fire severity (Coop et al., 2022; Higuera & Abatzoglou, 2021). To leverage this potential solution, targeted studies and management-focused data products are required. This includes better maps of aspen's current distribution to inform management actions, quantification of aspen's influence on fire intensity and severity, and opportunities for managing this species into the future given changing climate and future habitat suitability. In this dissertation, I explore the use of satellite remote sensing, geospatial analyses, and machine learning to provide data products and empirical insights to address these questions in the Southern Rockies.

Background

Quaking aspen ecology and management

Quaking aspen is the most widely distributed tree species in North America and often considered keystone, especially where it exists as the dominant deciduous forest type such as in the interior western U.S. (Campbell & Bartos, 2001; Rogers et al., 2020). Aspen forests provide important ecosystem services including biodiversity, wildlife habitat and forage, water conservation, recreational and economic value, soil and forest carbon sequestration, and resilience following disturbance (Rogers et al., 2014, 2020). Forests dominated by aspen are also considered less prone to high intensity fire compared to surrounding conifer types (Shinneman et al., 2013). Aspen also provides critical forest resilience in some regions through initial recovery of forest carbon following multiple compound disturbances (Buma & Wessman, 2013). Given the importance of this forest type, local, state, and federal agencies have prioritized its management across its range.

Aspen's persistence on the landscape is linked to climatic suitability, disturbance type and periodicity (Bartos, 2001; DeByle & Winokur, 1985; Landhäusser et al., 2010; Rehfeldt et al., 2009). Evidence points to mesoscale synchrony in aspen establishment across the western U.S. following widespread fire activity and/or favorable moisture conditions, highlighting the importance of both disturbance history and climate conditions for aspen persistence (Kaye, 2011). In some cases, increasing synchronous disturbance (e.g., drought, bark beetle, and wildfire) may favor future dominance of aspen in some regions due its ability to respond through root suckering and even from seed establishment (Andrus et al., 2021; Kulakowski et al., 2013; Landhäusser et al., 2010, 2019; Nigro et al., 2022). However, a drier climate and altered fire regimes are likely to have varied impacts on this foundational species across its range (Krasnow & Stephens, 2015; Rosenblum, 2015; Shinneman & McIlroy, 2019; Worrall et al., 2013). Across the interior western U.S., aspen forests have experience both decline in some regions (Worrall et al., 2010, 2013) and expansion in others (Kulakowski et al., 2004, 2013) with projected future climatic suitability showing evidence for both trajectories (Rehfeldt et al., 2009; Hart et al. *In review*). Much of this variation can be linked directly with past land management, fire suppression, insect and disease outbreak, residential and recreational development and changes in suitable temperature and moisture conditions (Rogers et al., 2020). In any case, the effects of short- and long-term declines or increases in aspen cover are of particular interest to forest managers in the intermountain west who want to maintain or expand existing stands for resource benefit or fire hazard reduction.

In the mountain west, aspen exists along a functional type gradient of seral to stable, with important implications for management, fire activity, and ecological trajectories (Morris et al., 2019; Rogers et al., 2014). Seral aspen stands tend to follow a successional pathway, where early establishment and dominance of aspen gives way to more mixed aspen-conifer stands within a relatively short period. In contrast, stable aspen stands are self-sustaining, often for many ecological rotations (lifecycles) with little to no conifer encroachment. These functional types represent key indicators for potential fire activity, with seral aspen exhibiting greater likelihood for extreme fire intensity and severity compared to stable aspen (Shinneman et al., 2013). Recognition of functional types in management of aspen forests is critical to developing effective prescriptions and understanding the varying levels of potential for fire hazard reduction (Rogers et al., 2014).

Management actions in stable aspen forests often involve coppice silviculture, or the removal of large overstory trees (either aspen or conifer), which stimulates suckering response due to changes in light and soil temperature. In general, stable aspen stands experience individual tree or small group mortality at a given time. The use of selecting logging or group clearfell can be highly effective for improving aspen stand condition in the absence of wildfire or other disturbances, especially in areas where sudden aspen decline (SAD) has been observed (W. D. Shepperd et al., 2015). In stable aspen forests, stand age and condition influence the regeneration capacity and help predict response to management actions. In seral aspen stands, a variety of management actions can be deployed to invigorate new growth and maintain stand condition and functioning by replicating stand replacing disturbance events like wildfire or wind throw. Management decisions in aspen forests should be guided by what functional type exists, the adjacent ecosystem structure (e.g., neighboring forest types, topography, and water availability), and topography and climate so that prescriptions are applied based on the locally-relevant context (Rogers et al., 2014).

Aspen as a "living fire break"

Aspen has been associated with less flammable traits including higher surface fuel moisture, greater canopy base height, and lower canopy bulk density (DeByle & Winokur, 1985; DeRose & Leffler, 2014; Nesbit et al., 2023). With these fire-moderating traits, aspen may act as a natural buffer or a "*living fire break*" to extreme fire behavior. Early explorations of this concept in the interior western U.S. highlighted the lower occurrence of fire in aspen stands (DeByle et al., 1987) and the capacity for aspen to improve suppression effectiveness in the Southern Rockies (G. Fechner & Barrows, 1976). More recently, palaeoecological, experimental, and geospatial analysis has shown that aspen forests are less likely to burn in some cases, especially in the boreal mixed hardwood forests of North America (Alexander, 2010; Bebi et al., 2003; Cumming, 2001; Girardin & Terrier, 2015; Krawchuk et al., 2006). However, aspen stands do burn and may even exhibit extreme fire behavior under extreme weather, demonstrated by simulated fire potential in aspen stands of Northern Utah (DeRose & Leffler, 2014). A recent extensive literature review found that studies have referenced the presence of aspen reducing fire occurrence, fire behavior, and fire severity, but this effect is dependent on many factors, including the percentage of aspen vs conifers in the overstory, load and type of understory fuels, weather, and season (Nesbit et al., 2023). The same study determined that more information is needed to understand if, how, when, and where aspen mediates fire behavior. This is especially needed in the context of recent extreme fire years in the western U.S. (Cunningham et al., 2024; Higuera & Abatzoglou, 2021).

The concept of *living fuel breaks* or sometimes referred to as "green fuel breaks" (Wang et al., 2021) is not necessarily a new concept, especially for aspen forests (G. H. Fechner, 1976). However, the lack of widespread analysis of these techniques, especially comparing their efficacy to more traditional fuels treatments, limits decision-makers who would be able to implement such strategies. Beyond the comparison to tradition fuels treatments, which is needed, there remains a more fundamental knowledge gap about how distinct forest types, particularly aspen, burn during recent extreme wildfire activity and whether the concept applies moving forward (i.e., under projected extreme fire activity). While there is widespread scientific evidence for distinct fire regimes in different forest types, there have been few studies which examine the direct influence of aspen, for example, on modulating fire behavior under different landscape scenarios (e.g., weather, topography, and other factors).

In the Southern Rockies, stakeholders including the Colorado State Forest Service, Rocky Mountain National Park, Summit County Parks and Open Space, Town of Breckenridge and The Nature Conservancy have expressed interest in using management of aspen forests as a tool for reducing wildfire hazard. This dissertation, in part, aims to produce actionable science to help inform management of quaking aspen forests for fire hazard reduction and other resource benefits. Improving our understanding of contemporary fire behavior in aspen forests is an area of urgent need to inform management decisions, especially in the context of wildfire hazard reduction but also in the context of future fire likelihood and forest persistence following increasingly high severity wildfires (*refs*). It is unclear how these so-called "living fire breaks" moderate fire behavior or reduce hazard for communities, particularly during recent extreme fire years. With a general lack of quantitative evidence, particularly in the context of recent extreme fire years in the western U.S., there is a gap between management goals and scientific knowledge (Nesbit et al., 2023). Given its importance in western US forests and the growing interest in aspen management for wildfire mitigation, more information is needed to understand if, when, and how aspen moderates fire activity (Nesbit et al., 2023).

Remote sensing applications in fire ecology

Availability of remote sensing (RS) data before, during, and after fires has grown significantly over the past many decades, and has fundamentally changed the ways in which scientists are able to monitor changing fire activity (Szpakowski & Jensen, 2019). Since the launch of the Landsat missions in 1972, which was the one of the first satellite mission explicitly designed to study the Earth's surface, our capacity to monitor landscape dynamics, especially fire and vegetation classifications, at broad spatial scales has fundamentally changed and the amount of available data has increased exponentially (Hermosilla et al., 2022). Alongside increasing availability of RS data products, computing resources and analysis techniques have also grown. This has ushered in a new era of fire science, one in which we increasingly monitor and study fire activity and effects from space.

In the context of aspen, applications of RS data are a promising avenue for monitoring its distribution and relationship to fire. For example, the unique canopy characteristics of aspen forests, especially relative to adjacent conifer types, facilitate the use of both passive optical and active radar remote sensing data to map its distribution. Elevated canopy chlorophyl content of aspen forests gives them a unique spectral signature that can be easily distinguished by multispectral or hyperspectral data, particularly in landscapes where it is the dominant deciduous forest type. Beyond the spectral uniqueness of aspen canopies, their structure also differs from adjacent conifer forests with higher canopy bulk density, for example. This presents an opportunity for active remote sensing including radar and LiDAR, which enable characterization of canopy roughness and structure. Combined, passive and active remote sensing, alongside machine learning classifiers, is a promising avenue for developing improved maps of aspen's distribution and facilitating long-term monitoring of its range and health.

Passive and active RS data also provide avenues for assessing fire activity and post-fire impacts across large spatial scales. Optical RS has been applied extensively to map post-fire ecosystem impacts such as burn severity using the spectral differences between pre- and post-fire multispectral imagery which show strong correlations with field-based measurements of severity (Roy et al., 2006). These methods form the basis for national-scale burn severity mapping such as the Monitoring Trends in Burn Severity (MTBS; Eidenshink et al., 2007) which has been widely applied in the U.S. over the past two decades . In tandem, active fire detection based on middle-infrared radiance and thermal RS has become a crucial tool for fire managers and researchers to detect, monitor, and assess global fire activity (Wooster et al., 2021). Aggregation of active fire pixels has been used to delineate fire events and recreate daily fire progression maps, providing crucial data to understand the drivers of fire growth patterns and changes in fire regimes and impacts related to extreme fire spread (Balch et al., 2020, 2024; Coop et al., 2022; McFarland et al., 2025; Scholten et al., 2024). Radiance in the middle-infrared is also leveraged to calculate the fire radiative power (FRP), a useful proxy for fire intensity as it relates well to the heat of a fire and biomass burning patterns. All told, these data represent key opportunities for the application of RS to understand the distribution of aspen forests and their relationship to fire activity such as spread, intensity, and severity.

Research Aims

This dissertation examines the application of remote sensing, geospatial analysis, and statistical learning to assess the distribution of quaking aspen forests, their influence on fire activity, and future opportunities for management of this important forest type in the Southern Rockies. In Chapter One, we demonstrate the capability of multispectral and radar imagery from the Sentinel missions to map the distribution of aspen forests across the SRM. These data present an opportunity for fine-scale mapping of aspen forests, identifying small stands which are important from a management perspective. In Chapter Two, we assess the influence of forest composition, structure, and landscape factors on satellite-derived Fire Radiative

Power (FRP) and Composite Burn Index (CBI), elucidating the relationship between forest type, specifically focused on aspen, on fire intensity and severity. We combine wall-to-wall forest composition information from the USFS TreeMap alongside VIIRS active fire detections and Landsat-based burn severity. In Chapter Three, we combine new results describing the future habitat suitability of aspen alongside future fire probability with contemporary wildfire hazard, population density, and forest composition to highlight regions of the SRM which can be targeted for active management of aspen forests for resource benefit, including fire hazard reduction.

1 CHAPTER ONE

Gold in the hills: Mapping quaking aspen using seasonal multispectral and radar imagery in the Southern Rockies, USA

Adapted from: Cook, M., Chapman, T., Hart, S., Paudel, A., Balch, J., 2024. Mapping Quaking Aspen Using Seasonal Sentinel-1 and Sentinel-2 Composite Imagery across the Southern Rockies, USA. Remote Sensing 16, 1619. https://doi.org/10.3390/rs16091619

1.1. Introduction

Across the interior western United States, quaking aspen (Populus tremuloides Michx.) is the dominant deciduous tree species in primarily mixed-conifer forests (DeByle & Winokur, 1985; Rogers et al., 2020). This important forest type provides ecosystem services, including biodiversity, wildlife habitat, recreational value, soil carbon sequestration, and vegetation recovery (Rogers et al., 2020). Aspen respond readily to canopy opening events (e.g., wildfire) and its persistence on the landscape is closely linked to disturbance type and periodicity (Bartos, 2001; Gill et al., 2017; Landhäusser et al., 2010; Rogers et al., 2014). Increasing synchronous disturbances (e.g., drought, bark beetle, and wildfire) may favor future dominance of quaking aspen in some regions (Andrus et al., 2021; Landhäusser et al., 2010; Nigro et al., 2022). However, a drier climate and altered disturbance regimes are likely to have varied impact on this foundational species across its range (Krasnow & Stephens, 2015; Rosenblum, 2015; Shinneman & McIlroy, 2019; Worrall et al., 2013). With growing focus on aspen ecology and management in the context of climate change and forest resiliency, production of high-resolution, accurate maps of its distribution at scales relevant to forest management activities is necessary.

Current nationwide maps of quaking aspen forest cover are developed using Landsat imagery at a 30-m spatial resolution (e.g., Picotte et al., 2019) and often fail to identify small stands, which offer prolific root suckering and expansion when managed or following disturbance (Landhäusser et al., 2019; W. D. Shepperd et al., 2015). There are three relevant 30-m maps of aspen distribution widely available for land managers in the Southern Rockies and US: 1 – the LANDFIRE Existing Vegetation Type (Landfire EVT) (Picotte et al., 2019), 2 – the United States Forest Service (USFS) National Individual Tree Species Parameter maps (USFS ITSP) (Ellenwood et al., 2015), and 3 – the USFS TreeMap (Riley et al., 2022). Of these, only the Landfire EVT is provided in more than one time stamp. The remaining databases provide a snapshot in time as valuable baselines for managers. Collectively, these databases are limited in accuracy, their ability to detect small patches of aspen, and in their temporal range. For example, one of the more commonly used land cover maps in the US, the Landfire EVT, has an accuracy of 60-63% within aspen classes across the southwest US region for the 2016 product (https://www.landfire.gov/remapevt_assessment.php, accessed March 31, 2023). The USFS ITSP (c. 2014) and TreeMap (c. 2016) uniquely provide additional information from the USFS Forest Inventory and Analysis (FIA) plot data such as basal area and stem density but provide only a snapshot in time and have similar moderate accuracy for the aspen class. Developing new, higher-resolution maps will improve on these existing products at scales relevant to quaking aspen management.

Remote sensing science has benefited in recent years from increasingly available free and open imagery and improved cloud computing resources, facilitating the application of large scale analysis of the Earth's surface (Gorelick et al., 2017; Hermosilla et al., 2022). In particular, the Sentinel missions, developed to support the Copernicus Programme and administered by the European Space Agency, have improved LULC mapping efforts across broad geographic regions (Phiri et al., 2020). The Sentinel missions consist of a constellation of satellites carrying a range of technologies, including microwave (radar) and multispectral imaging. These data are made free and open to the public through the Copernicus Programme free, full, and open data policy. Importantly, Sentinel products are also hosted in the Google Earth Engine (GEE) platform, which provides access to petabytes of earth systems data co-located with powerful cloud-computing resources (Gorelick et al., 2017).

The combination of spatial, spectral, and temporal resolutions of the Sentinel-2 (S2) Multispectral Instrument (MSI) is particular useful for mapping vegetation with distinct phenological patterns (Phiri et al., 2020). Since 2015, S2 has provided global multispectral imagery at finer spatial (10-60 m), spectral (13-band), or temporal (5-day) resolutions compared to similar satellite missions such as Landsat (30-90 m, 4-8 bands, and 16-day) or Satellite Pour L'Observation de la Terre (1.5-6 m, 4-band, and 1-3 day). The four narrow red-edge bands captured by

S2 improve species-level mapping, estimation of canopy chlorophyll content, and derivation of metrics such as gross primary productivity (Bayle et al., 2019; Clevers & Gitelson, 2012; Lin et al., 2019; Wong et al., 2019). The 5-day temporal resolution increases availability of cloud-free images and facilitates analysis of land surface phenology and generation of seasonal cloud-free image composites (Kollert et al., 2021). Seasonal imagery improves species discrimination in forested regions, especially for deciduous types with distinct phenology (Immitzer et al., 2019; H. Li et al., 2021; Macintyre et al., 2020; Persson et al., 2018).

However, as with any optical imagery, persistent cloud cover, haze, and snow cover are common issues affecting data acquisition and quality. In the case of vegetation mapping with multispectral imagery, multi-temporal image gap-filling can help overcome this challenge while retaining seasonal characteristics of the land surface (Kollert et al., 2021). Additionally, combining multispectral images with sensors less affected by atmospheric and environmental conditions, such as radar and microwave, can improve availability and quality of data.

The Sentinel-1 (S1) provides cloud-penetrating synthetic aperture radar (SAR) backscatter imagery at the same spatial and temporal resolution as S2, providing an important complementary data source for applications in land surface monitoring. As an active remote sensing system, SAR measures the amplitude and phase of the backscatter signal, which corresponds to the physical properties (e.g., roughness) of the land surface (Barber, 1985). In forested systems, the wavelength of radar signal emitted from the sensor determines the sensitivity and depth of penetration into the canopy (Udali et al., 2021). The S1 collects dual-polarized C-band SAR backscatter at a nominal frequency range, from 4-8 GHz (3.75-7.5 cm wavelength) in the microwave region of the electromagnetic spectrum. In this region, there is minimal penetration into the forest canopy, making it useful for characterizing tree canopy roughness and texture (Numbisi et al., 2018; Udali et al., 2021).

Recent studies have shown potential for multi-temporal optical and radar (e.g., S1 and S2) imagery to improve vegetation mapping, especially in areas with persistent cloud cover and heterogeneous vegetation types (Dobrinić et al., 2021; Lechner et al., 2022; Liu et al., 2018). The common spatial and temporal resolutions of the S1 and S2 facilitate the use of these two data sources in tandem for classifying vegetation type (Dusseux et al., 2014; Steinhausen et al., 2018). Radar imagery is particularly useful in characterizing deciduous forest canopy structure during winter months when there is often persistent snow cover and/or cloud cover (Dobrinić et al., 2021; Lechner et al., 2022). In deciduous forests specifically, the canopy structure changes at key phenological stages (e.g., onset of greenness increase, greenness maximum, onset of senescence, and greenness minimum), which may be characterized by multi-temporal S1textural data, improving forest species classifications (Kollert et al., 2021). Furthermore, because SAR is sensitive to changes in the canopy roughness, textural features derived from backscatter imagery have improved classification of forest type (Haralick et al., 1973; Numbisi et al., 2018). Given the advances in classification accuracy using the Sentinel suite in a variety of recent studies, the efficacy in different ecosystems should be explored.

In this study, we have three primary objectives: 1) develop methods for an open-source, accurate, and high-resolution (10 m) map of aspen cover across the Southern Rockies ecoregion (U.S. Environmental Protection Agency Level III) using combined S1 and S2 seasonal composite imagery with spectral indices and textural features; 2) assess the agreement of this Sentinel-based map with existing 30-m products; and 3) analyze and compare aspen patch size and total area across the Southern Rockies and within a targeted Colorado geography where aspen is currently a management focus. Finally, we provide access to results and input data through a public interactive GEE application and make all code and methodology available in public repositories. We anticipate that a higher resolution and more accurate map of aspen cover will facilitate targeted and effective management of aspen forests to increase the valued ecosystem services provided by this forest type.

1.2. Materials and Methods

1.2.1. Study Area

The Southern Rockies includes portions of southern Wyoming, central and western Colorado, and northern New Mexico. Extending nearly 130k km^2, the elevation of the region ranges from approximately 1,128-4,268 m above sea level and is characterized by two major mountain belts and intermontane valleys and parks. There are a diverse array of ecosystem types including lower montane/foothills, wet meadows, upper montane, subalpine, and alpine (R. K. Peete, 1988). Forested area accounts for an estimated 72% (93.6k km2) of the landscape (Landfire EVT, c. 2016), with dominant tree species including Engelmann spruce and subalpine fir (18.1%), ponderosa pine and Douglas-fir (17.2%), quaking aspen (10.1%), lodgepole pine (9.4%), and pinon and juniper woodland (7.8%) (Picotte et al., 2019). The Southern Rockies is characterized by a large proportion of federally managed lands (87.5%) including ten National Forests, two National Parks, and 57 federally listed wilderness areas (Johnson, 2023). Quaking aspen is the dominant deciduous forest type and persists on the landscape in both pure (stable) and mixed (seral) stands and their geographic distribution is highly linked with disturbance history (Rogers et al., 2014; W. Shepperd, 1990).

We evaluate our Sentinel-based aspen map across the Southern Rockies blocks and for a targeted geography in Colorado, the White River National Forest (NF), where quaking aspen is actively managed for wildlife habitat and wildfire risk reduction. The White River NF covers over 10,000 km^2 in central and western Colorado and encompasses many of the ecosystem types of the Southern Rockies. The region is also recreationally important with 11 ski resorts, ten peaks over 4,267 m, and eight wilderness areas encompassing nearly a third of the total area (https://www.fs.usda.gov/whiteriver; accessed March 31, 2023). The USFS manages 1,966 km^2 of both stable and seral stands of quaking aspen. Current management activities aim to promote aspen regeneration in existing aspen stands, improve wildlife habitat by expanding aspen cover, and increase forest disturbance severity and recovery by promoting aspen in conifer stands. Managers are using mechanical harvests (coppice silviculture) and prescribed fire to achieve these outcomes.

Large area image classification presents unique challenges, particularly in the generation of representative and accurate training and validation data, collection of satellite imagery, and assessment of model performance (Hermosilla et al., 2022). To overcome these challenges, we divided the Southern Rockies into 129 equal area (50 km2) spatial blocks (Figure 1). These blocks provide an analytical unit to generate training and validation data (Section 1.2), imagery composites (Section 1.3.1 and 1.3.2) and perform spatial block cross-validation during model training (Section 1.4).

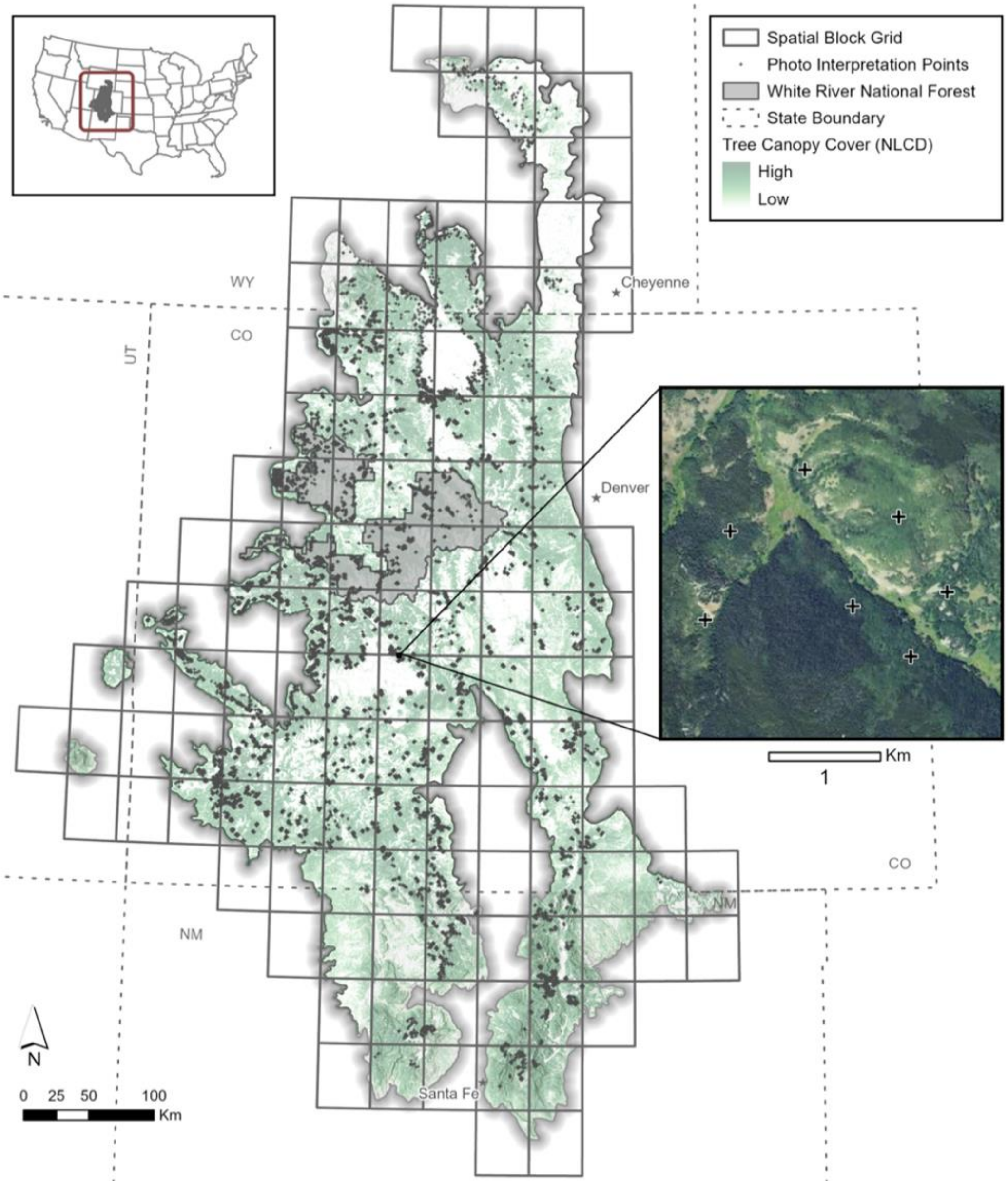

Figure 1.1 *Map of the Southern Rockies study area with spatial blocks, case study landscape, aspen reference data and forest canopy cover. Inset map showing aspen photo points overlain with National Agricultural Imagery Program (NAIP, ca. 2019).*

1.2.2. Image Reference Data

To train and validate the classification models, we generated presence and background learning data for the study region. In binary classification algorithms, presence (or the positive class) represents the target land cover type or species, and background (or the negative class) captures a representative sample of all other cover types. This approach is particularly useful for applications where the desired result is a single land cover type or species and is commonly used in applications of habitat suitability modeling (Deng et al., 2018).

Quaking Aspen Reference Data

Availability of field-based measurements of quaking aspen forest cover in the region is limited, particularly data aligned with Sentinel pixels. To overcome this challenge, we created a database of aspen presence using photo interpretation of high-resolution (1 m) aerial imagery from the United States Department of Agriculture (USDA) National Agricultural Imagery Program (NAIP, c. 2017) (Davis, D., 2011). We created a binary mask of aspen forest cover using the USFS TreeMap (c. 2016) basal area estimates derived from the USFS FIA. We identified pixels where live basal area was greater than 10 stems/ha, a potential minimum unit for established aspen stands in the Southern Rockies (DeByle & Winokur, 1985). For each spatial block, we placed 10 random points inside the mask and applied a 5 km buffer which served as a spatial support to aid interpretation. An interpreter was trained to identify aspen from NAIP imagery and attempted to label a minimum of 10 pixels of aspen within the spatial support unit. If there were no obvious stands of aspen, a new random point was generated in the block. A random sample of these presence points was taken with a minimum distance of 100 m to limit effects of pseudoreplication. The resulting database includes 12,609 points across 95 spatial blocks in the Southern Rockies.

Background Reference Data

Background reference data are representative of other major land cover types across the Southern Rockies and were derived from the Landfire EVT Sub-class property (c. 2016). To account for regional variation in cover types, proportional stratified samples were generated for each spatial block. The total number of samples in each block was set to ten times the number of presence points and divided amongst classes proportional to their area. A minimum sample size of 10 was set for each class in the block to ensure representation of minority classes, resulting in 73,031 samples across Landfire EVT sub-classes (Table 1).

Table 1-1 *Distribution of background samples across all spatial blocks with at least 100 aspen presence points.*

Landfire EVT Sub-class	Number of Samples
Evergreen closed tree canopy	23,957
Mixed evergreen-deciduous shrubland	13,421
Evergreen open tree canopy	12,991
Perennial graminoid grassland	7,637
Annual Graminoid/Forb	3,537
Evergreen shrubland	3,273
Sparsely vegetated	2,869
Mixed evergreen-deciduous open tree canopy	1,016
Developed	896
Non-vegetated	808
Perennial graminoid	716
Evergreen dwarf-shrubland	669
Evergreen sparse tree canopy	624
Deciduous open tree canopy	617

	Total	**73,031**

1.2.3. Satellite Imagery

We collected freely available Sentinel-1 and Sentinel-2 imagery for one year (2019) in the GEE data catalog (Gorelick et al., 2017). To develop seasonal imagery composites which are consistent across a large and diverse geographic region, we use phenological characteristics of aspen forests to identify temporal windows of key stages of development. Collection and preparation of median seasonal radar composites is described in *Section 1.2.1* and optical imagery collection and compositing is described in *Sections 1.2.2* and *1.2.4*, respectively. In addition, we calculated spectral vegetation indices and radar textural features which are described in *Section 2.2.3*.

Sentinel-1 Synthetic Aperture Radar (SAR)

We collected winter (December-February) and summer (June-August) imagery from the Sentinel-1 (S1) C-Band Ground Range Detected (GRD), which collects data in dual polarization mode (VV and VH). These seasonal windows capture two distinct development stages of the forest canopy: peak (summer) and dormancy (winter). The S1 GRD collection was processed to analysis-ready data involving border noise correction and speckle filtering (Mullissa et al., 2021). We combined both orbital passes (ascending and descending) for each polarization mode and calculated the median backscatter coefficient for the seasonal windows. In total, 556 individual S1 images were used to generate the median composites (324 for summer and 232 for winter).

Sentinel-2 Multispectral Instrument (MSI)

We collected all Sentinel-2 (S2) Multispectral Instrument (MSI) Level-2A surface reflectance scenes for the entire year across the Southern Rockies (5,137 tiles). Each surface reflectance tile includes four spectral bands at 10-m spatial resolution, six bands at 20-m, and three bands at 60-m. The 60-m bands (coastal aerosol, water vapor, SWIR-cirrus), which are uninformative for vegetation analysis, were excluded from the collection and remaining bands were resampled to a common 10-m spatial resolution (**Table 1-2**).

Table 1-2 *Original Sentinel-1 and Sentinel-2 bands with abbreviations, names, center wavelengths, and seasonal windows.*

Satellite	Abbrev.	Name	Center Wavelength	Seasonal Windows*
Sentinel-1	VV	Vertical-vertical	5.5cm	Peak Greenness / Dormancy
	VH	Vertical-horizontal	5.5cm	
Sentinel-2	B2	Blue	490 nm	Summer / Autumn
	B3	Green	560 nm	
	B4	Red	665 nm	
	B5	Red-edge 1	705 nm	
	B6	Red-edge 2	740 nm	
	B7	Red-edge 3	783 nm	
	B8	Near Infrared	842 nm	
	B8A	Red-edge 4	865 nm	
	B11	Shortwave Infrared 1	1610 nm	
	B12	Shortwave Infrared 2	2190 nm	

Additional Spectral and Textural Feature

In addition to the S1 backscatter and S2 spectral bands, we calculated a suite of additional textural features and vegetation indices (Table 2). Given that radar backscatter imagery is sensitive to canopy surface roughness, textural features of

S1 data can provide valuable information for discriminating forest types. Specifically, the Gray Level Co-Occurrence Matrix (GLCM) calculates textural features from image data by assessing the patterns of pixel intensities and spatial arrangement (Haralick et al., 1973). The derivatives of GLCM have been shown to improve land cover classifications from radar data (Farwell et al., 2021; Haralick et al., 1973; Numbisi et al., 2018). We derived GLCM entropy, contrast, variance, and correlation using a 7x7 kernel for each of the winter and summer VH and VV polarization modes resulting in 16 additional features for classification.

Six vegetation indices targeting forest canopy productivity, moisture, and chlorophyl content were derived from the S2 bands. These included the Chlorophyll Index Red-edge (CIRE), Modified Chlorophyll Absorption in Reflectance Index (MCARI), Inverted Red-edge Chlorophyll Index (IRECI), Specific Leaf Area Vegetation Index (SLAVI), Modified Normalised Difference Water Index (MNDWI), and the Red-edge Normalised Difference Vegetation Index (NDVI705).

Table 1-3 *Spectral vegetation indices and radar textural features. The formula and associated reference to calculate each index is provide where relevant. Indices and textural features were calculated for each seasonal window.*

Satellite	Index	Abbreviation	Formula	Seasonal Windows	Reference
Sentinel-1	GLCM Entropy	VV_ent, VH_ent	GLCM 7x7	Peak / Dormancy	(Farwell et al., 2021)
Sentinel-1	GLCM Variance	VV_var, VH_var	GLCM 7x7	Peak / Dormancy	
Sentinel-1	GLCM Correlation	VV_corr, VH_corr	GLCM 7x7	Peak / Dormancy	
Sentinel-1	GLCM Contrast	VV_contrast, VH_contrast	GLCM 7x7	Peak / Dormancy	

Sentinel-2	Chlorophyll Index Red-edge	CIRE	(B8 / B5) – 1	Summer / Autumn	(Gitelson et al., 2003)
Sentinel-2	Inverted Red-edge Chlorophyll Index	IRECI	(B8 – B4) / (B5 / B6)	Summer / Autumn	(Frampton et al., 2013)
Sentinel-2	Specific Leaf Area Vegetation Index	SLAVI	B8 / (B4+ B12)	Summer / Autumn	(Kobayashi et al., 2020)
Sentinel-2	Modified Chlorophyll Absorption in Reflectance Index	MCARI	((B5 – B4) – 0.2 * (B5 – B3)) * (B5 / B4)	Summer / Autumn	(Dobrinić et al., 2021)
Sentinel-2	Red-edge Normalized Difference Vegetation Index	NDVI705	(B6 – B5) / (B6 + B5)	Summer / Autumn	(Evangelides & Nobajas, 2020)
Sentinel-2	Modified Normalized Difference Water Index	MNDWI	(B3 – B11) / (B3 + B11)	Summer / Autumn	(Jiang et al., 2020)

1.2.4. Seasonal Sentinel-2 Composites

To generate median spectral image composites which are representative of key phenological stages of aspen, we extracted 1) the spectral response of aspen reference data for each image in the annual collection, and 2) the phenological characteristics within the USFS TreeMap mask (*Section 1.3.1*) from the Visible Infrared Imaging Radiometer Suite (VIIRS) Land Cover Dynamics data product (VNP22Q2), which provides global land surface phenology (GLSP) metrics at yearly interval (Zhang et al., 2018). For the S2 time-series, we excluded any observations which were occluded by clouds or shadows using the Cloud Score Plus (Pasquarella et al., 2023) with a threshold value for occluded pixels of 0.60. We then calculated the median bi-weekly surface reflectance for each reference point in the time-series for the S2 bands and vegetation indices. The median and range of phenology metrics (in day-of-year) were calculated at the spatial block unit for the VIIRS time-series (2013-2022). The timing of phenological transition varies across spatial block units and years and is heavily influenced by elevation (**Figure S1**). A more detailed description of the phenology assessment across the Southern Rockies is provided in Appendix S1. Using these data, we defined two ecologically relevant temporal periods for image composites: summer (median onset of greenness increase to the 10th percentile onset of greenness decrease, May 25-August 13, 2019), and autumn (minimum mid-senescence phase to the 90th percentile onset of greenness minimum, September 2-November 14).

For each seasonal window, we filtered out images with greater than 80% cloud cover and 10% snow cover. We joined each image in the collection to its corresponding Cloud Score Plus image. The Cloud Score Plus provides a single pixel occlusion score based, enabling flexible and accurate masking of cloud and cloud shadows (Pasquarella et al., 2023). A binary cloud mask for each image was created with a cloud score threshold of 0.60 and used to remove occluded pixels. Seasonal image composites were created by calculating the per-pixel median surface reflectance value. A total of 3,956 S2 tiles were used with per-spatial block averages of 146 (+/- 71) tiles for summer and 73 (+/- 30) tiles for autumn.

1.2.5. Topographic Data

Inclusion of topographic information is shown to improve the accuracy of forest type classifications, especially in regions with complex elevation patterns (Dobrinić et al., 2021). We include a digital elevation model (DEM) from the United States Geological Service (USGS) 3-dimensional Elevation Program (3DEP) 1/3 arc-second (10 m) elevation product. In addition, we calculated aspect and slope from the DEM, both of which may influence the distribution of aspen forest cover across the landscape (W. Shepperd, 1990).

1.2.6. Image Classification

We developed a binary random forest (RF) classification of aspen cover. For image classification tasks, RF is a robust method which is less sensitive to overfitting while also minimizing computational expense with large input data (Belgiu & Drăguț, 2016; Deng et al., 2018). In order to account for spatial autocorrelation in the training and testing data, we implemented 10-fold spatial block cross-validation during model development and calculated the average model performance metrics and confidence intervals (Karasiak et al., 2021). For each fold, a 70:30 ratio was used to split valid spatial blocks (i.e., blocks which contain reference data) into training and testing sets respectively. Within each subset, the presence and background learning data were extracted, resulting in different subsets of reference data for each fold. Models were trained with 1001 trees and the number of random variables used at each split was set to the square root of the number of input variables. We assessed model performance across different combinations of classification scenarios and selected the best performing combination of input features to use for the final classification.

Model Selection and Accuracy Assessment

We assessed model performance using a set of common metrics based on the confusion matrix for each k-fold model and classification scenario. From the confusion matrix, we calculated the precision, recall and F1-score. To account for class imbalance in our training data, the F1-score was adopted to assess model performance because it typically performs better than overall accuracy in imbalanced classifications (Uhl & Leyk, 2022). We selected the best performing classification scenario based on the average F1-score across folds. For the best performing scenario, we identified and removed multicollinear bands and performed feature selection to identify the most parsimonious model for classification in GEE. While the predictive ability of RF is likely unaffected by multicollinearity, the assessment of feature importance is sensitive to its presence (Belgiu & Drăguț, 2016). We tested for multicollinearity using the 'multi.collinear' function in the rfUtilities (Evans & Murphy, 2018) package in the R Statistical Programming Language (R Core Team, 2022) with a permutated (N=1001, p<=0.05) leave-one-out method. We removed features from best performing classification scenario based on the frequency that they were identified in the permutation tests (frequency > 0). We then used the 'rf.modelSel' function to identify the most parsimonious set of features based on out-of-bag error rate to use in the final classification model in GEE, thereby improving computation time and minimizing noise (Evans & Cushman, 2009).

We assessed the accuracy of the final model based on the binary classification of the probability surface generated by the RF model. Typically, predicted classes are defined based on a single probability threshold between 0-1 (e.g., probability > 0.5 belongs to class 1). We tested the sensitivity of model performance using a moving threshold where the confusion matrix is calculated for 100 values between

0-1 for each of the 10 folds. At each threshold in the sequence, we classified the testing data into aspen (1) or non-aspen (0) and calculated the precision, recall, and F1-score. We identified the optimal threshold for classification based on the average maximum F1-score across folds.

Feature Importance

We retrieved feature importance from the final model, calculated in GEE as the sum of decrease in Gini impurity index over all trees in the forest (Nembrini et al., 2018). We stored the feature importance values for each fold and present the median values with confidence intervals.

1.2.7. Agreement with Existing Products

We assessed the agreement between our Sentinel-based aspen map and three existing 30-m products: the Landfire EVT (c. 2016), USFS ITSP (c. 2014), and USFS TreeMap (c. 2016). We compare both the accuracy of our testing data (i.e., aspen presence data held out for model testing) as well as the pixel-based agreement across the Southern Rockies and the White River NF for each product. Each of these reference products were reclassified into aspen and non-aspen classes and resampled to a common 10-m spatial resolution to match the Sentinel-based map. For the USFS ITSP and TreeMap, we used the basal area metric (> 10 stems/ha) to reclassify the grids into aspen and non-aspen. A confusion matrix was created using the testing data across the region and for each spatial block across the Southern Rockies and for the White River NF for the pixel-based assessment. From the confusion matrices, we calculated the precision, recall, and F1-score and present the distribution of these metrics across the study regions.

1.2.8. Case Study: Landscape Patch Dynamics

To highlight the utility of the Sentinel-based map for management activities, we calculated patch- and class-level landscape metrics across the Southern Rockies and within the White River NF. We compare landscape metrics between the Sentinel-based map and the three reference datasets. These metrics included landscape-level (total area, patch density, and proportion of the landscape) and patch-level (patch size and perimeter to area ratio) statistics. All metrics were calculated using the pylandstats Python package (Bosch, 2019).

1.3. Results

1.3.1. Annual Spectral Response of Quaking Aspen Forests

The annual surface reflectance of quaking aspen forests highlights the patterns of phenology, canopy development and environmental conditions in the study region (**Figure 2A**). During winter (December-March), surface reflectance is highly variable as the canopy is in dormancy and stands are often covered in snow, especially at higher elevations. As the canopy develops, a peak in the near-infrared (NIR) and red-edge wavelength occurs around the first week or two of July and corresponds with a mature forest canopy. As the canopy transitions to early autumn, there is a drop in NIR reflectance and increase in both the visible and shortwave-infrared (SWIR) which corresponds to a decrease in green vegetation. A similar pattern is observed for the S2-MSI spectral indices (**Figure 2B**). The largest difference in reflectance between summer and autumn windows occurs in the NIR and red-edge regions of the spectrum, although there are significant spectral changes across all S2 bands (**Figure 1.2C**) and spectral indices (**Figure 1.2D**).

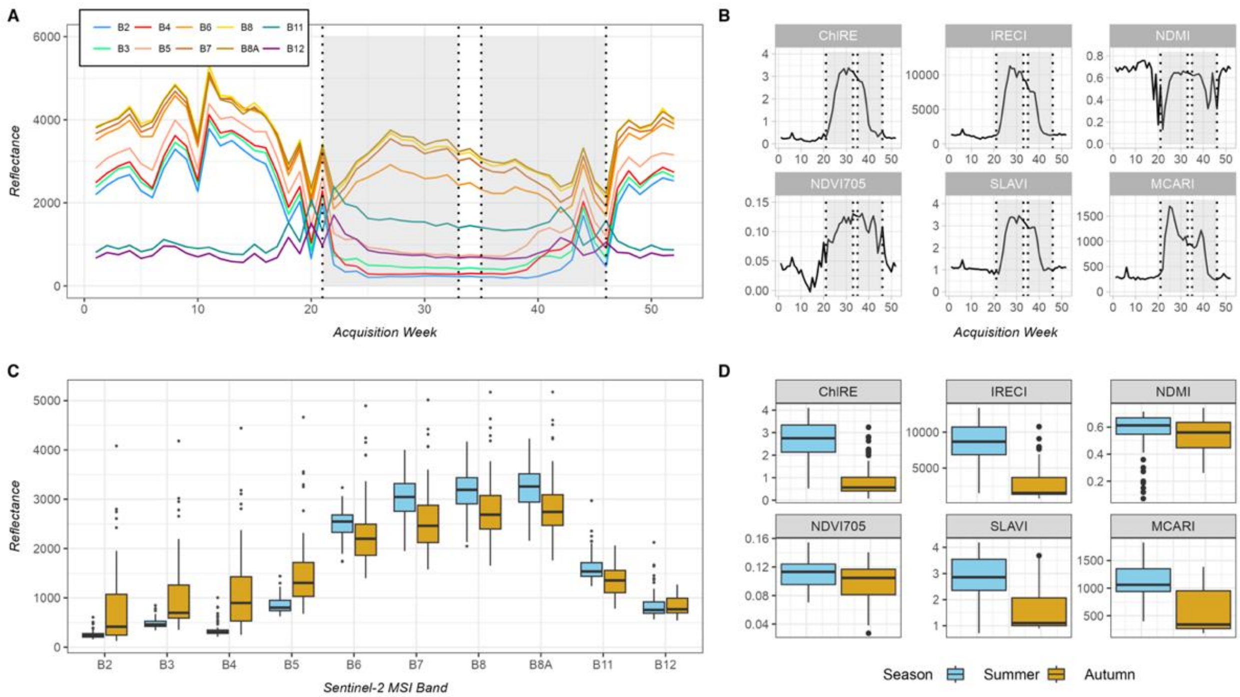

__Figure 1.2__ Annual (A-B) and seasonal (C-D) spectral response of aspen presence data (c. 2019). Grey shading defines the temporal windows. (A) Median bi-weekly surface reflectance values for S2 bands; (B) Median weekly response of derived spectral indices; (C) Seasonal differences in S2 bands from image composites (summer and autumn); (D) Seasonal difference in spectral indices.

1.3.2. Model Selection and Accuracy Assessment

We selected the final classification model based on the results from the scenario testing. The best performing classification scenario included all features from both S1 and S2 and topographic data with an average F1-score of 0.91 (+/- 0.01, **Figure 3**). The worst classification scenarios were those in which only S1 data was used (F1-score 0.46-0.62). There was a significant increase in classification accuracy for single-season S2 data (i.e., summer or autumn alone). Combining both the seasonal S2 composites along with spectral indices increased the average F1-score by 0.3 compared with just the summer S2 and indices, whereas the addition of S1 only improved the F1-score by an additional 0.1. Thus, our final scenario included all S1 and S2 features for each seasonal window along with topographic features. For this best performing classification scenario, we removed 21 collinear bands and identified a set of 17 which minimized the out-of-bag error rate for the most parsimonious classification. We achieved an average F1-score of 0.931 (+/- 0.008) for the final model.

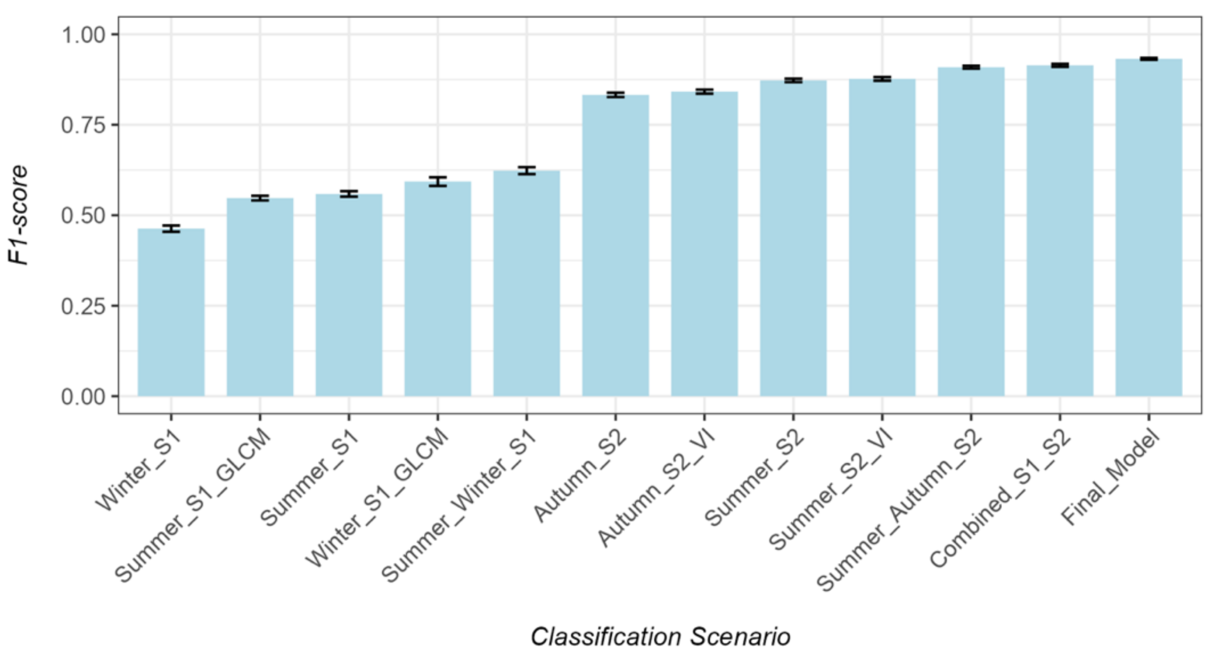

Figure 1.3 *Results from the classification scenarios. We report the average and standard error F1-score across folds for each scenario. Topographic data (elevation, slope, and aspect) were included in all scenarios.*

We extracted the feature importance from the final model based on the sum of decrease in Gini Impurity Index for each model fold. While there were 17 features in the final model, we present only the top 10 most important (**Figure 4**). The Modified Normalised Difference Water Index (MNDWI) from the autumn S2 composite was the top predictor across all folds. Elevation was the second most important feature followed by the Chlorophyll Index Red-edge (CIRE) and Band 3 (green) from the summer S2 composite and the VV polarization band from the summer S1 composite. Just outside of the top 5 features is the Specific Leaf Area Vegetation Index (SLAVI) from the summer S2 composite. The remaining features in the top 10 are the red bands for both summer and autumn S2, Band 5 (red edge) for the summer S2, and autumn CIRE. Of the 17 bands in the final model, the radar textural features were the least important in classifying aspen forests.

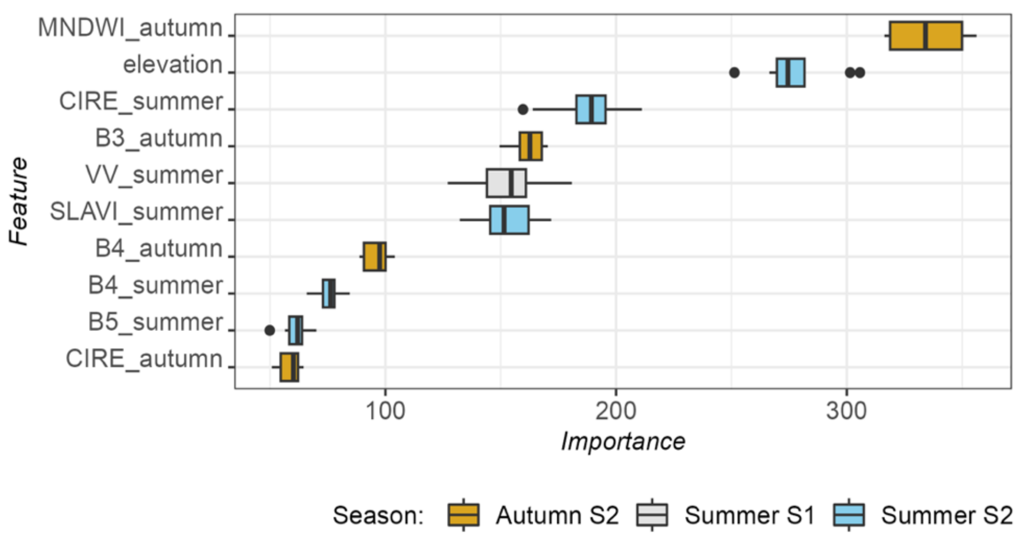

Figure 1.4 *Feature importance for the top 10 features across folds for the final model measured as the sum of decrease in Gini impurity index. Color shade indicates the seasonality.*

The resulting high-resolution (10 m) Sentinel-based map of quaking aspen forest cover represents the average probability across the 10 folds for the final model (**Figure 5A, 5C**). The optimum probability threshold for classification of 0.42 was used to classify the final map into aspen and non-aspen pixels based on the maximum F1-score achieved across the range of thresholds tested for each fold

(**Figure S2B**). A more detailed description of the threshold testing and model performance can be found in **Appendix S2**. Across the Southern Rockies, we estimate 9,482 km2 (7.4% of total land area) as quaking aspen forests. Within the White River NF, we mapped 1,658 km2 (16.3% of total land area).

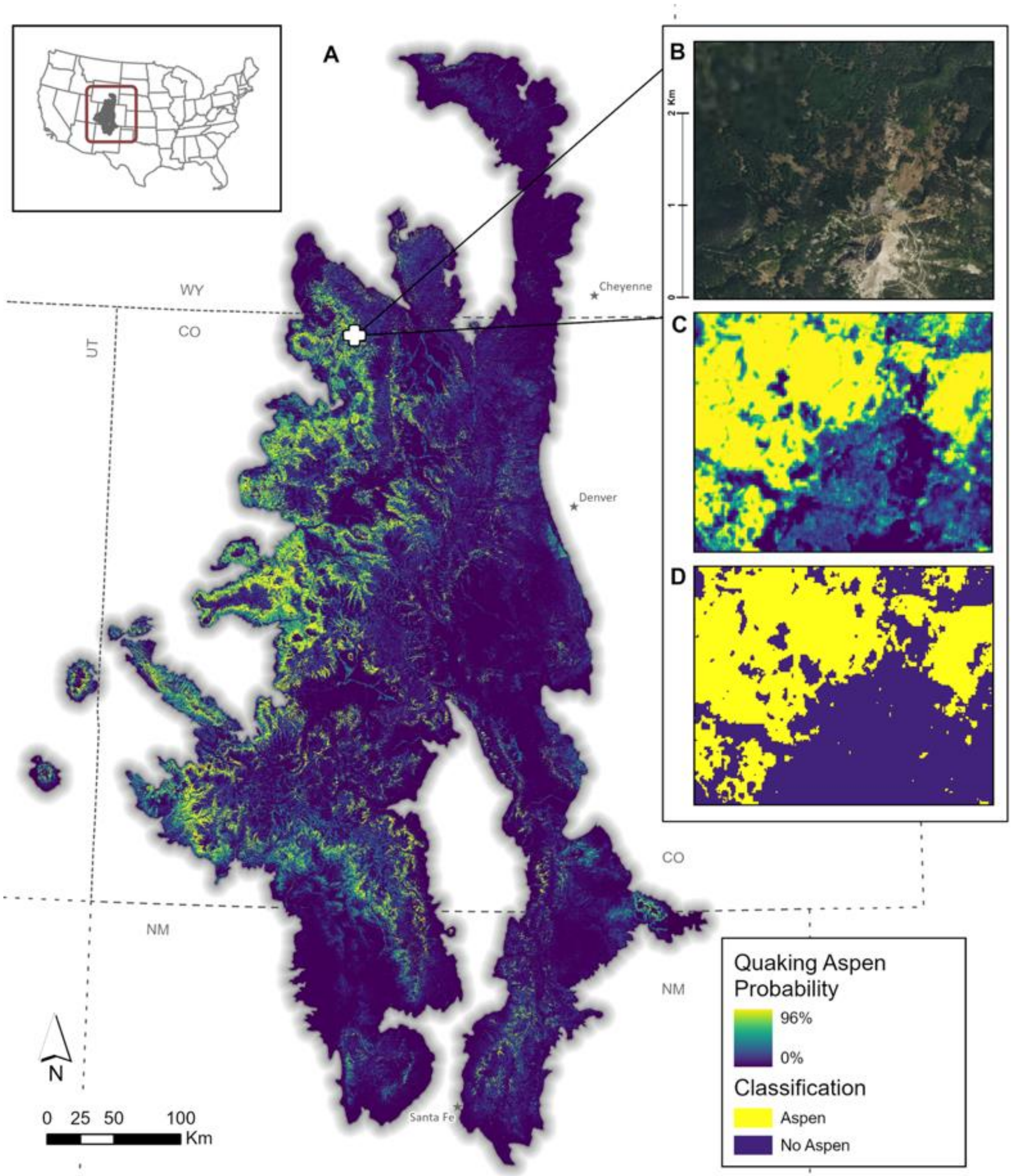

Figure 1.5 *Map of quaking aspen canopy cover with reference location (Hahns Peak, Steamboat Lake State Park, Routt County, CO). (A) Aspen canopy probability (0-100%); (B) NAIP image for the reference; (C) Aspen canopy cover probability (0-100%) for the reference location; (D) Aspen classification based on the optimum threshold of the probability (0.42).*

1.3.3. Agreement with Reference Datasets

We tested the agreement of the Sentinel-based map with three existing products using both the testing data from model training and a pixel-based approach across the entire study region and within the White River NF. Based on testing data (i.e., aspen presence points held out of model training), we see high overall agreement between all products with average F1-score ranging from 0.829-0.865 compared to the 0.931 for the Sentinel-based map (**Table 1.4**). However, a notable pattern emerges regarding precision and recall. The Sentinel-based map demonstrates higher precision (0.9516) relative to recall (0.9116). This suggests that while the map is correctly predicting aspen presence 95% of the time, it may be more restrictive, missing about 9% of true aspen presence. Conversely, all three reference products exhibit lower precision than recall. For example, the USFS TreeMap correctly predicts aspen presence just 80% of the time but identifies 93% of all true aspen presence. This indicates that while existing products are relatively accurate, they may be more likely to include non-aspen areas in their predictions based on the testing data

Table 1-4 *Precision, recall, and F1-score for aspen test data across the three reference datasets and for the Sentinel-based map.*

Data Source	**Precision**	**Recall**	**F1-score**
Sentinel-based map	0.9516	0.9116	0.9311
USFS TreeMap	0.8087	0.9302	0.8652
LANDFIRE EVT	0.8168	0.8995	0.8562
USFS ITSP	0.7959	0.8669	0.8299

In the pixel-based agreement assessment between the three existing products and the Sentinel-based map, we calculated the precision, recall, and F1-score across spatial blocks in the Southern Rockies and for the White River NF. There was significant spatial variability in all metrics across spatial blocks with some regions performing significantly better than others (**Figure 1.6**). Interestingly, we observe an opposite relationship between precision and recall when comparing the maps directly suggesting that the Sentinel-based map remains restrictive in classifying aspen presence compared to the existing products. Given the higher accuracy of the Sentinel-based map based on testing data (**Table 1.4**), this supports the finding that existing products likely over-predict areas of aspen presence. Additionally, the White River NF exhibits significantly higher precision, recall, and F1-score for all existing products than the median across spatial blocks (**Figure 1.6**). This region is characterized by extensive aspen forests, suggesting that the agreement may be higher in areas with more consistent aspen cover. Still, the higher precision than recall in the pixel-based assessment indicates that there is likely overestimation occurring for the three reference products. Along with assessment of the test data, the Sentinel-based map shows more accurate identification of actual aspen forests on the landscape.

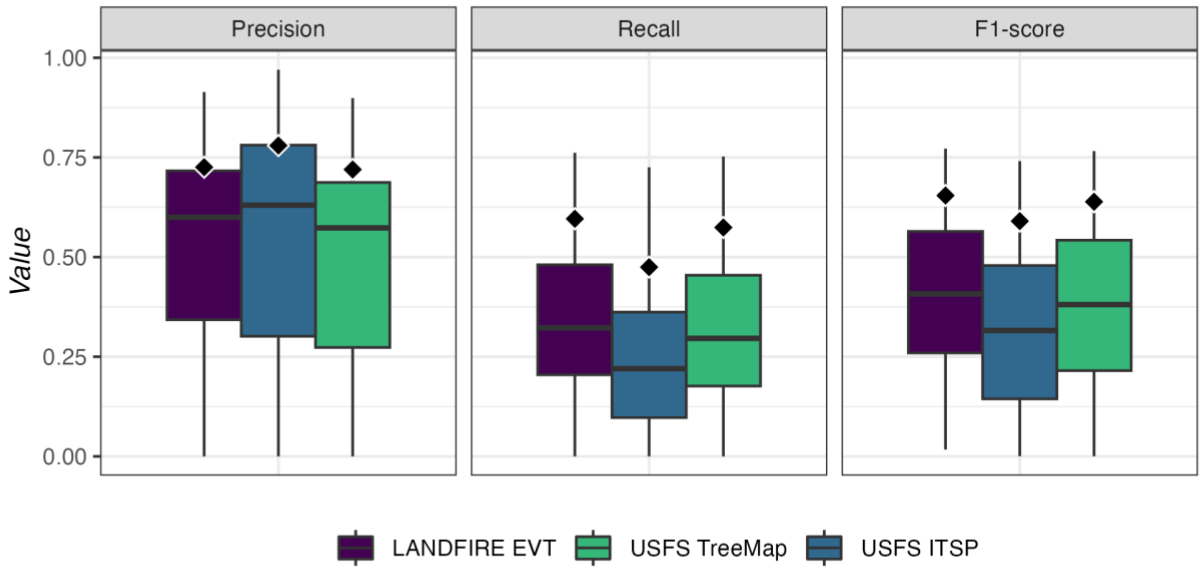

Figure 1.6 *Distribution of pixel-based precision, recall, and F1-score of existing products compared to the Sentinel-based map across spatial blocks within the Southern Rockies. Diamonds indicate the values for the targeted geography (White River NF).*

1.3.4. Landscape and Patch Dynamics

We assessed the landscape patch dynamics for the Sentinel-based map and the three existing products by spatial block across the Southern Rockies and for the White River NF. The Sentinel-based map estimates 43-118% less total aspen area across the Southern Rockies and 21-64% less in the White River NF compared to existing products (**Figure 1.7A**). The average patch size varies greatly across the Southern Rockies, highlighting the regional difference in stand characteristics. For the Sentinel-based map, the average patch size is 0.53 ha (+- 23) in the Southern Rockies and 0.74 ha (+- 22) in the White River NF, significantly smaller than existing products (**Table 1.5, Figure 1.7B**). Some regions are dominated by large stands of pure aspen (> 22 ha), whereas others are defined by many small, more dispersed stands (**Figure 1.7B and 1.7C**). Notably, the Sentinel-based map identifies 28-93% more individual patches across the Southern Rockies and White

River NF. Given the higher accuracy of the Sentinel-based map and the trend in over-prediction of aspen areas from existing products, these results suggest that the higher-resolution map is better able to characterize the actual landscape configuration of aspen forests.

Table 1-5 *Landscape patch dynamics summarized across spatial blocks for the Southern Rockies. We report the total area, number of patches, average patch density, average patch size, and average perimeter to area ratio.*

Data Source	Total Area (Km2)	Number of Patches	Patch Density	Average Patch Size (ha)	Average Perimeter/Area Ratio
Sentinel-based	9,384.41	1,760,386	35.73	0.53	2,745.57
LANDFIRE	13,441.59	728,370	14.22	1.85	1,060.98
USFS TreeMap	13,931.85	1,268,131	24.82	1.10	1,145.88
USFS ITSP	20,477.69	266,762	4.82	7.68	941.75

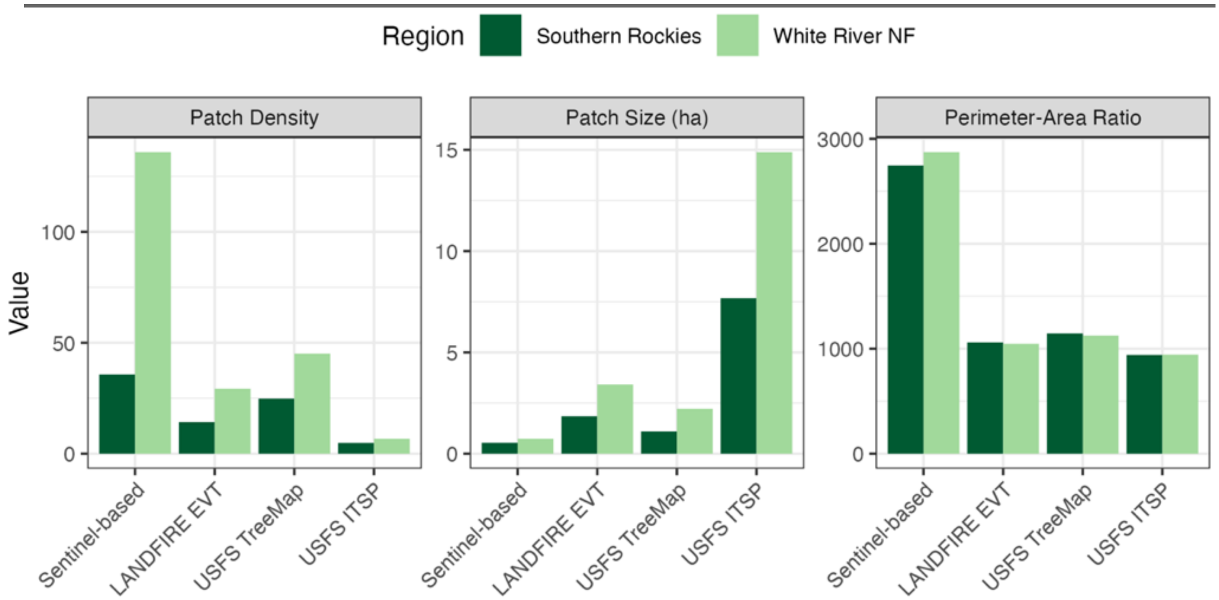

Figure 1.7 *Comparison of patch metrics for the Southern Rockies and the White River NF for the Sentinel-based map and the three existing products. The White River NF is dominated by large, often pure stands of quaking aspen which is highlighted in the much larger average patch density and patch size when compared to the Southern Rockies.*

1.4. Discussion

This overall effort provides a high-resolution quaking aspen forest cover map from 2019 for the Southern Rockies. We map 9,482 km2 (7.4% of total area) of aspen forest cover within the SRME and 1,658 km2 (16.3% of total area) within the White River NF region. Leveraging the GEE cloud-compute platform, we were able to map quaking aspen forests across a large geographic region. We used multi-temporal composite satellite imagery, presence and background learning data and a spatial block cross-validation approach to train a random forest classification model which achieved high accuracy (average F1-score of 0.93). We demonstrate that combining seasonal spectral composites (summer and autumn) significantly improves classification accuracy of quaking aspen forests, while the addition of S1 imagery only marginally improves accuracy. S2 spectral indices targeting canopy moisture and chlorophyl content were important in the classification of aspen forests. Furthermore, we assessed the agreement of this new high-resolution map with existing products, identifying spatial consistencies across the region while achieving a higher level of accuracy when compared to training data. The higher-resolution map facilitates improved understanding of landscape dynamics such as the average patch size, patch density, and overall area. These metrics provide key insights into the management of individual stands across diverse areas.

Like previous studies using Sentinel data to classify forest species, we achieve high classification accuracy (average F1-score of 0.93), especially when leveraging multiple seasonal image composites. Previous studies have shown the effectiveness of multi-temporal S2 imagery for vegetation mapping in heterogeneous environments (Dobrinić et al., 2021; Immitzer et al., 2019; H. Li et al., 2021; Macintyre et al., 2020; Persson et al., 2018). However, these studies often use single S2 tiles to retrieve cloud-free images across time for a given location. Large-area image classification is impacted by persistent cloud-cover and variations in the timing and availability of cloud-free images on a single day (Hermosilla et al., 2022). We show that multi-temporal gap-filling and compositing methods to generate cloud-free images is an effective method for overcoming these challenges. Additionally, existing data on land surface phenology is helpful in identifying ecologically relevant temporal windows to create seasonal imagery composites. This method can be applied to other species with unique phenological characteristics.

In western US mixed conifer forests, quaking aspen canopies contain higher levels of canopy moisture and chlorophyl content than other species. We showed that spectral indices from S2 seasonal composites which leverage the red-edge and SWIR bands to estimate canopy moisture and chlorophyl content are important features for classification. For example, two of the most important features in the final model were the Modified Normalized Water Index (MNDWI) and the Chlorophyl Red-edge Index (CIRE) for the summer image composite. Leveraging unique canopy characteristics to created targeted spectral indices improves discrimination of forest species, particularly deciduous species.

In comparison with three primary existing products, we achieve higher precision in the prediction of aspen presence. Existing maps are developed at a coarser spatial resolution (30-m) and tend to over-predict areas of aspen cover, as highlighted by the tradeoffs between precision and recall when comparing the products using known locations of aspen presence. For the Sentinel-based map, we achieve significantly higher precision than recall which contrasts with existing maps. This suggests that the new map is highly accurate in correctly identifying aspen pixels but may be more restrictive. Conversely, existing products typically do identify aspen forests accurately but tend to include many non-aspen areas in their classifications. However, these trends vary across the Southern Rockies as shown in the distribution of the pixel-based agreement metrics across spatial blocks. Areas with higher consistency between the Sentinel-based map and existing products based on the pixel-level confusion matrices seem to occur in regions with more consistent or homogenous aspen forest cover. Landscape heterogeneity, aspen stand dynamics (e.g., pure or mixed/seral), or various forest densities may influence the success of predictions using remotely sensed data. This underscores the importance of spatial assessments, as the results provide an opportunity to investigate areas with poor precision or recall for model tuning and classification improvements in the future. In these areas, development of more precise training and validation data may improve the overall ability of the model to distinguish aspen forests from other land cover types.

Furthermore, the landscape dynamics of aspen forests vary widely across the Southern Rockies, with some areas dominated by pure or stable stands and others characterized by mid-late successional seral stands. Using the Sentinel-based map, we demonstrate the effectiveness for higher-resolution data to provide detailed insights into the landscape configuration based on metrics like average patch size, patch density, and perimeter to area ratio. We show that these metrics vary across both the Southern Rockies and White River NF. Importantly, the Sentinel-based map can also detect smaller stands (<0.09 ha) and greater perimeter to area ratio, suggesting it is able to better characterize the landscape configuration of aspen forests. These insights are critical in developing management plans targeting different stages of successional development in aspen forests.

Together, this effort provides a crucial tool for land managers in determining where to prioritize active management of aspen forests. Quaking aspen is a shade-intolerant species capable of vegetation regeneration from root suckers, as such it readily occupies canopy openings (Long & Mock, 2012; W. D. Shepperd et al., 2015). These characteristics have been used to regenerate and even expand aspen patches using coppice silviculture techniques. The improved capability to map patch dynamics at fine spatial resolution and high accuracy is useful for forest managers who are planning silvicultural management activities which maximize the potential for expansion of aspen patches into new areas. These smaller patches can offer prolific root suckering when managed or following disturbances (Long and Mock 2012; Shepperd et al. 2015). Combined with other datasets including habitat suitability, wildfire or other disturbance risk, and others, these new maps have the potential to assist forest management at both temporal and spatial scales relevant to the ecology of the species.

While we achieve high classification accuracy in this new map, there are improvements that could be made. Addition of field-based measurements of aspen forests across the region would improve accuracy assessment and model refinement. Collecting data from existing field studies, citizen science databases (e.g., iNaturalist), or species occurrence databases (e.g., the Global Biodiversity Information Facility) may provide both additional accuracy assessment opportunities and model improvements while limiting the need for time-intensive photo interpretation efforts. Future efforts may include more state-of-the-art classification techniques such as neural networks and object-oriented classification, which would take advantage of the spatial characteristics of aspen stands. Moreover, the use of upcoming hyperspectral imaging campaigns, very high spatial resolution imagery, or other active remote sensing such as LiDAR will undoubtedly offer continued improvements. The methods presented in this research are fully open and reproducible, enabling others to contribute as the availability of remotely sensed products and cloud-compute resources continues to grow.

1.5. Conclusion

As human- and climate-related impacts to forested areas continue to grow, the development of new high-resolution and accurate maps of forest species is critical to effective management activities which improve resilience, reduce hazard for communities, and maintain important ecosystem service benefits. We demonstrate an effective method for large-area forest species classification and provide an improved map of quaking aspen forests for the Southern Rockies. Given the uncertainty around aspen growth dynamics in a changing climate, this product is an important source of information for forest managers and will benefit management of quaking aspen forests.

2 CHAPTER TWO

Quaking aspen's influence on fire intensity and severity is moderated by forest composition, structure, and fire weather in the Southern Rockies

2.1. Introduction

Forest composition, or the abundance, dominance and diversity of forest species, has an important influence on fire activity and post-fire ecosystem impacts (Hagmann et al., 2021). Alongside climate and topography, forest composition and species traits help govern fire regimes and fire effects at a variety of spatial and temporal scales (Johnstone et al., 2016). Tree species composition and structure (e.g., density, height, diameter), for example, help drive fire intensity, or how hot a fire burns, and fire severity, or the consumption of organic matter (Keeley, 2009). Fire intensity and severity influence suppression difficulty (Thompson et al., 2018), impacts to the built environment (Penman et al., 2014), and ecosystem responses such as post-fire tree recruitment (Chapman et al., 2020; Meigs & Krawchuk, 2018). Given recent extreme fire activity and changes to the composition, structure and fire regimes of western North American forests (Hagmann et al., 2021; Hessburg et al., 2021), there is an urgent need to understand the influence of forest species composition and structure on contemporary fire intensity and severity.

The modification of forest composition and structure is a viable management tool often leveraged to reduce wildfire hazard to communities and ecosystems (Prichard et al., 2021). These management actions often involve reduction of fuels through mechanical treatment or prescribed fire, thereby reducing the potential for extreme fire activity (Agee & Skinner, 2005; S. L. Stephens et al., 2009). However, this presents a persistent management problem where treatments must be revisited to maintain positive benefits. Furthermore, while far more prescribed fire is ultimately needed to restore increasingly fire-starved ecosystems in the western U.S. (Parks et al., 2025), its use is limited by policy restrictions, public support, and a shortening window of appropriate weather conditions for burning (Schultz et al., 2019; Swain et al., 2023). The promotion of "fire-resistant" species, which may provide natural buffers to extreme fire behavior that are more self-sustaining, presents a complimentary management tool to reduce extreme fire behavior (Girardin & Terrier, 2015). With increasing fire activity and hazards, particularly across the western U.S. (Parks & Abatzoglou, 2020), assessments of which species may provide these benefits and under what conditions they are likely to do so are needed.

In some regions of western North America, quaking aspen (Populus tremuloides Michx.) is one forest species potentially capable of reducing extreme fire hazard (G. Fechner & Barrows, 1976). Aspen, which is also the most widely distributed tree species in North America and often considered a keystone species (Rogers et al., 2020), has been characterized by fire-moderating traits such as lower canopy bulk density, higher canopy base height, and greater leaf moisture content (DeByle & Winokur, 1985; W. Shepperd, 1990; Shinneman et al., 2013). Existing in a functional gradient of seral (e.g., having a conifer component) to stable (e.g., pure stands), aspen exhibits varying fire regimes and degrees of fire resistance (Rogers et al., 2014; Shinneman et al., 2013). Generally, seral aspen exhibits more extreme fire behavior compared to stable aspen and, in turn, fire activity drives the persistence of either functional type (Morris et al., 2019; Shinneman et al., 2013). Evidence points to fire weather and stand condition influencing the fire behavior in aspen, where even pure stands are likely to burn when the conditions align (DeRose & Leffler, 2014). However, with these potentially fire-moderating traits, aspen may offer a natural buffer, a so-called living fire break, to extreme fire intensity and severity. Despite this recognition, there remains a knowledge gap between management and scientific understanding of how, when, and where aspen moderates fire, especially relative to other forest types and during recent extreme fire activity at regional-to-continental scales (Nesbit et al., 2023).

Widespread availability of satellite remote sensing data before, during, and after wildfires presents a unique opportunity to quantify the influence of aspen on wildfire activity across large spatial scales. Burn severity mapping, which is based on differences between pre- and post-fire multispectral imagery, is one of the most commonly applied uses of satellite remote sensing in fire ecology (Szpakowski & Jensen, 2019). Satellite-based metrics of burn severity, such as the composite burn index (CBI), have been shown to correlate well with field-based measurements, enabling large-scale assessments of ecosystem impacts and their drivers (Parks et al., 2019). In tandem, active fire detection, which relies on middle-infrared (~ 4 μm) imagery, has become a crucial tool for monitoring global fire activity (Wooster et al., 2021). Spectral radiance in the middle-infrared is used to calculate fire radiative power (FRP), which is a measure of the energy released by actively burning fires and is highly correlated with the rate of biomass consumption per unit time (Kaufman et al., 1998; Schroeder et al., 2010; Wooster et al., 2003). Studies have applied FRP to, for example, track wildfire smoke emissions (F. Li et al., 2019, 2020) and investigate the relationship between energy released and fire size (Laurent et al., 2019). However, as a proxy for fire intensity, FRP has been underutilized to assess the influence of forest composition and structure, fire weather, and landscape factors on fire activity. The harmonization of satellite-derived burn severity metrics such as CBI and fire intensity proxies like FRP alongside forest inventories is a promising approach to exploring these relationships.

To investigate the influence of aspen and other forest types on fire intensity and severity during recent (2017-2023) wildfires, we harmonized satellite-based FRP and CBI with imputed wall-to-wall forest inventory data derived from the United States Forest Service (USFS) Forest Inventory and Analysis (FIA) program. Using Bayesian spatial hierarchical modeling, we investigate three primary questions: (i) how do dominant forest types influence FRP and CBI relative to aspen; (ii) how does forest composition and structure, such as forest canopy cover, live basal area, tree height and diameter, influence FRP and CBI; and (iii) where aspen co-occurs with other forest types, how does its dominance, measured as the proportion of live basal area, influence FRP and CBI both with and without mediating effects of fire weather. To account for landscape and climatic effects on fire activity, we include variables describing the topography and fire weather. Given the spatial-temporal dependence of wildfires, we also include random effects for day-of-burn and a structured spatial model, uncovering the landscape patterns of FRP and CBI. The results of this study have important implications for management of aspen and other common forest types in the context of fire intensity and burn severity in the Southern Rockies. We also highlight a novel application of satellite-derived FRP as a proxy for fire intensity to investigate the biotic and abiotic controls and spatial patterns of fire heat. These methods can be applied across large geographic regions to answer a variety of important questions related to forest and fire management.

2.2. Materials and Methods

2.2.1. Study System and Wildfire Census

The Southern Rockies includes portions of southern Wyoming, central and western Colorado, and northern New Mexico (**Figure 2.1**). Aspen is the dominant deciduous forest type (**Figure 2.2**), encompassing an estimated 9,482 km^2, 7.4% of total land area (Cook et al., 2024). In this region, aspen co-occurs with all major forest types including ponderosa mixed-conifer, lodgepole, and spruce-fir, and across a wide range of elevation and site conditions (Bartos, 2001). We collected a census of recent (2017-2023) wildfire events from the ICS-209-PLUS (St. Denis et al., 2023; updated through 2023). Since 2017, 113 wildfires burned approximately 1.68M acres including five large events (>100k acres): Calf Canyon / Hermit's Peak (New Mexico, 2022), East Troublesome (Colorado, 2020), Cameron Peak (Colorado, 2020), Mullen (Colorado/Wyoming, 2020) and Spring Creek (Colorado, 2018). Where possible, we obtained fire perimeters from the Monitoring Trends in Burn Severity (MTBS; Eidenshink et al., 2007) using the link to MTBS in the ICS-209-PLUS database. For fire events without an MTBS identifier, we gathered perimeter data from FIRED (Balch et al., 2020). These fire perimeters were used to locate the associated active fire detections (*Section 2.3*).

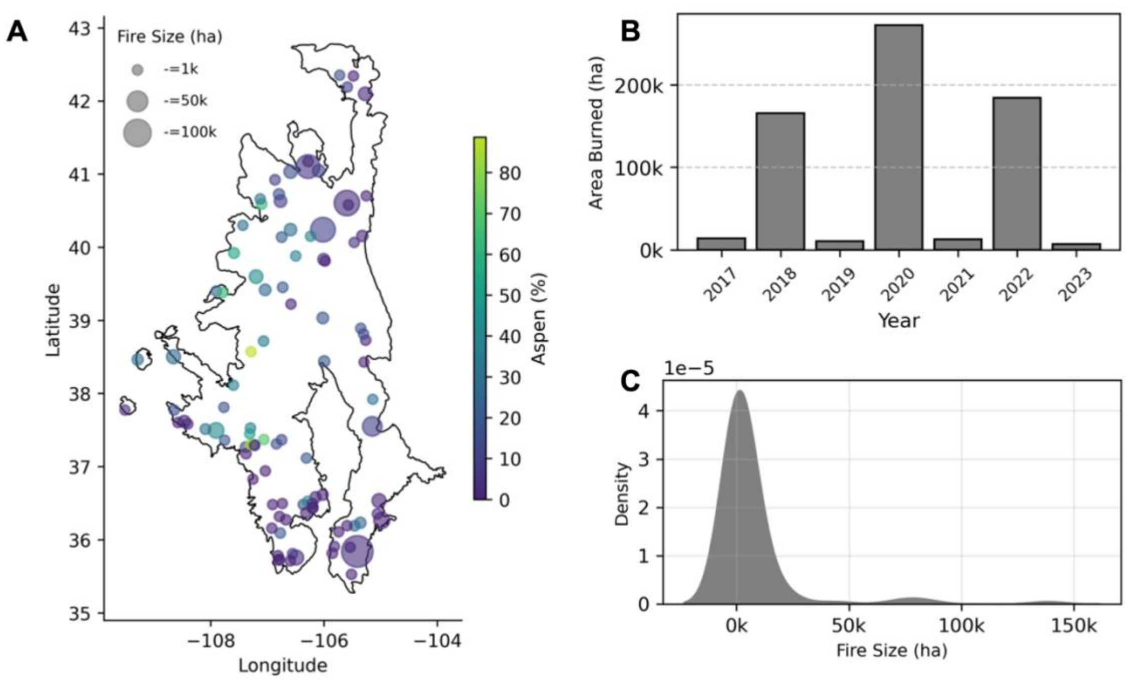

Figure 2.1 *Study region and wildfire census data (2017-2023). (**A**) Map of the Southern Rockies and fire census. Size of points represents burned area; color represents the proportion of forested area that is aspen; (**B**) Annual area burned; (**C**) Fire size distribution.*

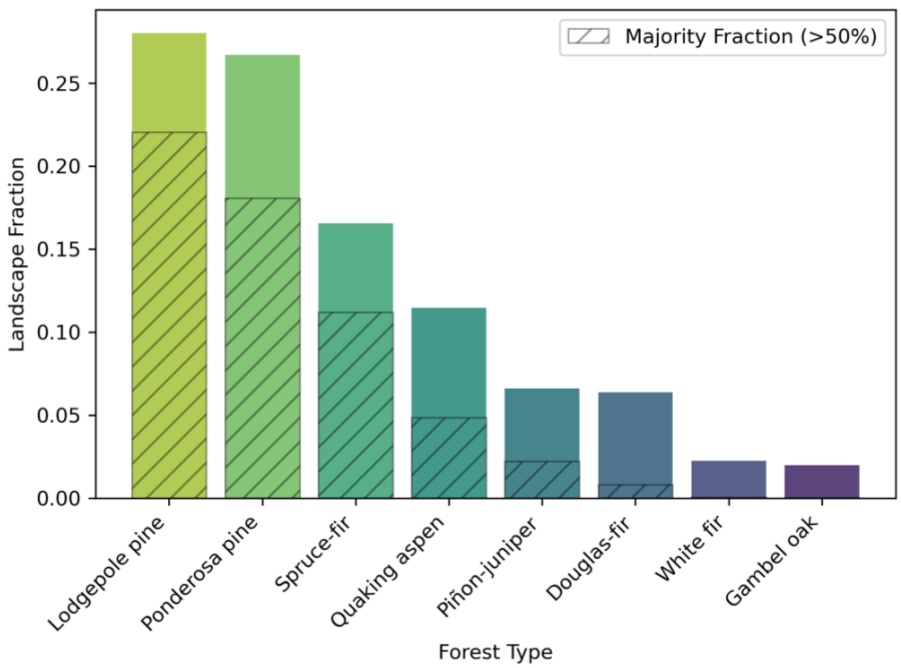

Figure 2.2 *Distribution of major forest types within burned areas in the fire census. Hatching indicates the proportion of area where that forest type was the gridcell majority (>50% of forested proportion).*

2.2.2. Active fire detections and fire radiative power (FRP)

Active fire detections from the Visible Infrared Imaging Radiometer Suite (VIIRS) Collection 2 Active Fire product (Schroeder et al., 2014) were collected across the study region. These data were produced in 6-minute temporal satellite increments (swaths) at 375 m spatial resolution at-nadir from VIIRS sensors aboard the NASA/NOAA Suomi National Polar-orbiting Partnership (S-NPP; VNP14IMG) and Joint Polar Satellite System (JPSS-1 or NOAA-20; VJ114IMG) satellites. Acquisitions from these satellites occur twice daily around 1:30AM and 1:30PM at mid latitudes. We remotely queried the cloud-hosted active fire swaths using the *earthaccess* Python library (A. Barrett et al., 2024) for all burn dates in the fire census. From the swaths, we extracted the spatial coordinates of active fire pixels and their attributes including the swath sample position, detection confidence, acquisition datetime, and fire radiative power (FRP). Only detections meeting the "nominal" or "high" confidence were retained. We used the swath sample position to assign along-scan and along-track pixel dimensions to account for changes in pixel area as the sample gets further from nadir (F. Li et al., 2018; Schroeder et al., 2014). For each detection, coordinates were spatially buffered by the per-sample dimensions to generate the "true" ground area for each pixel (**Figure B2**). We identified duplicate detections resulting from adjacent scans by flagging those which were acquired at the same datetime and had >30% spatial overlap. In cases where duplicates were identified, we retained the detection with the higher FRP value.

To aggregate FRP retrievals into a consistent unit of analysis, we created a regular grid of 375 m cells (the approximate resolution of the VNP/VJ114IMG fire products at nadir) across the entire Southern Rockies and assigned FRP based on fractional overlap of true pixel areas (**Figure 2.3**). This involved first converting FRP to watts/km^2 for a consistent area-based measurement. Then, FRP was assigned to gridcells based on the fractional overlap (*FRP * gridcell overlap %*). Only gridcells which had greater than 50% spatial overlap with detections were retained for analyses, limiting the contribution of gridcells with low fractional FRP. The total number of acquisitions, day/night counts, datetime of acquisition, and FRP summary statistics (cumulative, maximum and percentiles) were assigned to the grid cells. For analysis, this study focused on the *cumulative* FRP to capture the total fire intensity throughout the fire event and to avoid the often-extreme diurnal fluctuations in FRP. Finally, detections were assigned a fire ID based on spatial overlay with the fire census and where acquisition datetimes aligned with the ignition and cessation dates.

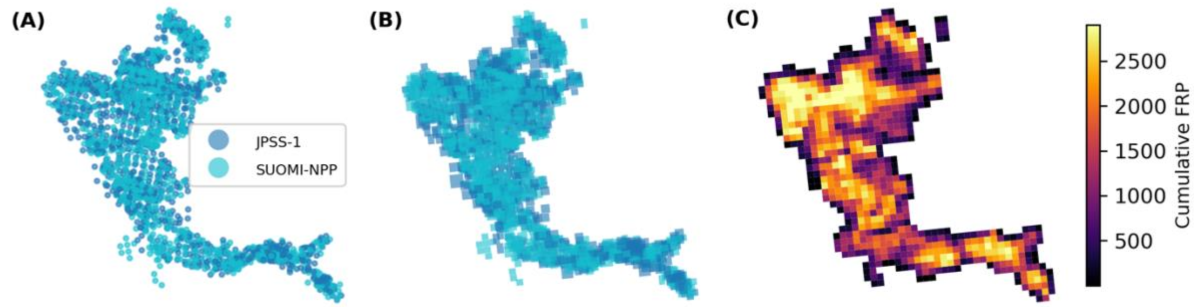

Figure 2.3 *Aggregation of VIIRS active fire detections (AFD) onto a regular grid for the Williams Fork Fire (2020). (**A**) Pixel centers of AFD from both satellites (S-NPP and JPSS-1); (**B**) Pixel ground area based on swath position (relative nadir position); (**C**) Maximum FRP based on fractional overlap aggregation.*

2.2.3. Composite Burn Index (CBI)

We created burn severity rasters for each wildfire in the census using pre- and post-fire Landsat 8 imagery following methods from Parks et al. (2019) in the Google Earth Engine cloud-compute platform (Gorelick et al., 2017). While this method produces a variety of burn severity metrics based on spectral indices, we retained only the bias-corrected CBI (CBIbc) for analysis as this metric adjusts values at the extreme low/high ends of the range, better quantifying the variability in burn severity (Parks et al., 2019). We calculated zonal statistics of CBIbc within our 375m gridcells to align the spatial scale with FRP aggregations. Specifically, the average, standard deviation, and percentiles were calculated for each gridcell. For analysis, we use the 90th percentile of CBIbc which emphasizes higher burn severity while still accounting for some within-cell variability.

2.2.4. Forest Composition and Structure

To assess the influence of forest composition and structure on FRPc and CBIbc, we gathered information from the ca. 2016 USFS TreeMap (Riley et al., 2022). TreeMap imputes Forest Inventory and Analysis (FIA) plot identifiers onto 30 m2 LANDFIRE (Picotte et al., 2019) pixels based on a set of LANDFIRE biophysical characteristics including topography, vegetation type, and disturbance (Riley et al., 2021, 2022). The FIA is a nationally consistent forest inventory monitoring program consisting of thousands of systematically located and revisited 675 m2 plots at a density of one plot per 24.3 km2 (Gray et al., 2012; Riley et al., 2021). While representing a sparse network of field plots, the TreeMap demonstrates good agreement with existing vegetation, enabling estimation of wall-to-wall forest characteristics (Riley et al., 2021, 2022). We use the TreeMap to, (i) identify gridcell majority forest cover type, and (ii) estimate forest composition and structure metrics from the Tree Table, which links TreeMap pixels to their imputed FIA tree-level data. Each gridcell is composed of approximately 182 TreeMap pixels (30 m2 spatial resolution). We focused efforts on commonly occurring forest types in the Southern Rockies including lodgepole pine, ponderosa pine, spruce-fir (Engelmann spruce and subalpine fir), Douglas-fir, white fir, pinon-juniper, Gambel oak, and quaking aspen (Appendix 2).

For (i), we used the algorithmic forest type (FORTYPCD), which closely aligns with LANDFIRE existing vegetation type, to calculate the proportion of gridcell forested area for each forest type present. The majority forest type simply represents the type with the maximum proportional area in the gridcell. For (ii), following methods from Riley et al. (2021), we linked TreeMap pixels to their imputed tree-level information (the TreeMap Tree Table) using the TM_ID attribute. We calculated the live basal area of each measured tree using its diameter (DIA in the Tree Table), which was then multiplied by the number of trees per acre it represents (TPA_UNADJ in the Tree Table) and summed for each species in the plot. We converted this to live basal area per pixel using a conversion factor (0.222395 acres/pixel). The total live and dead trees per pixel (TPP), hereafter referred to as tree abundance, was also calculated using this conversion factor. These metrics were then multiplied by the total number of pixels for each FIA plot identifier in the gridcell to estimate the total live and dead basal area, total live and dead tree abundance, average tree height and average diameter for each species. We derived common forest stand structure metrics at the gridcell level including the stand density index (SDI), average stand diameter (measured as the diameter of a tree with the average basal area), and the average height to diameter ratio (HDR). These metrics represent important forest structure characteristics and minimize statistical correlations between the raw values of live basal and area and tree abundance, for example (Figure SX).

In addition, we used the ca. 2016 remap LANDFIRE (Picotte et al., 2019) to calculate gridcell average forest canopy cover (%), as this metric has the lowest agreement between TreeMap and FIA tree-level measurements (Riley et al., 2022). Given the importance of forest canopy structure in the context of FRP retrievals and potential interception of radiative energy (Roberts et al., 2018), we calculated the canopy percent from LANDFIRE, which derives these measurements more directly from satellite data rather than from imputed forest inventories.

2.2.5. Climate and Topography

Elevation data were sourced from a 1/3 arc-second (~10 m) digital elevation model, which was used to calculate elevation, slope, and aspect. Aspect was converted to northness by taking the cosine of aspect in radians, where values closer to one indicate north-facing slopes. Gridcell average Topographic Position Index (TPI), derived at a 270 m resolution (Theobald et al., 2015), was also calculated to represent the landscape position (e.g., valley bottom, ridgetop). To characterize fire weather, we gathered vapor pressure deficit (VPD), energy release component (ERC), and wind speed from gridMET, a daily 4 x 4 km gridded meteorological product (Abatzoglou, 2013). Both VPD and ERC represent atmospheric and fuel aridity and correlate well with fire activity (Abatzoglou & Williams, 2016). For ERC, we calculated the deviation from the 15-year average (ERCdv) to represent the more extreme fuel dryness in the western U.S. during recent history (Parks & Abatzoglou, 2020). Gridcells were spatially aggregated by the first VIIRS detection day and the average VPD, ERCdv, and wind speed was calculated.

2.2.6. Statistical analysis

To assess the influence of forest composition and structure on FRPc and CBIbc, we fit Bayesian hierarchical spatial models using the Integrated Nested Laplace Approximation (INLA) framework, implemented in *R-INLA* (R Core Team, 2024;

Rue et al., 2009). Unlike traditional Markov Chain Monte Carlo (MCMC) methods, INLA leverages deterministic (Laplace) approximations, providing a computationally efficient alternative for Bayesian inference that has been widely applied in recent years (e.g., Gomez-Rubio, 2020; Niekerk et al., 2019). These models are particularly well-suited for dynamic ecological systems, offering precise inference on spatial processes and rapid computation of posterior distributions (Beguin et al., 2012; Engel et al., 2022; Niekerk et al., 2019; Sadykova et al., 2017). *R-INLA* allows fitting complex hierarchical models to account for structured and unstructured random effects such as fire-level variability, temporal day-of-burn effects, and spatial dependence. We fit separate models for FRPc and 90th percentile CBIbc to address three primary aims: 1) establish the differences between dominant forest types on fire heat and burn severity *relative to aspen*, 2) assess how forest composition and structure effect FRPc and CBIbc, and 3) quantify how these relationships are mediated by VPD.

We fit separate models for FRPc and CBIbc in *R-INLA* to address aims (1) and (2) and establish the difference between major forest types *relative to aspen* and the influence of forest structural metrics including percent cover of the majority forest type, SDI, HDF, and average live basal area for all species present in each gridcell. A categorical variable for the gridcell majority forest type (i.e., percent of forested area) was included using aspen as the baseline level, allowing us to compare the differences between forest types relative to aspen. We included interactions between species and their structural metrics as well as fixed effects for gridcell topography and day-of-burn fire weather. Only species which contributed to at least 10% of the total live basal area in a gridcell were retained to address potential noise in the forest inventory data. For aim (3), to test the influence of aspen co-occurrence and dominance, we identified fires which had any pre-fire aspen cover (N=65). Aspen dominance was measured as the proportion of total live basal area. An interaction term between the gridcell majority forest type and aspen dominance was used to test the effect of aspen co-occurrence across major forest types, including gridcells where aspen was the majority type. To assess the influence of fire weather mediation, an interaction term was set with VPD (i.e., majority *forest type* * *aspen dominance* * *VPD*).

2.2.7. Model parameters and assessment

Models were parameterized using the gaussian family for log-transformed FRPc and gamma for 90th percentile CBIbc based on their observed distributions. Penalized complexity priors were used for fixed and random effects to allow for flexibility in model variance. We used weakly informative priors to allow the data to speak and because the choice of priors did not significantly influence model estimates (which suggests that there is good evidence for model effects in the data). Baseline models without random and spatial effects were compared to increasingly complex model structures using fit statistics, specifically Watanabe-Akaike information criterion (WAIC) and conditional predictive ordinates (CPO), two measures of model robustness and predictive power, respectively, commonly used to compare model outputs in *R-INLA* (Gomez-Rubio, 2020). For FRPc models only, additional covariates were included to represent the cumulative detection overlap percentage and the proportion of daytime detections within each grid to account for the aggregation method (*Section 2.3*). This is crucial, as some gridcells have a larger proportion of nighttime detections and thus lower FRPc. For all models, we also included a covariate for the mean gridcell forest canopy percent, as previous studies have shown a correlation between FRP and fire size (Laurent et al., 2019). Other fixed effects included a gridcell distance to fire edge, the gridcell forest canopy percent, diversity of species contributing to the total live basal area (H-BA), total live and dead tree abundance (TPP), topography, and fire weather. Prior to fitting models, we tested correlations between predictor variables using a Spearman correlation coefficient (**Figure B5**).

2.2.8. Spatial mesh grid

Wildfires are inherently spatially dependent processes, requiring careful assessment of model covariates. To account for these spatial processes, we implemented the Stochastic Partial Differential Equation (SPDE) approach, which is a key innovation within the INLA framework for modeling spatial processes (Lindgren et al., 2011). The SPDE efficiently approximates continuous spatial Gaussian random fields (GRFs) using sparse precision matrices, linking GRFs to Gaussian Markov Random Fields (GMRFs) through a triangulated mesh representation (Bakka et al., 2018). We developed a spatial mesh for the Southern Rockies designed to reflect the expected within-fire spatial processes and minimize the influence of between-fire dependence (**Figure 2.4**). The mesh parameters, including maximum edge, cutoff, offset, and priors were chosen to balance computational efficiency with observed spatial process based on fire-specific semivariograms fit using the gstat R package (Gräler et al., 2016). More detailed information about the mesh creation and SPDE model definitions can be found in the supplement and in Figure 3 in Section 3.1.

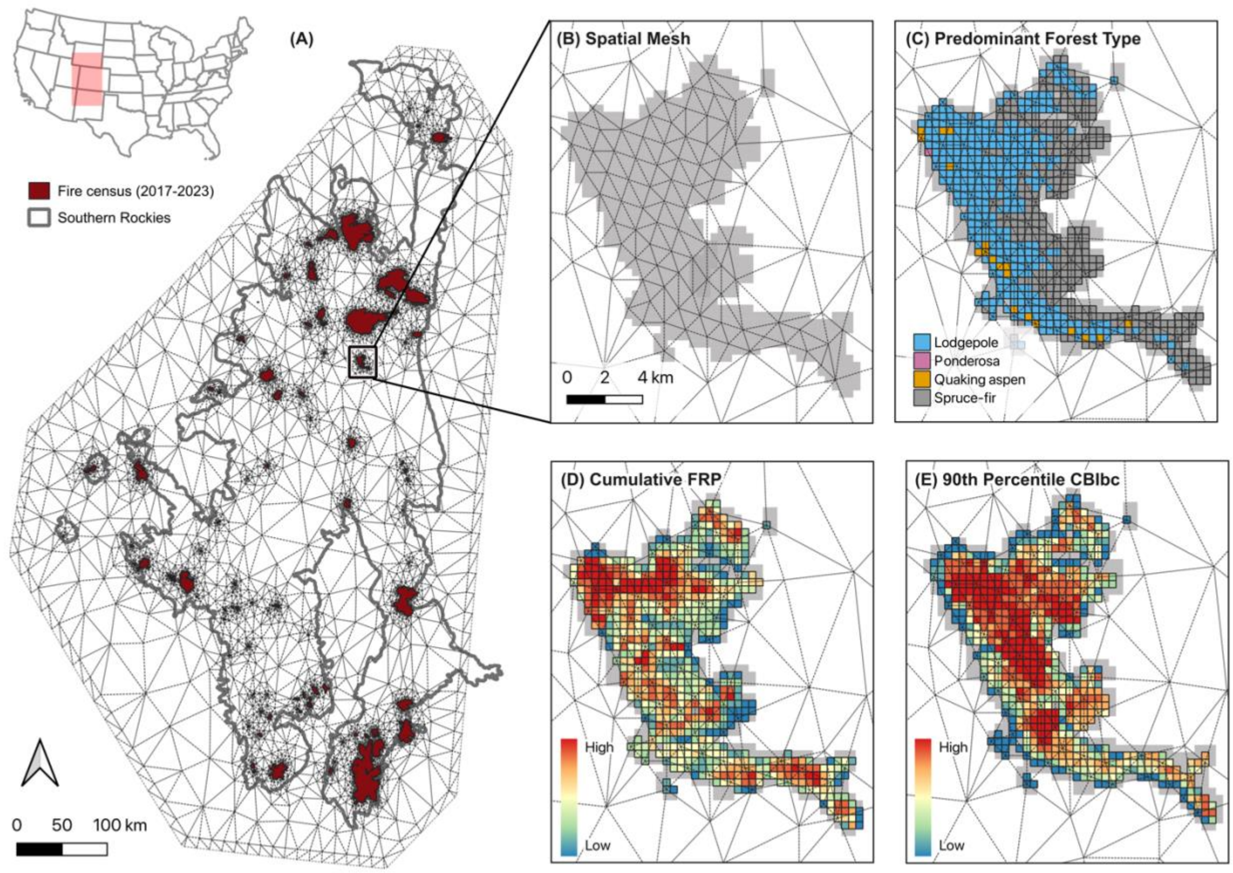

Figure 2.4 *Southern Rockies study region with spatial mesh grid and inset for the Williams Fork Fire, CO (2020). (**A**) Full spatial mesh with all fire census in red. The mesh is designed to capture within-fire variability while relaxing the intra-fire spatial dependence as seen by the wider triangular mesh between fire events. (**B**) Spatial mesh for the Williams Fork Fire, CO (2020) showing the within-fire spatial dependence with smaller triangles. (**C**) Predominant forest type aggregated to gridcells, defined by the pixel count majority from TreeMap FORTYPCD. (**D**) Aggregated cumulative FRP (W/km^2). Where gridcells remain gray, there were no daytime observations. (**E**) 90th percentile CBIbc.*

2.3. Results

2.3.1. Differences between dominant forest types relative to aspen

In the Southern Rockies, dominant forest types influenced FRPc and CBIbc *relative to aspen*, demonstrated by the posterior distribution of effects (**Figure 2.5**). For FRPc, lodgepole pine showed the strongest positive baseline effect, with +20.9% higher FRPc than aspen (95% CI: 18.3%, 23.6%). Douglas-fir, white fir, ponderosa pine, and spruce-fir forest types also showed significant positive effects relative to aspen, although the credible intervals for white fir were wider, suggesting more uncertainty in the model estimates. Gambel oak and pinon-juniper had negative effects on FRPc relative to aspen, although the credible intervals were more extreme and passed zero for Gambel oak, indicating insignificance in model estimates. For all forest types except Gambel oak, the effect on CBIbc was significant and positive, showing that burn severity is typically higher in other forest types relative to aspen. Again, the credible intervals were wide for Gambel oak suggesting uncertainty in the model estimates or a wide range of effects relative to aspen. Douglas-fir and white fir showed the greatest positive effect on CBIbc, with a +23.3% (95% CI: 19.6%, 27.1%) and +22.3% (95% CI: 13.9%, 31.2%) increase relative to aspen, respectively. For both models, inclusion of fire-level random effects alongside a spatial model significantly improved fit statistics demonstrated by the improved WAIC and CPO (**Table 2-1**).

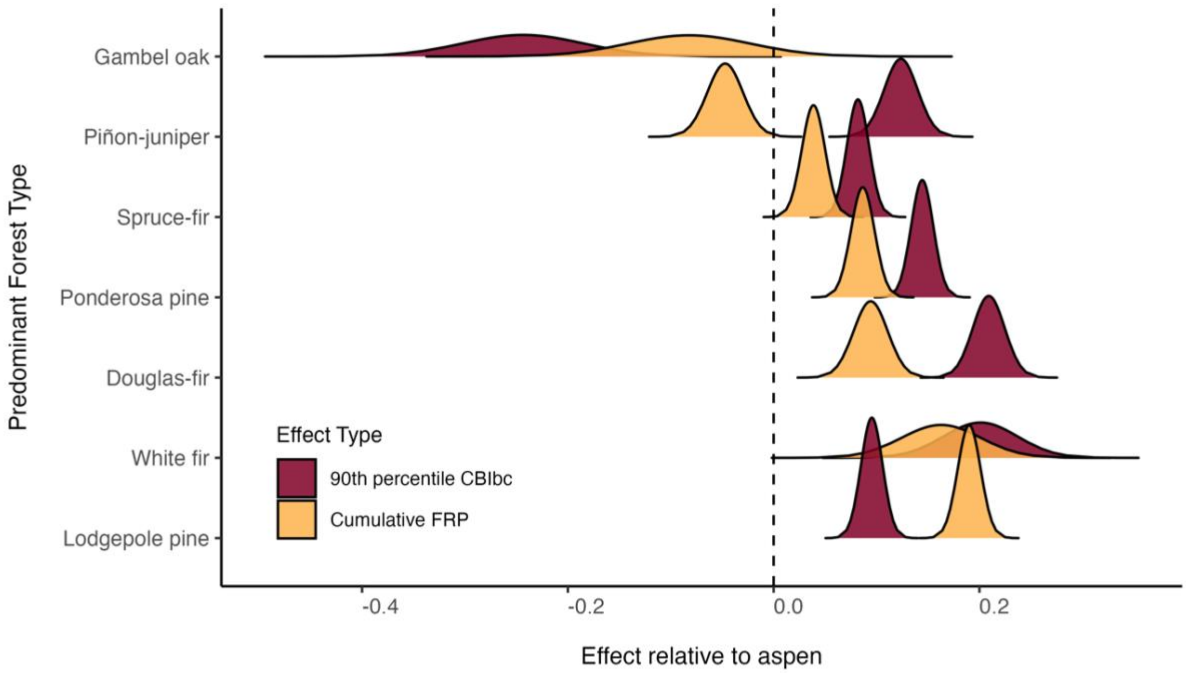

Figure 2.5 *Posterior distributions of effects of predominant forest types on FRPc and CBIbc relative to aspen as the baseline. Lodgepole, Douglas-fir, white fir, ponderosa pine, and spruce-fir forest types had significant positive effects on both FRPc and CBIbc. Gambel oak and pinon-juniper forests showed a lower FRPc though credible intervals pass zero for Gambel oak and credible intervals are wide. Pinon-juniper relative to aspen but a higher CBIbc. Except for Gambel oak, all forest types showed significant positive effects on CBIbc relative to aspen.*

Table 2-1 *Model fit statistics and effective number of parameters. Spatial models with random effects for fire event and day-of-burn were far more complex (greater number of effective parameters) and performed significantly better based on WAIC and CPO.*

Response	Model	WAIC	Mean CPO	Effective # of Parameters
FRP	**W/Fire + Temporal + Spatial Effect**	**261898.96**	**0.34**	**4700.02**
FRP	W/Fire + Temporal Effect	282012.54	0.31	506.49
FRP	W/Fire Random Effect	288571.70	0.30	145.79
FRP	Baseline	295284.82	0.29	53.99
CBI	**W/Fire + Temporal + Spatial Effect**	**264356.09**	**0.36**	**4159.85**
CBI	W/Fire + Temporal Effect	273861.08	0.34	501.89
CBI	W/Fire Random Effect	278836.15	0.33	495.64
CBI	Baseline	293617.54	0.30	51.99

2.3.2. Effect of composition and structure

Forest composition and structure influenced FRPc and CBIbc, with aspen clearly demonstrating a moderating effect based on posterior distributions (**Figure**

2.6). We characterized composition and structure using the gridcell proportion of the majority forest type (percent cover), species-level SDI, HDR, and average live basal area. Aspen percent cover had a significant negative effect on both FRPc (**Figure 2.6A**) and CBIbc (**Figure 2.6B**). For every standard deviation increase in aspen percent cover, there was a -8.1% (95% CI: -9.4%, -6.6%) reduction in FRPc and -13.1% (95% CI: -14.4%, -11.8%) reduction in CBIbc (**Table B1, B2**). This effect was prominent for aspen compared to other forest types, although percent cover of ponderosa, Douglas-fir, and lodgepole pine had significant positive effects on FRPc. Increasing percent cover of ponderosa and pinon-juniper also had significant positive effects on CBIbc. The influence of species-level SDI, HDR, and average live basal area were less pronounced for aspen, however, significant effects did emerge. For every unit increase in aspen SDI, FRPc reduced by an average of -1.6% (95% CI: -3.0%, -0.01%). Increasing aspen HDR also had a significant negative effect on both FRPc and CBIbc though no discernable effect of average stand diameter was found. In spruce-fir forests, the average stand diameter and HDR had significant negative effects on FRPc but had insignificant effects on CBIbc. Ponderosa forests showed a strong positive effect of HDR on both FRPc and CBIbc.

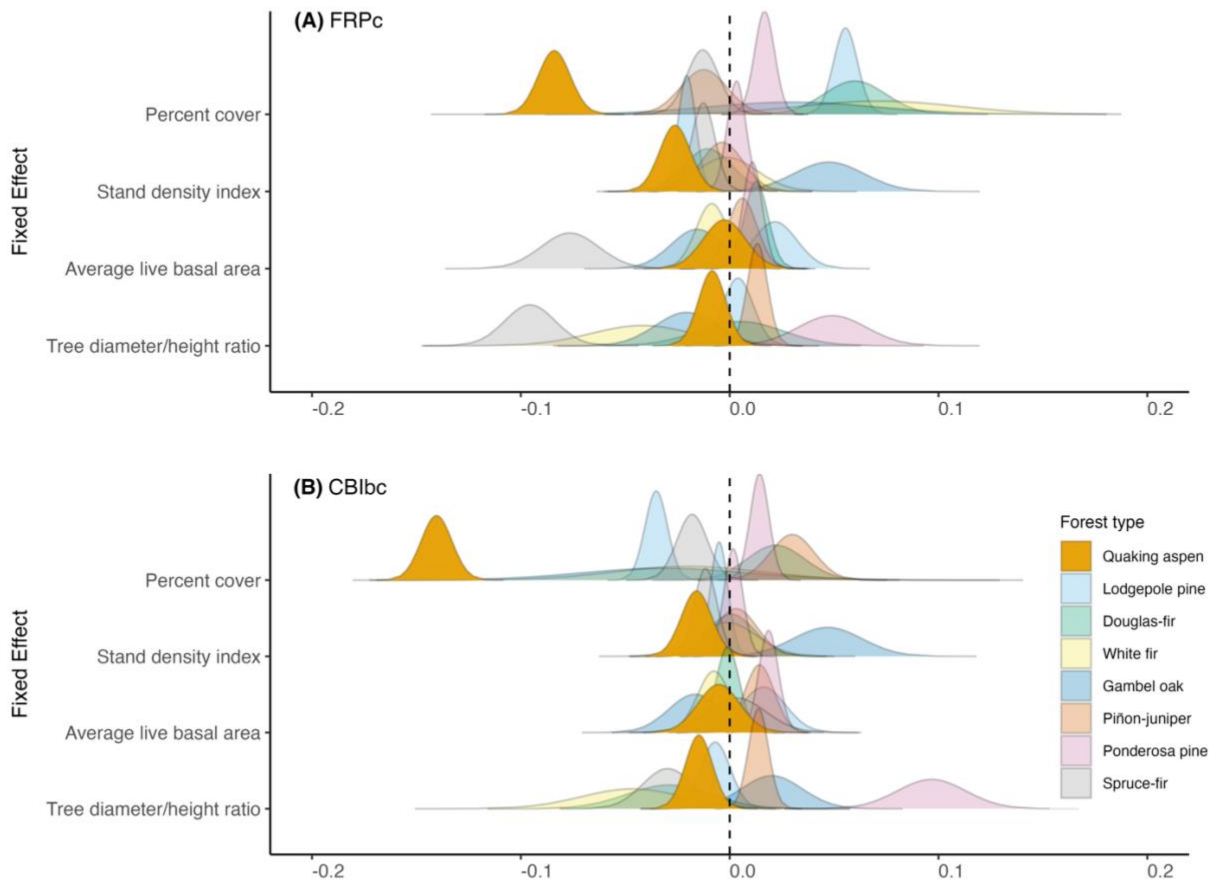

Figure 2.6 *Posterior distribution of effects for forest type-specific composition and structure metrics on (**A**) FRPc, and (**B**) CBIbc. We assessed the percent cover of the gridcell majority forest type, forest-specific stand density index (SDI), average live basal area, and height-diameter ratio (HDR). Posterior distributions which overlap zero are uncertain/insignificant.*

2.3.3. Topography and fire weather

Topography and fire weather influenced FRPc and CBIbc alongside forest composition and structure, with some key differences (**Table B1, B2**; **Figure B7**). Elevation, for example, had a significant negative effect on FRPc, but a non-significant effect on CBIbc. Topographic features such as ridges and hilltops, characterized by higher TPI, had significant positive effect on both responses. Steeper slopes had a weak but significant positive effect on both responses. North-facing slopes tend to weakly decreased FRPc but have little effect in our models on CBIbc. Fire weather generally had a stronger positive effect on FRPc than CBIbc in our models. For every unit increase in VPD, there was a 16.2% (95% CI: -13.3%, -11.9%) increase in FRPc. In the case of CBIbc, VPD showed a weak negative effect with credible intervals passing zero, indicating insignificance. ERCdv had a positive effect which was strongest for FRPc (+10.7% for every unit increase), though positive and significant for CBIbc as well (**Table B1, B2**).

2.3.4. Aspen co-dominance and fire weather mediation

Where aspen co-occurs with other major forest types, its proportional live basal area (i.e., *dominance*) influenced FRPc and CBIbc differently, and these effects were often mediated by VPD (**Figure 2.7, Table B1**). Where aspen was the majority, increasing dominance significantly decreased FRPc (-5.4% for every unit increase) and CBIbc (-8.7% for every unit increase). However, VPD-mediation had a pronounced influence, with the effect of aspen dominance either diminishing greatly (CBIbc, **Figure 2.7b**) or becomes slightly positive with a non-significant effect (FRPc, **Figure 2.7a**). In lodgepole forests, the effect of increasing aspen dominance on FRPc was significant and negative (-3.5% for every unit increase), with VPD-mediation further increasing the magnitude of this effect (-5.7%). The influence of aspen dominance was strongest in lodgepole forests for FRPc and weaker for CBIbc where only VPD-mediation showed a significant but weak signal for reducing burn severity in lodgepole forests. In spruce-fir, ponderosa, Douglas-fir, and pinyon-juniper, increasing aspen dominance showed either a positive or non-significant effect on FRPc *without* VPD-mediation. However, this effect on FRPc became negative and significant for ponderosa, Douglas-fir and pinon-juniper when interacting with VPD, suggesting that as fire weather was more extreme aspen dominance had a larger effect on reducing fire activity in these forest types. This influence was pronounced, with -17.8% reduction in FRPc in ponderosa forests when interacting with VPD compared to a +6.8% increase in effect without VPD-mediation, for example. In spruce-fir forests, VPD-mediation moved the influence of aspen dominance to a non-significant effect on FRPc, demonstrating a lack of evidence for aspen moderation in this forest type. In the case of CBIbc, spruce-fir forests did benefit from aspen dominance during more extreme fire weather, with a reduction by X% in burn severity for every unit increase in aspen dominance. For Gambel oak and white fir, which are relatively rare in the sample (**Figure B1**), the effects of aspen dominance exhibited extreme credible intervals for both models. These forest types rarely co-occur with aspen in great proportions (**Figure B5**), which helps explain the wide credible intervals and uncertain estimates.

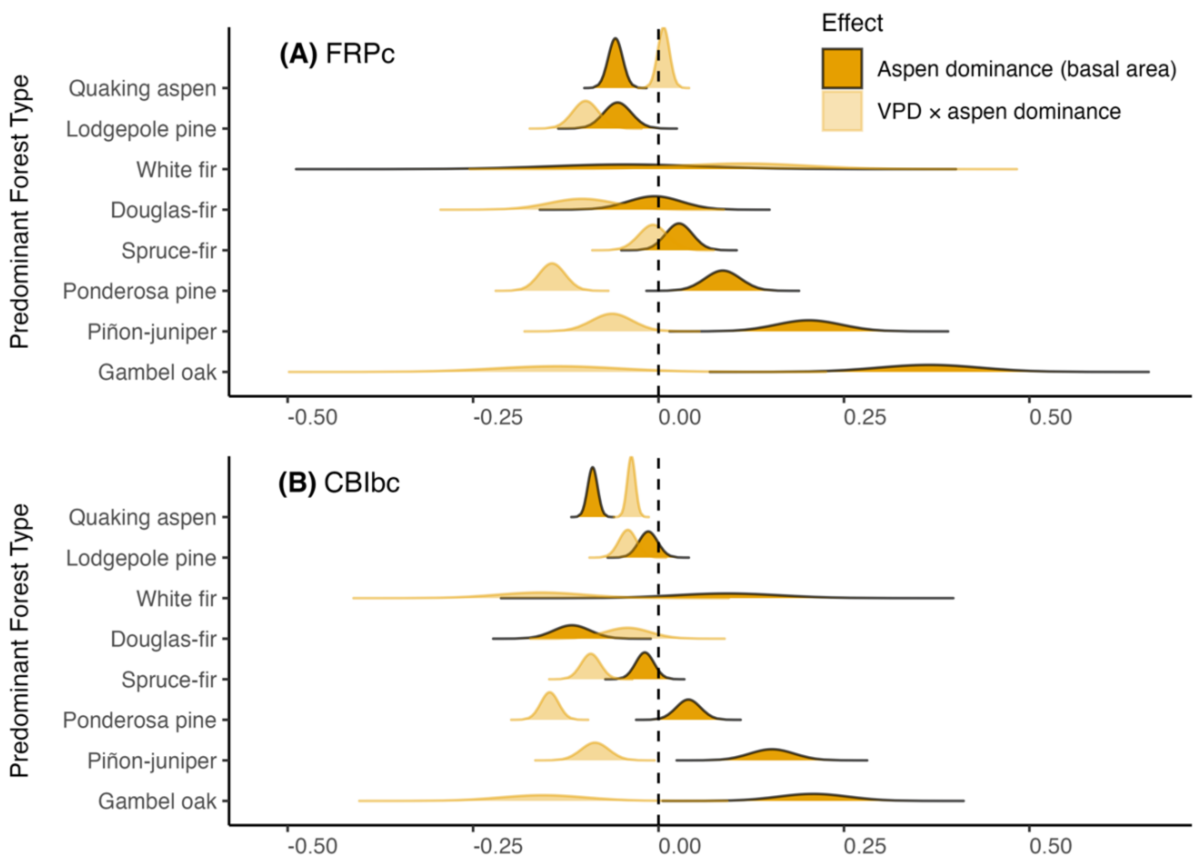

Figure 2.7 *Posterior distribution of effects on (**A**) FRPc, and (**B**) 90th percentile CBIbc, for the influence of quaking aspen dominance relative to co-occurring major forest types with and without VPD mediation. Light orange ridges represent the VPD-mediated effect which was modeled as an interaction term (forest type:aspen dominance * VPD). For both models, terms were included to account for other fire weather, topography, fire-dependent random effects, day-of-burn temporal random effects, VIIRS aggregation information and spatial effects (see Section 2.7).*

2.3.5. Spatial patterns in FRP and CBI

Substantial spatial structure emerged for both FRPc and CBIbc, defined by the SPDE structured random effects model implemented in *R-INLA* (**Figure 2.8**). Semivariogram analysis provided an initial assessment of the expected spatial range, suggesting an expected mean range for FRPc of ~2.2 km and ~2.9 km for CBIbc. Results from the SPDE indicate alignment with these expectations alongside fixed and random effects, with slight differences. For FRPc, the mean effective range of spatial dependence was 0.016 degrees (~1.6 km), suggesting a fine-scale clustering and influence of localized conditions unexplained by fixed or random effects. A relatively large standard deviation (mean 0.769) indicated moderately strong spatial variation in FRPc, and residual spatial effects left unexplained by the model. In the case of CBIbc, the effective range of spatial dependence increases to 0.078 (~7.8 km), suggesting more broad-scale spatial patterns in burn severity compared to FRPc. With a lower standard deviation (mean 0.088), the spatial variation in CBIbc is significantly reduced compared to FRPc and may be better explained by the fixed and random effects such as forest composition and structure, fire weather and topography.

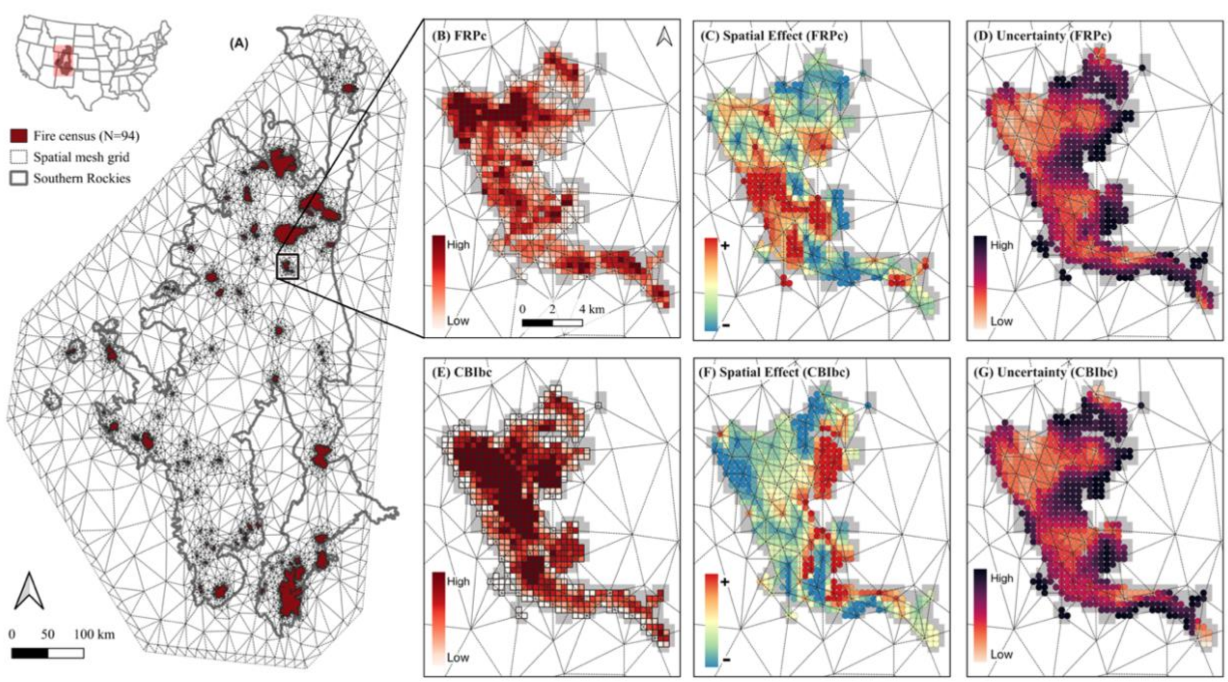

***Figure 2.8** Results from the spatial model (SPDE); (**A**) Spatial mesh grid covering the Southern Rockies; (**B**) Cumulative FRP (FRPc); (**C**) Spatial effect of FRPc; (**D**) Uncertainty in the spatial effect of FRPc; (**E**) 90th percentile CBIbc; (**F**) Spatial effect of CBIbc; and (**G**) Uncertainty in the spatial effect of CBIbc.*

2.4. Discussion

Significant differences between FRPc and CBIbc relative to aspen emerged across forest types in the Southern Rockies during recent wildfires. Aspen forest composition and structure had significant moderating effects on fire intensity and severity compared to other forest types. For example, we found that compared to lodgepole pine, aspen averaged 20.9% lower FRPc and 10.0% lower CBIbc. In this forest type, and where lodgepole and aspen co-occur, every unit increase in proportional live basal area decreased FRPc by -3.5% and (-5.7% with VPD-mediation), highlighting the capacity for aspen to reduce fire intensity in lodgepole forests even under more extreme conditions. The results of this study have widespread implications for forest and fire management in the context of fire hazards, suppression and response, and fuels treatments. We introduce a novel index, FRPc, as a proxy for fire intensity and successfully harmonize this with satellite-derive burn severity, imputed wall-to-wall forest inventory data, and characteristics of topography and weather to elucidate the biotic and abiotic controls on fire intensity and post-fire ecosystem impacts.

2.4.1. Aspen turns down the heat during recent wildfires

Aspen forests had a strong moderating effect on both FRPc and CBIbc, especially where it was the dominant forest cover. Lodgepole pine, Douglas-fir, white fir, ponderosa pine, and spruce-fir forests types all exhibited significantly higher FRPc and CBIbc *relative to aspen* while holding landscape and climatic effects such as forest composition and structure, fire weather, and topography at their means. This result aligns with expectations of fire activity in aspen forests, which is generally considered to be lower than adjacent conifer forest types (Nesbit et al., 2023). Previous studies have shown that fire activity is determined also by aspen stand structure and function type (e.g., seral or stable), where stable stands are less likely to burn than seral stands (Shinneman et al., 2013). Our results support this during recent wildfires in the Southern Rockies, with a -8.1% reduction FRPc for every unit increase in aspen percent cover (**Figure 2.6A**) – indicating a more pronounced cooling effect of aspen forests when they make up a greater proportion of the landscape area. Where aspen co-occurs with other forest types, significant moderating effects emerged especially when interacting with VPD (**Figure 2.7**). In lodgepole, for every unit increase in aspen dominance (proportion of live basal area), there was -3.5% effect on FRPc and -5.8% in CBIbc, respectively (**Table B1, B2**). Importantly, this moderating effect was more pronounced when interacting with VPD, suggesting that even under more extreme fire weather conditions aspen may reduce fire intensity and severity where it co-occurs with lodgepole. Conversely, the influence of aspen dominance in ponderosa, pinon-juniper, and Douglas-fir weakly increased fire intensity and severity in some cases *except* when interacting with VPD. While this dynamic deserves more attention in subsequent studies, it indicates that under more extreme fire weather aspen may provide a buffer in these forest types. Given associations between increasing VPD and increasing fire activity in the western US (Abatzoglou & Williams, 2016), this is potentially significant finding. However, These forest types often occupy low-elevation sites where the future habitat suitability of aspen is in question (Hart et al., *In review*). This VPD-mediation also highlights an important consideration in areas already dominated by aspen forests – the influence of increasing dominance becomes insignificant when fire weather is more extreme. This aligns with simulated studies of aspen fire behavior in northern Utah, where torching and crowning events were just as likely in aspen compared to conifer when fire weather was more extreme (DeRose & Leffler, 2014). Still, both FRPc and CBIbc are lower in aspen forests relative to other types, this effect may just be diminished by extreme fire weather. Future efforts should focus on this dynamic to untangle the influence of fire weather on fire behavior in different forest types.

2.4.2. Forest composition and structure effects align with expected fire regime characteristics

Forest-specific fire regime characteristics emerged when assessing the influence of structural metrics on fire heat and burn severity. For example, the interesting relationships between SDI and HDR corroborate expected fire regime characteristics in aspen, ponderosa pine and spruce-fir forests. The SDI relates the total number of trees per unit area to their average stem diameter where low values represent less dense stands and high values represent dense, high volume stands. Significant effects of aspen SDI emerged showing that as SDI increases, FRPc and CBIbc decreases by -2.6% and -1.6%, respectively (**Figure 2.7**). This indicates that where aspen stands were more densely packed (*i.e.*, representative of a more stable functional type) they reduce both heat and severity of fire. Similarly, as aspen HDR increased, FRPc and CBIbc both decreased weakly but significantly. High HDR implies tall, slender trees which is more indicative of seral aspen forests with little understory regeneration and a few large individuals. This aligns with expected fire regime characteristic in stable aspen types which generally experience lower intensity fire than seral types (Shinneman et al., 2013). Similar interesting effects emerged in spruce-fir forests for FRPc but not for CBIbc. In these forest types, significant negative effects of SDI (weak but significant), average live basal area, HDR indicate that densely packed forests tend to have lower FRPc. High-elevation dense spruce-fir forests are characterized by relatively high surface fuel and soil moisture which is often retained later in the year than other forest types and can have significant limitations on fire intensity under most conditions. Still, these forests readily burn at high severity when conditions align, a possible explanation for the lack of significant effects on CBIbc. Relative to aspen, spruce-fir forest types only demonstrated a weakly positive effect on FRPc (**Figure 2.3**) and the influence of aspen dominance on reducing fire heat was only uncovered when interacting the VPD (**Figure 2.7**), suggesting that specific fire weather conditions influence the flammability of spruce-fir relative to aspen, aligning with expectations that spruce-fir is more climate-limited than fuel-limited. For ponderosa pine, which is a low-elevation dry conifer forest type historically evolved with high frequency, moderate to low severity/intensity wildfire (Kaufmann et al., 2006), opposite effects emerged. These forests have been particularly impacted by a century of fire-exclusion leading to a forest structure that is characterized by densely packed even-aged stands and resulting in changing fire behavior (Battaglia et al., 2018; Veblen et al., 2000). We found significant positive effects on FRPc and CBIbc for ponderosa where average live basal area and HDR increases and a weak positive effect of SDI (**Figure 2.7**). This aligns with expectations, where smaller individual trees and dense forest structure results in higher fire intensity and severity compared to a more open park stand structure. These findings are significant, as these methods provide an accurate way to assess the influence of forest composition and structure on *observed* fire behavior; an important consideration when planning fuels treatments or assessing their effectiveness in different forest types and fire regimes.

2.4.3. Opportunities, limitations and future directions

Broadly speaking, the methods of this study are widely applicable to other regions, forest types, and satellite-derived information. We demonstrate a novel application of satellite-derived FRP as a proxy for fire intensity and our results highlight the potential of these data to understand how landscape factors influence fire intensity, an important measure of how difficult a fire will be to control. These data could, for example, be leveraged to monitor fuel treatment effectiveness, the influence of beetle-kill on fire intensity, and understand the influence of more fine-scale measurements of live fuel moisture. The VIIRS data in particular offer an important source of *globally* available FRP information. The aggregation of active fire detections in the present study could also be used to integrate data across sensors, such as VIIRS, MODIS, and GOES, to fill the spatial and temporal gaps in detections. As new satellites come online, such as the FireSat constellation scheduled for 2026, these methods may become more applicable with higher temporal and spatial resolution imagery measuring fire activity and heat.

While we demonstrate a successful harmonization of satellite-derived FRP and CBI with imputed forest inventory data, there are some considerations for future work. These data still represent a sparse network of field sampling locations (one plot per 24.3 km^2), introducing uncertainty into our estimates of forest structure. Future efforts will benefit from integrating this approach with other satellite-based or field measurements on forest composition and structure to better define these relationships. Despite this uncertainty, our results indicate agreement with expectations of fire intensity and severity in common forest types of the Southern Rockies, highlight important advancement in the integration of satellite-derived FRP as a proxy for fire intensity with wall-to-wall forest metrics from TreeMap and the information provided in the *Tree Table* provides unique estimates of understory and mixed-forest composition which have been understudied at landscape scales.

2.5. Conclusion

This study demonstrates the influence of forest composition and structure on fire intensity and severity and elucidates the potential moderating influences of quaking aspen forests in the Southern Rockies. From a management perspective, the expansion of aspen forests may reduce the risk of extreme fire behavior under certain conditions, although this influence is likely mediated by the specific forest structure and the fire weather conditions. The moderating influence of aspen forests is more stable in lodgepole-dominated areas and targeted management of aspen in these forests is likely to provide a larger benefit of wildfire risk reduction. Given this information, aspen management in lodgepole forests can be targeted to provide a potential buffer in regions near communities where wildfire risk and suppression difficulty are high. This study provides important insights into the effects of not only aspen forests, but other predominant forest types and their structure, on observed fire intensity and severity in the Southern Rockies, with implications for wildfire risk reduction and forest management planning activities.

Overall, this effort contributes a significant advancement in the use of satellite-derived FRP as a proxy for fire intensity and demonstrates successful harmonization of these data with burn severity, forest inventory data, fire weather, and topography. The results have widespread implications for management of aspen and other forest types in the context of fire hazards and fuels management in the Southern Rockies and the open-source methods provide a framework for future research using satellite-derived FRP.

3 CHAPTER THREE

The fiery future of quaking aspen: management opportunities for wildfire hazard reduction in the Southern Rockies

3.1. Introduction

Management of quaking aspen (Populus tremuloides Michx.) is a primary focus for many agencies, municipalities, and private landowners, especially in the Southern Rockies. As a keystone species (Campbell & Bartos, 2001), aspen forests provide wildlife habitat, recreational and economic value, water conservation, post-disturbance forest resilience, and potential fire-resistance (Rogers et al., 2014). Recent evidence suggests that where aspen is dominant, it moderates fire intensity and burn severity, especially in high elevation lodgepole forest types in the Southern Rockies (Cook et al., In prep). Aspen has also recently been associated with lower fire growth rates and fire perimeter formation in southwestern dry conifer forests, having clear implications for management as fire breaks (Harris et al. In review). The concept of aspen as fire breaks is not new (e.g., G. Fechner & Barrows, 1976), however, given this mounting evidence, especially in the context of recent extreme fire activity (Bowman et al., 2017; Coop et al., 2022; Cunningham et al., 2024), there is growing interest in these so-called *living fire breaks*. Aspen management, including expansion, maintenance, and introduction, has the potential to augment existing fuels treatments and create a more fire-resilient landscape, especially in the context of a growing wildland urban interface (WUI) and increasing structure loss from western wildfires (Higuera et al., 2023). Beyond the potential hazard reduction benefits benefit, aspen forests provide crucial resilience in post-disturbance landscapes through prolific resprouting following canopy opening events (Bartos, 2001; Long & Mock, 2012) and their intentional management may even the odds in the context of observed declines in forest resilience in the western US (Stevens-Rumann et al., 2018). However, planning such management activities should consider the current and future conditions favorable for aspen and where targeted management may have the biggest benefits to society in the context of increasing fire activity and effects.

Changing climatic conditions are having and will continue to have profound impacts on fire activity and vegetation distribution, with clear implications for aspen forest persistence. Suitable habitat for aspen in the Southern Rockies is likely to change under future climate scenarios, with an 8.1% reduction in average suitability expected by 2040 (Hart et al., In review). Much of this loss will occur at low elevation dry sites where increasing temperature and changes in precipitation will have profound effects on current aspen forests and their persistence into the future (Hart et al., In review). At the same time, up to 17,017 km2 will remain suitable and up to 11,725 km2 of newly suitable habitat may become available for expansion, mostly at higher elevation sites which will be more favorable to aspen in the future (Hart et al., In review). From a management perspective, these regions represent priorities for maintaining current aspen stands, improving stand condition, or facilitating expansion into new areas. They also represent areas where wildfire activity could promote this expansion naturally, as the persistence of aspen on the landscape is driven by disturbance type and frequency, particularly wildfire (Kulakowski et al., 2004; Morris et al., 2019; Rosenblum, 2015). In some areas of the Southern Rockies, synchronous disturbances of drought, bark beetle, and fire have strained the capacity for conifer regeneration and may favor future dominance of aspen, at least where it was present pre-disturbance (Andrus et al., 2021; Tepley & Veblen, 2015).

There is also mounting evidence for an increasingly fiery future in the Southern Rockies. Recent decades have featured increases in fire occurrence and fire size (Iglesias et al., 2022), area burned at high severity (Parks & Abatzoglou, 2020), human-caused wildfire activity (Balch et al., 2017; Nagy et al., 2018), fire speed (Balch et al., 2024; Coop et al., 2022), and structure impacts (Higuera et al., 2023). These trends are likely to continue under future climate scenarios with implications for forest persistence and impacts to the built environment (Abatzoglou et al., 2021; Coop et al., 2022; Syphard et al., 2019). Recent evidence also points to an unprecedented increase in the size of the of the largest fires in the western US, and increasing fire occurrence and area burned overall (J. J. Stephens et al., n.d.). In the context of aspen forest persistence, these projected changes will have varied effects. On the one hand, areas where aspen habitat suitability is expected to increase may benefit from more fire on the landscape especially in lieu of much-needed prescribed fire. Conversely, regeneration failures at low-elevation dry sites which are experiencing more frequent fire and where aspen suitability is declining may lead to large-scale loss of aspen forests. Planning management activities focused on aspen retention or expansion should thus consider these factors, especially where the goal of management actions is to reduce future fire hazard for communities.

Management of aspen forests is dependent on topoedaphic site conditions, adjacent vegetation, functional type (e.g., stable or seral), and land use (Long & Mock, 2012; Rogers et al., 2014). Seral aspen stands tend to follow a successional pathway, where early establishment and dominance of aspen gives way to more mixed aspen-conifer stands within a relatively short time (Morris et al., 2019). Seral stands are regulated by stand-replacing disturbance events and harvest activities, with disturbance intensities often much higher (Shinneman et al., 2013). In contrast, stable aspen stands are self-sustaining, often for many ecological rotations (lifecycles) with little to no conifer encroachment (Rogers et al., 2010). This functional type is characterized by continuous regeneration and recruitment, often experiencing individual tree or small group mortality at a single time and is thus prone to less intense disturbance events (though, landscape scale disturbances like wind, fire, drought, insect outbreak still occur) (Rogers et al., 2010; W. Shepperd, 1990). These functional types represent key indicators for potential fire activity, with seral aspen exhibiting greater likelihood for extreme fire intensity and severity compared to stable aspen (Shinneman et al., 2013). Coppice silviculture, which involves cutting stems to stimulate the suckering response of aspen, is a commonly applied management technique to simulate disturbances and invigorate new growth in lieu of prescribed fire (Long & Mock, 2012). In some cases, especially in stable aspen types experiencing decline, this can achieve quite prolific regeneration (W. D. Shepperd et al., 2015). This response is driven by changes in root and soil temperature and light availability, which stimulates the growth of aspen suckers belowground. Although seedling-based establishment has become more common than previously thought and may play an important role in the future of aspen management (Landhäusser et al., 2019), this suckering capacity still drives a large portion of aspen response to disturbance and management.

To support management of aspen forests in the Southern Rockies, particularly for potential wildfire hazard reduction, we harmonize a suite of data products related to contemporary aspen canopy cover and patch characteristics, existing vegetation type, built environment and human population, and fire hazard potential alongside future projections of fire activity and aspen habitat suitability to produce maps of priority areas for aspen management. These maps and data provide a critical resource for forest managers and communities who are faced with an increasing wildfire hazard and are interested in aspen management for hazard reduction or forest resilience. Beyond the fire hazard, aspen forests may stabilize otherwise changing forest resilience following increasingly high severity firesand compound disturbances. This overall effort enables data-driven decision making for this important forest species now and into the future.

3.2. Materials and Methods

To assess landscape priorities for quaking aspen management in the Southern Rockies now and into the future, we harmonized a diverse suite of variables describing (1) trends in *future* fire occurrence and changes in aspen habitat suitability, and (2) the *contemporary* aspen distribution, patch metrics, fire hazard, forest characteristics, and characteristics of the built environment. We aggregate these data at the fireshed scale (The Fireshed Registry, n.d.), a unit of analysis that is operational and translates to actionable decision-making for communities and managers. Firesheds represent an average of 10,315 hectares and are developed based on probabilistic wildfire transmission to buildings, delineating areas where fires are likely to occur and impact communities. We aggregate each variable, described in more detail below, to the fireshed scale using zonal statistics and an aggregation method appropriate for the data based on native resolution and data type (e.g., geospatial raster or vector). The resulting database represents a rich combination of environmental and social-ecological information which is relevant to management decision making.

3.2.1. Aspen habitat suitability

To assess the future habitat suitability for quaking aspen, we leverage new data based on future climate projections downscaled in the Southern Rockies (Hart et al., In Review). These data were produced at ~90m spatial resolution using an ensemble modeling approach and derived from two Shared Socioeconomic Pathway (SSP) climate scenarios (SSP245 and SSP585). Following methods in Hart et al. In review, we calculated the change in near future (2041-2070) habitat suitability compared to the historical baseline (1981-2010) for both scenarios. We calculated the average change in aspen habitat suitability for both scenarios at the fireshed scale (**Figure 3.1**).

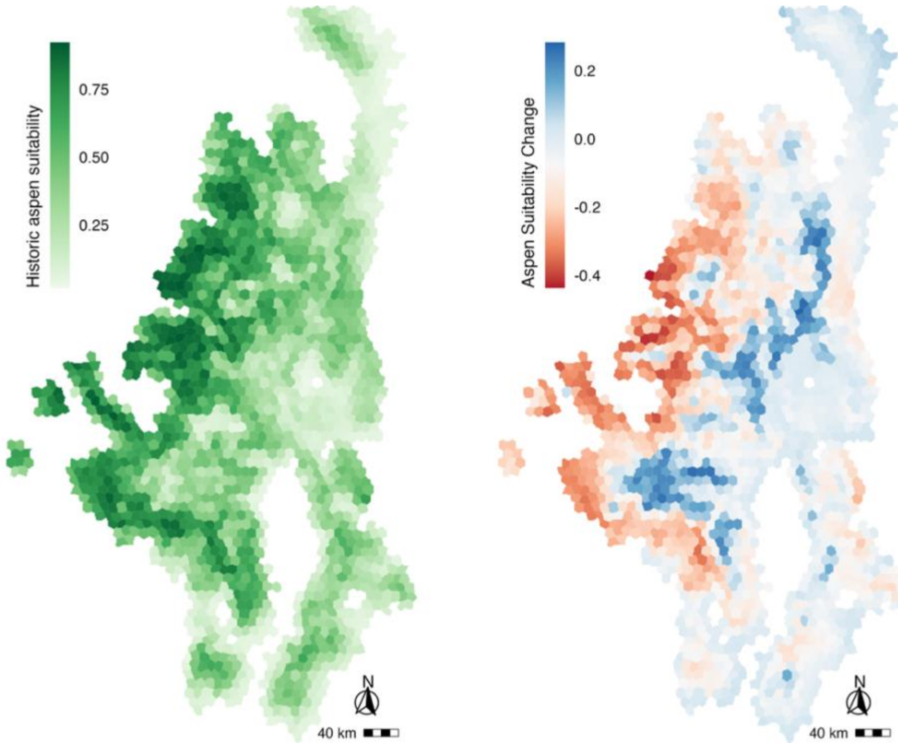

Figure 3.1 *Aspen habitat suitability summarized at the fireshed scale. (**A**) Historic (1981-2010) climatic and topographic aspen habitat suitability; (**B**) Change in future quaking aspen suitability based on the SSP585 scenario and difference between historic (1981-2010) and future (2041-2070). Warm colors represent areas of expected decreased suitability. Aspen habitat suitability is likely to decrease significantly in parts of the western slope of the Southern Rockies, particularly at lower elevation and drier sites. Conversely, higher elevation forests may see an increase in aspen suitability under future climate scenarios (represented in cool colors).*

3.2.2. Projected future wildfire activity

To assess future wildfire activity, we leveraged a new dataset providing annual projections of area burned and large fire occurrence (counts) from 2023-2060 based on ensemble climate models and population growth estimates for US EPA Level IV ecoregions (J. J. Stephens et al., n.d.). For both fire counts and burned area, we calculated the ecoregion-level trend using a median-based linear model

(MBLM), which estimates a Thielsen temporal trend. For each fireshed, we assigned a US Level IV ecoregion based on majority spatial overlap and joined to the future fire trends using the ecoregion code (**Figure 3.2**).

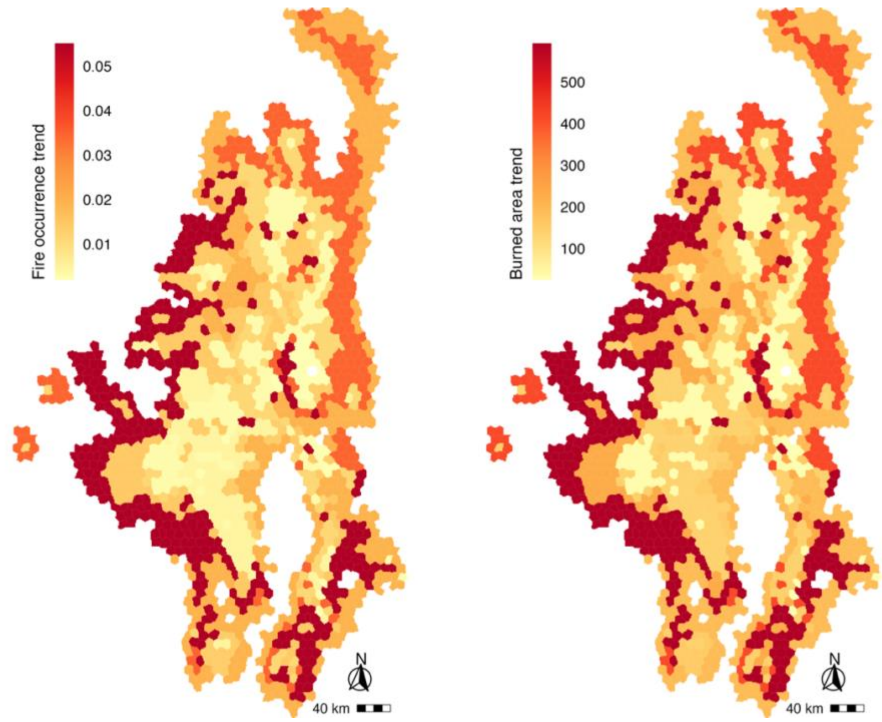

Figure 3.2 *Trends in projected future (2023-2060) fire counts (**A**) and area burned (**B**) across Southern Rockies firesheds. All trends were significant (|p|<0.05). Many low-elevation regions are expected to increase in fire activity substantially, though all regions demonstrate a positive and significant trend.*

3.1.1. Contemporary fire hazard and risk

To summarize contemporary fire hazard, we gather information from the Wildfire Risk to Communities (2nd Edition) which provides nationally-consistent information for the purpose of comparing relative wildfire risk among communities (Wildfire Risk to Communities, n.d.). Specifically, we use the ca. 2023 USFS Wildfire Hazard Potential (WHP; Dillon et al., 2015), Housing Unit Impact (HUI), and Conditional Flame Length (CFL). The WHP is built upon outputs from the Large Fire Simulator (FSim) including burn probability and flame length probability, alongside spatial fuels and vegetation from ca. 2020 LANDFIRE and past fire occurrence from the FPA-FOD (1992-2020). These data provide useful information to evaluate fire hazard and prioritization of fuels treatments across the landscape. We calculate the 95th percentile WHP within each fireshed.

3.1.2. Historic wildfire activity

We gathered summaries of both historic fire activity and contemporary fire hazard for the Southern Rockies. To assess historic fire, we summarized the number and cause of ignitions and cumulative area burned from multiple sources. First, we summarized the ignition type (e.g., human, natural, and undetermined) and area burned gathered from the FPA-FOD from 1992-2020 and supplemented by the latest ICS-209-PLUS release for 2021-2023. Most of the area burned (55.1%) since 1992 was a result of human-caused ignitions (**Figure X**). To assess prior burned area in our database, we calculate the cumulative area burned for each gridcell from the Monitoring Trends in Burn Severity (MTBS; *ref*). So, each gridcell is assigned its cumulative area burned from 1984-2023 representing the most recent release of the MTBS database.

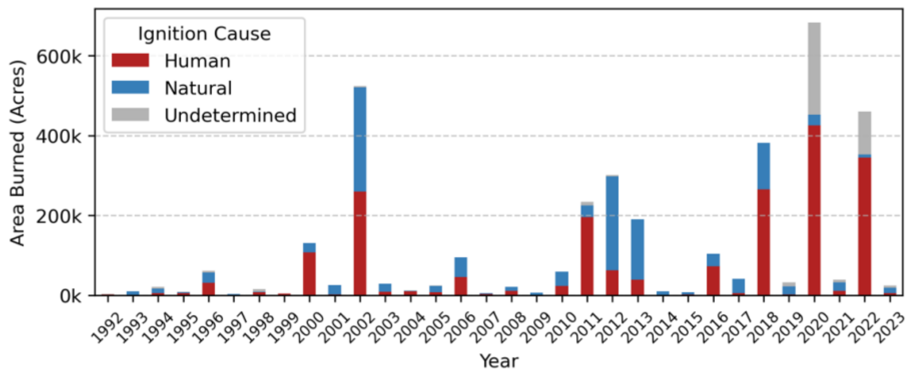

Figure 3.3 *Southern Rockies annual area burned by ignition cause (natural, human, or undetermined) between 1992-2023. Fire data from 1992-2020 is from the FPA-FOD and 2021-2023 from the ICS209-PLUS. Human-caused ignitions accounted for 55.1% of all fires in this database, 33.8% were natural, and 11.1%.*

3.2.3. Built Environment and Wildland Urban Interface

To assess the contemporary distribution and characteristics of the built environment and the wildland urban interface/intermix (WUI), we leverage a variety of regional and global data sources (**Figure 3.4**). The Combustible Mass of the Built Environment (COMBUST) is a novel dataset which brings together numerous sources of information to describe the total volume of structures and estimated indoor mass based on property records, zoning codes and climatic conditions (Uhl et al., *In prep*). In this data, *combustible* is defined by building materials which are known to be flammable, helping to estimate not only the footprint of the built environment, but how flammable it is. To assess the distribution of the WUI, we aggregated the percent cover of grassland and forested interface/intermix from the SILVIS global 10m data (Schug et al., 2023). We merged these classes into a combined WUI designation and summarized the percent cover within each fireshed. In addition, each fireshed was assigned the average distance to WUI using a Euclidean distance approach calculated as the average distance to a WUI pixel.

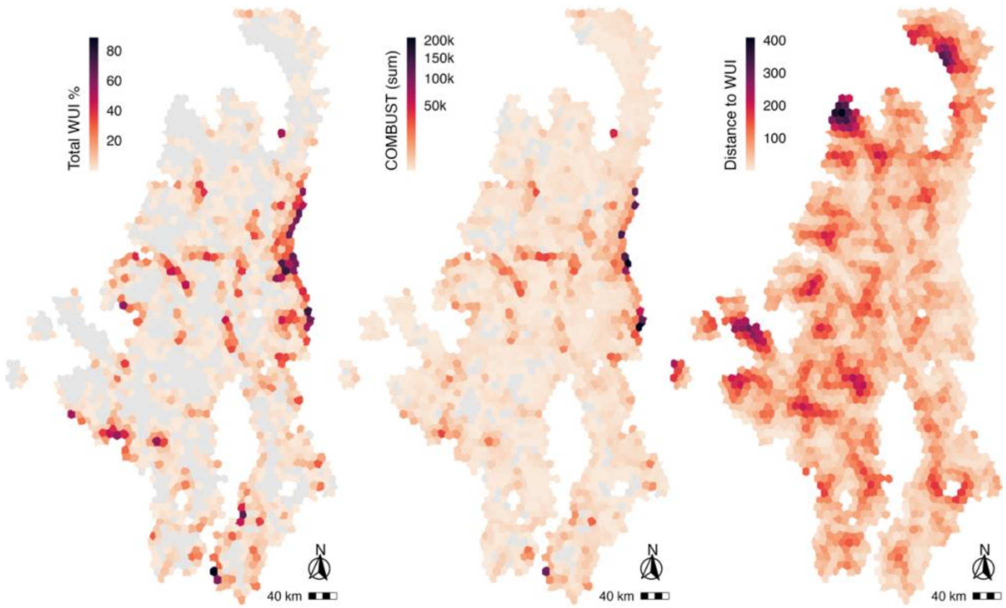

Figure 3.4 *Built environment characteristics summarized by firesheds in the Southern Rockies; (**A**) Total wildland urban interface/intermix (grassland and forested) percent cover; (**B**) Total combustible mass of the built environment (COMBUST; units).*

3.2.4. Contemporary aspen canopy, patch size, and existing vegetation

We summarized contemporary aspen canopy cover, patch distribution, and existing vegetation types within firesheds across the Southern Rockies using (i) new high-resolution maps of contemporary aspen forest canopy cover (Cook et al., 2024), and (ii) ca. 2023 LANDFIRE existing vegetation type (EVT), forest cover, and forest height. Specifically, for (i) we calculated the percent canopy cover of aspen within firesheds as well as the patch metrics including the number of patches, average patch size, density, and area of largest patch using the *pylandstats* Python package (Bosch, 2019) (**Figure 3.5**). For (ii) we calculated the percent cover of all LANDFIRE EVT classes in each fireshed. We identified the top four EVT classes in each fireshed as well as the percent cover for specific types relevant to aspen ecosystems including ponderosa, lodgepole, Engelmann spruce and subalpine fir, pinon-juniper, Douglas-fir, white fir, sagebrush, and Gambel oak.

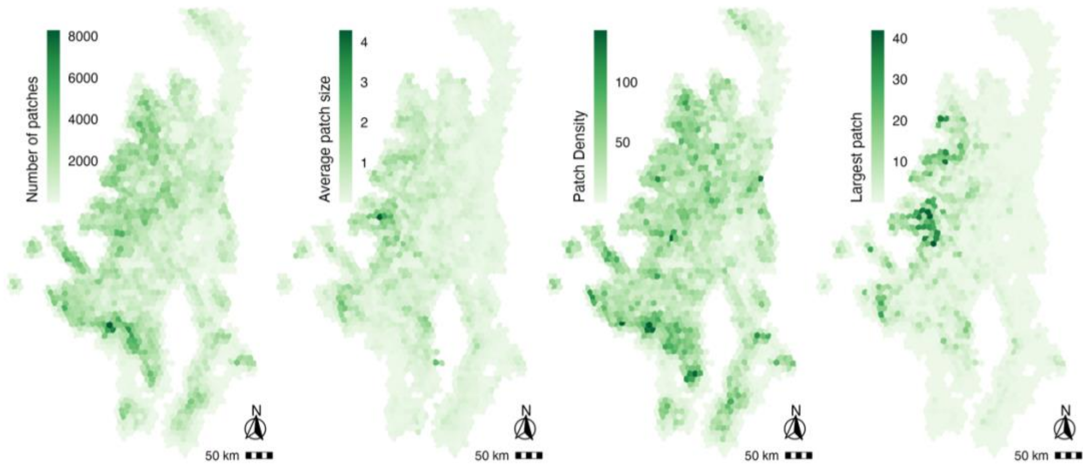

Figure 3.5 *Aspen patch metrics including the number of patches, average patch size, patch density, and largest patch index (the proportion of the landscape of the largest patch).*

3.2.5. Statistical Analysis

To assess opportunities for aspen management in the Southern Rockies now and into the future, we use two primary approaches. First, we apply bivariate mapping to identify spatial correlations between projected future fire occurrence and changes in aspen habitat suitability. A bivariate map visualizes the relationship between two distinct variables on the same map, showing regions where they align or diverge. This provides an intuitive way to classify firesheds where, for example, there is a large positive trend in future fire activity and increasing aspen habitat suitability. Within bivariate classes, we summarize contemporary aspen distribution, patch metrics, and wildfire hazard to contextualize future conditions relative to existing aspen cover.

Second, we use self-organizing maps (SOM), an artificial neural network (ANN) unsupervised clustering algorithm, to further distinguish unique opportunities for aspen management. Like other unsupervised clustering algorithms, such as *k*-means, SOM identifies topological relationships within high dimensional data and maps these to a 2-dimensional grid, or nodes (Wehrens & Buydens, 2007). These nodes represent groups of similar observations, in this case firesheds, based on the set of input variables. However, they do not themselves represent specific spatial units. To delineate firesheds into potential management units, we extend the SOM using hierarchical clustering of the codebook vectors, an output of the model which represents the average fireshed characteristics for each node. This approach leverages the stored topologies to identify broader groups of firesheds with similar characteristics. Importantly, variable weighting can be leveraged to guide node definitions based on specific criteria. We present the results of a single "scenario" using balanced weights across categories of variables. Specifically, we group variables into four major categories: aspen-specific, fire activity and disturbance, social hazard, and forest characteristics (**Table 3-1**). We trained a SOM in the *kohonen* R package (Wehrens & Buydens, 2007) with 5001 iterations, initial learning rate of 0.02 and hexagonal grid structure.

Table 3-1 *Variables considered for input to SOM analysis including their respective "category", name, abbreviation, fireshed aggregation method (if relevant), and data source.*

Category	Variable	Abbreviation	Aggregation method	Data source
Aspen	Contemporary aspen canopy cover (hectares)	aspen_ha	Sum	Cook et al., 2024
	Average patch size	patch_size	n/a	Cook et al., 2025

	Patch density	patch_den	n/a	Cook et al., 2026
	Largest patch index	big_patch	n/a	Cook et al., 2027
	Change in aspen habitat suitability (SSP585; 2041-2070)	delta585	Average	Hart et al., *In review*
Historic & future fire activity / disturbance	Trend in projected fire occurrence (2023-2060)	trend_count	Average	Stephens et al., *In review*
	Historic burned area (1984-2023)	burned_pct	Cumulative sum	MTBS
	Disturbance (%)	disturbed	Percent cover	LANDFIRE
Fire hazard / vulnerability	Population density	pop_den	Average	WorldPop
	Structure count	msbf_count	Sum	Microsoft Building Footprints
	WUI (%)	wui	Percent cover	SILVIS
	Distance to WUI	wui_dist	Average	SILVIS
	Housing unit impact	hui_p90	90th percentile	USFS
	Wildfire hazard potential	whp_p90	90th percentile	USFS
	Combustible mass of the built environment (COMBUST)	combust	Sum	Uhl et al., *In prep*
Forest characteristic	Forested percent	forest_pct	Percent cover	LANDFIRE
	Conditional flame length	cfl_p90	90th percentile	USFS
	Forest canopy percent	lf_canopy	Average	LANDFIRE
	Forest canopy height	lf_height	Average	LANDFIRE

We assess the cluster definitions using radar plots showing the relative contributions of variables to each cluster, as well as the distribution of each variable within clusters. This provides a way of contextualizing the results in a way that is meaningful from a management perspective. Additionally, we crosswalk clusters with our bivariate map classes to better define management scenarios in the context of future environmental conditions. Finally, given the efficiency of SOM analysis and the flexibility to guide clustering through variable weighting, we deployed this workflow in a shiny application (Chang et al., 2025). This application provides users with an interface to set weighting on specific variables and display both the fireshed clusters and the contributing factors visualized using radar plots.

3.3. Results

3.3.1. Alignment of future fire and aspen habitat suitability

We identified firesheds where projected trends in future fire activity and changes in aspen habitat suitability align in the Southern Rockies using a bivariate mapping approach (**Figure 3.6**). Importantly, 93 firesheds (9,861 km^2) emerged with both the highest projected increase in fire occurrence and either low change or increasing aspen habitat suitability. While representing only 5.4% of firesheds, these regions may be primed for effective aspen management into the future, with an estimated 13,347 ha (133.8 km^2) of contemporary aspen canopy cover and an average patch size of 0.14-0.19 ha (**Table 3-2**). An additional 557 firesheds (57,774 km^2) are likely to experience some increases in fire occurrence and *increasing* aspen habitat suitability. Here, management of existing aspen (~1,116 km2 with an average patch size of 0.10-0.29 ha) including improving stand health or promoting expansion may have greater success within the next few decades. These regions may also represent priority landscapes for seedling-based establishment of new stands as there may be higher quality sites for this purpose. However, they may also face fewer challenges associated with environmental changes and thus require less intensive active management to maintain positive benefits. On the other hand, we identified 405 firesheds (41,896 km^2) with moderate to high trends in future fire occurrence and average *decreasing* aspen habitat suitability. Here, we estimate a total of 343,325 ha (3,433 km^2) of contemporary aspen canopy cover with an average patch size of 0.34-0.43 ha. This represents roughly 35% of total estimated aspen canopy cover in the Southern Rockies. Active management and monitoring of these stands may represent a conservation priority for both potential fire hazard reduction and forest resilience in the face of changing environmental conditions. Although, for example, establishment of new stands from seedling may be less successful here, opportunities still exist for maintaining or improving stand condition through silvicultural techniques or prescribed fire thereby promoting regeneration of older stands. Crucially, these regions also include 226,983 building footprints (28% of total) across Southern Rockies firesheds, including a population of ~387,000 (29% of total).

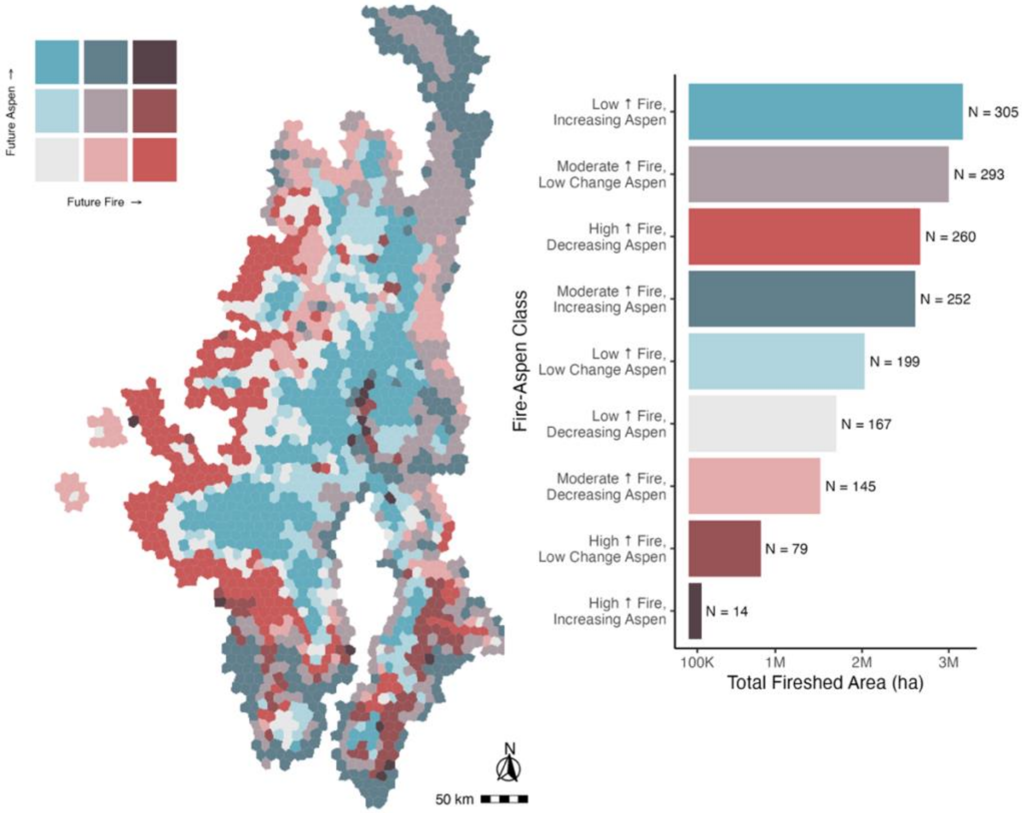

Figure 3.6 *Intersection of the trend in future fire occurrence and change in future aspen habitat suitability under the more severe climate scenario (SSP585). (**A**) Bivariate map of the Southern Rockies showing firesheds where future fire and aspen suitability intersect or diverge; (**B**) Total land area (hectares) in each bivariate mapping classes.*

Table 3-2 *Descriptive statistics of bivariate classes showing the mean wildfire hazard potential, trend in burned area, change in aspen suitability, and contemporary aspen cover sorted by wildfire hazard potential.*

Bivariate Class	N	Aspen area (ha)	Average patch size (ha)	Change in aspen suitability (mean)	Trend in fire occurrence (mean)	Wildfire Hazard Potential (mean)
High Increasing Fire, Decreasing Aspen	260	264305	0.43	-0.255	0.06	1750
High Increasing Fire, Increasing Aspen	14	2783	0.19	0.011	0.06	1812
High Increasing Fire, Low Change Aspen	79	10564	0.14	-0.063	0.06	3122
Low Increasing Fire, Decreasing Aspen	167	339213	0.85	-0.176	0.01	958
Low Increasing Fire, Increasing Aspen	305	106209	0.29	0.094	0.01	689

Low Increasing Fire, Low Change Aspen	199	125954	0.42	-0.055	0.01	1004
Moderate Increasing Fire, Decreasing Aspen	145	79020	0.34	-0.169	0.03	1311
Moderate Increasing Fire, Increasing Aspen	252	5449	0.11	0.016	0.02	829
Moderate Increasing Fire, Low Change Aspen	293	29320	0.18	-0.049	0.03	1595
Total	**1,714**	**962818**				

3.3.2. Priority firesheds for aspen management

We mapped firesheds with similar environmental and fire hazard characteristics using SOM analysis, delineating eight unique clusters with different implications for aspen management (**Figure 3.7A**). To crosswalk the results of this unsupervised clustering method, we assess the contribution of each variable to defining clusters using radar plots (**Figure 3.7B**). We also show the distribution of input variables within each cluster to help contextualize these differences (**Figure 3.8**). Additionally, we link these clusters to their respective bivariate class to better understand their distribution in the context of future conditions (**Table 3-3**). For example, Cluster 1 (C1) represents the largest group of firesheds (N=934) and is driven by low to moderate increases in fire occurrence and either low change or increasing aspen habitat suitability (**Table 3-3**). However, these regions are also further from WUI areas, meaning they may be better suited for aspen management in the context of conservation and forest resilience as opposed to fire hazard reduction. Conversely, clusters 2, 5, and 7 (N=379 combined) represent firesheds that are more closely linked with hazard potential and WUI designations. In these regions, managing aspen for hazard reduction may be an additional priority. Clusters 5 and 7 (N=92 combined) include most total building footprints, population, and higher than average hazard potential. These areas also have less contemporary aspen with smaller average patch size indicating the potential for improving stand health, expanding existing aspen patches, or possibly establishment of new stands, especially where the future habitat suitability is expected to remain consistent or increase. In the context of contemporary aspen distribution, clusters 3, 4, and 6 (N=387 combined) represent firesheds with greater aspen canopy area and higher patch size, density, and largest patch index. These firesheds also largely fall within regions that are expected to decrease in aspen habitat suitability (**Table 3-3**). These clusters represent areas where, for example, short-term conservation efforts and stand improvement may help even the odds under changing environmental conditions to protect large areas of existing aspen. An even smaller subset of firesheds fall within Cluster 8 and represent high levels of housing unit impact, forest cover, and conditional flame length. While representing a small proportion of total firesheds, these areas may benefit from greater proportions of aspen forests for reducing expected flame lengths and largely fall within high elevation regions where future aspen habitat suitability is likely to increase.

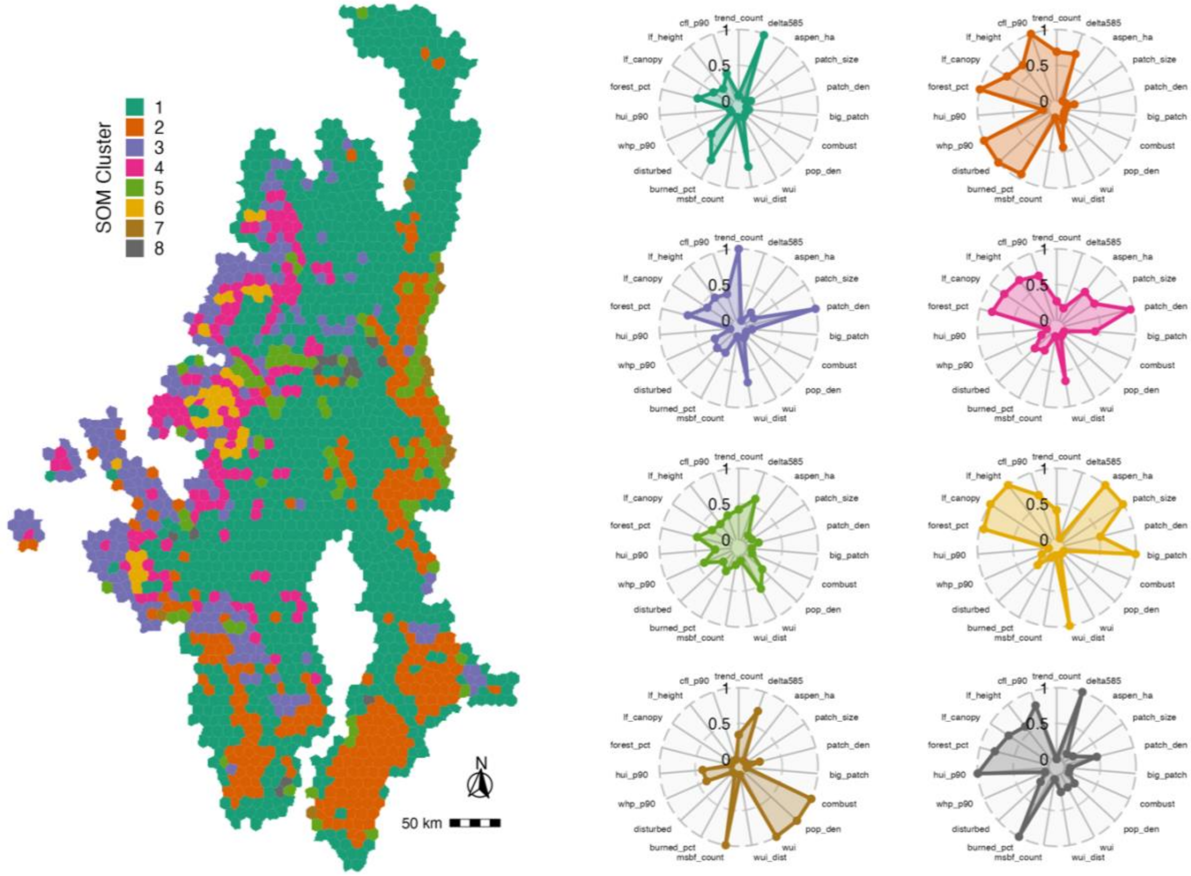

Figure 3.7 *Results from SOM analysis. (**A**) Map of cluster assignments by firesheds in the Southern Rockies; (**B**) Radar plots showing the contributions of variables to SOM cluster definitions.*

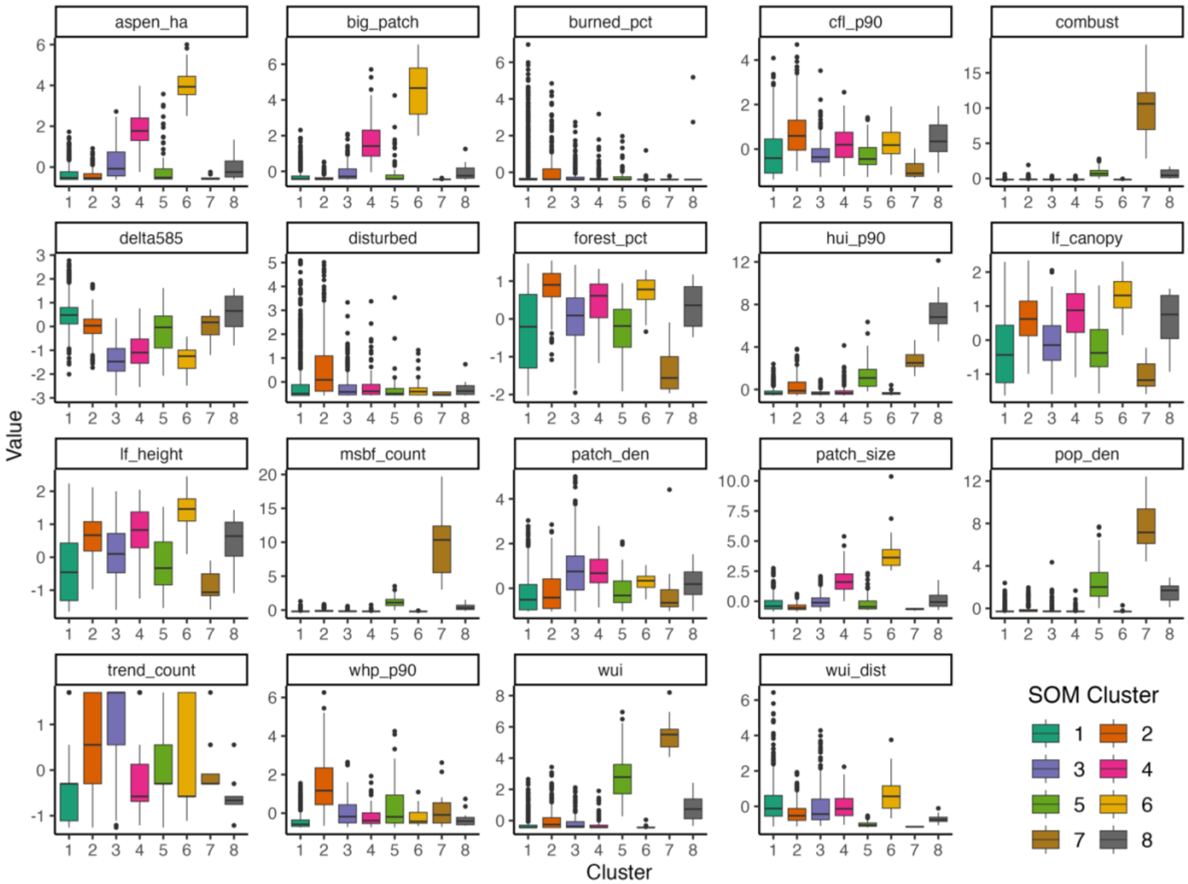

Figure 3.8 *Distribution of input variables by cluster. Variables were centered and scaled before analysis.*

Table 3-3 *Distribution of clusters within bivariate classes. Bold values signify the majority bivariate class for each cluster. Rows represent bivariate class, and columns represent cluster numbers (denoted with "C#").*

Bivariate Class	C1	C2	C3	C4	C5	C6	C7	C8
High Increasing Fire, Decreasing Aspen	6	46	**151**	31	13	12	1	0
High Increasing Fire, Increasing Aspen	7	7	0	0	0	0	0	0
High Increasing Fire, Low Change Aspen	9	64	6	0	0	0	0	0
Low Increasing Fire, Decreasing Aspen	46	9	12	**71**	4	**23**	0	2
Low Increasing Fire, Increasing Aspen	**274**	16	0	3	4	0	0	**8**
Low Increasing Fire, Low Change Aspen	144	25	6	18	5	0	0	1
Moderate Increasing Fire, Decreasing Aspen	55	24	38	10	15	0	3	0
Moderate Increasing Fire, Increasing Aspen	212	22	0	0	15	0	3	0
Moderate Increasing Fire, Low Change Aspen	181	**74**	4	2	**24**	0	**5**	3
Total	*934*	*287*	*217*	*135*	*80*	*35*	*12*	*14*

Table 3-4 *Summary statistics within SOM-based clusters showing aspen area, patch size (average), building footprints, population, wildfire hazard potential (unitless), and housing unit impact (unitless).*

Cluster	Aspen area (ha)	Average patch size (ha)	Microsoft Building Footprints	Population	Wildfire Hazard Potential	Housing Unit Impact
1	236,575	0.26	125,841	51,916	527	961013
2	53,051	0.15	96,876	51,573	3666	2201601
3	165,647	0.32	39,057	25,940	1322	754101
4	309,885	0.98	17,366	9,158	910	1152024
5	40,699	0.27	234,709	390,365	1838	4743802
6	147,955	1.82	1,659	294	895	600018
7	906	0.08	257,366	751,730	1723	8083984
8	8,100	0.36	19,842	44,826	736	19522489

3.4. Discussion

This overall effort produced an extensive database describing trends in *future* fire activity and aspen habitat suitability alongside *contemporary* information relevant to management of aspen forests for fire hazard reduction, conservation, and forest resilience. We present (1) a characterization of future conditions using bivariate mapping combining trends in future fire and projected changes in aspen habitat suitability, and (2) an application of hierarchical SOM analysis for prioritizing firesheds based on complex multidimensional data, enabling fireshed prioritization based on environmental and social-ecological conditions. We identified 93 (5.4%) firesheds with the greatest expected trend in future fire occurrence and either low change or increasing aspen habitat suitability, representing regions where future conditions may favor aspen dominance. Conversely, 405 (23%) firesheds make up regions where there is moderate to high increases in fire occurrence and yet *decreasing* aspen suitability. These areas are also characterized by large aspen stands (3,433 km^2 with an average patch size of 0.34-0.43 ha) suggesting that conservation, stand improvement, and monitoring are likely to be important moving forward under changing conditions. We further refine these regions using hierarchical SOM analysis, developing a method for scenario-based spatial planning. This approach delineates firesheds with similar social-ecological characteristics including the contemporary aspen distribution and patch dynamics and proximity to the WUI and expected fire hazard. As an unsupervised clustering algorithm, SOM is an efficient tool for identifying regions with similar environmental and hazard characteristics. This approach provides a way to further contextualize opportunities and challenges for aspen management in the context of broader environmental and social-ecological conditions. From a management perspective, this is a helpful exercise in scenario planning, potentially guiding the decision-making process at landscape scales.

The persistence, distribution, and functional type of quaking aspen on the landscape is linked with disturbance type and periodicity (Bartos, 2001; Long & Mock, 2012; Shinneman & McIlroy, 2019). This forest type exists in both seral (or having a conifer component) and stable (pure aspen stands) functional types, each of which are governed by disturbance, especially wildfire (Morris et al., 2019; Rogers et al., 2014). Some of the largest stands of aspen in the Southern Rockies likely resulted from individual synchronous pulses of regeneration following natural and human-caused disturbance (e.g., mining in the 18000s or large wildfires in the 1900s) (Kaye, 2011). However, for the past century, aggressive fire suppression, livestock grazing, and expansion of the Wildland Urban Interface (WUI) has altered disturbance regimes across this region (Hessburg et al., 2019), having a profound influence on aspen regeneration and persistence (Gill et al., 2017). In the Southern Rockies, for example, a lack of disturbance has driven widespread changes in aspen cover over the past century (Landhäusser et al., 2010). In the absence of fire as governing disturbance, these regions may require direct management to sustain and promote existing aspen stands into the future. The results of the present study help contextualize the opportunities for aspen management now and into the future, providing a framework for management decision making.

Importantly, our improved understanding of aspen patch distributions from analysis of high-resolution map products (e.g., Cook et al., 2024) better informs these decisions at the fireshed scale. For example, the western slope of the Southern Rockies is characterized by much larger patches of aspen forests and total area. Much of this region is expected to experience some decline in habitat suitability, indicating a need for conservation or management targeting improving stand condition. These areas also represent relatively lower density of human population and WUI meaning that management actions may be better suited for improving forest resilience or conserving existing aspen. Conversely, in regions with greater human population and wildfire hazard, the average aspen patch size is smaller. To improve the capacity for aspen forests to provide hazard reduction benefits in these regions, management should focus on increasing the average patch size, especially in areas that also provide tactical advantage for fire suppression near communities.

For example, areas defined by Cluster 5, which represents high levels of potential wildfire hazard and housing unit impact, have an average patch size of 0.27 ha, smaller than the average in the Southern Rockies as a whole (~0.51 ha). Management goals may focus on increasing this average patch size through silvicultural techniques, prescribed fire, or wildland fire use. The largest average patch size (1.8 ha) occurs in Cluster 6. However, these areas are further from the WUI and are less likely to provide hazard reduction benefits. Still, they may help define management goals in regions where that patch size is much smaller. Future work should focus efforts on understanding the relative effects of aspen patch size on fire behavior mediation.

3.5. Conclusion

Management of quaking aspen forests in the Southern Rockies is a primary focus for many municipalities, land management agencies, and non-governmental organizations. Under rapidly changing environmental and social-ecological conditions, planning management activities should be informed by the best available data and information. To this end, the present study provides a rich database describing the contemporary aspen canopy cover, patch metrics, fire hazard, built environment characteristics, alongside future projections of fire activity and aspen habitat suitability summarized at a relevant spatial scale. The maps and summaries provided herein can provide important frameworks for management decision making and scenario planning for this important forest species now and into the future.

SUMMARY AND CONCLUSIONS

Statement of importance

In an increasingly fiery future, one with greater risk to communities and potentially weakened capacity for resilience in western U.S. forests (Stevens-Rumann et al., 2018), intentional management of fire-resistant species may help even the odds. Quaking aspen is emerging as one such species, particularly in the Southern Rockies, that may play an important role in future forest resilience and wildfire hazard reduction in some areas. Rapidly growing WUI and development in hazard hotspots (Iglesias et al., 2021; Radeloff et al., 2018), changes in the frequency, severity, and speed of wildfire (Balch et al., 2024; Coop et al., 2022; Iglesias et al., 2022; Parks & Abatzoglou, 2020), and disturbance (or lack thereof) changes to forest persistence, composition and structure (Coop et al., 2020; Hagmann et al., 2021) will continue to put pressure on both ecological and human communities in the Southern Rockies. These changes require collective action, technological and scientific advancements, and intentional management to improve natural and built environment resilience to wildfire. The work presented in this dissertation represents contributions to this end, with an emphasis on quaking aspen forest management but with methods that widely apply to other forest types and geographic regions.

Summary of work

One underexplored “tool in the toolbox” for fire hazard reduction is the expansion of fire-resistant species like quaking aspen. Investigation of opportunities and challenges for managing fire-resistant species like aspen are needed to help inform decision making at a variety of spatial scales, especially in the context of changing habitat suitability and future fire activity (Hart et al., In review; Stephens et al., In review). This dissertation contributes to the growing body of knowledge around aspen as a fire-resistant species and presents analyses and data products which directly inform such management actions. Each chapter in this body of work presents novel datasets, findings and/or analysis approaches to facilitate this investigation of aspen as a living fire break. Beyond the important questions regarding aspen, the methods presented in this dissertation are widely applicable to other forest species and regions, contributing significant advancements and opportunities for future research.

In **Chapter One**, we demonstrate the effectiveness of combining multispectral and radar seasonal cloud-free composite imagery alongside a machine learning classifier to develop new high-resolution maps of quaking aspen canopy cover. These methods achieved classification high accuracy (0.93 average f1-score), significantly outperforming other similar land cover products in the region and demonstrating a promising approach for mapping individual forest species using Sentinel-1 and -2 imagery. We mapped 9,482 km^2 of aspen canopy cover with an average forest patch size of 0.53 ha (+/- 23 ha), which is 95% smaller than LANDFIRE existing vegetation type (1.85 ha), providing maps of small aspen stands which are critically important from a management perspective. Importantly, we also map 1.76M individual forest patches across the Southern Rockies, 28-93%

more than existing maps. This work is highlighted by advancements in large-area image classification and accuracy assessment focused on a single forest species, methods of which are highly applicable to other species and regions. Specifically, the preparation and composition of thousands of Sentinel images in the Google Earth Engine (GEE) platform demonstrates the capacity to leverage big data in a cloud-native format for generating cloud-free season composite imagery useful for image classification. Including multiple seasons of both multispectral and radar composites, alongside radar texture metrics emphasizing canopy characteristics, improved classification accuracy. This work is open and scalable, enabling generation of aspen canopy maps across larger geographic regions and temporal scales (e.g., annual cover maps). The results are presented in a GEE web application, providing a way to easily visualize the aspen cover maps and input satellite image composites. Following principles of open science, the code and data to recreate these maps or apply the methodologies elsewhere are provided in public GitHub and GEE repositories. These resources enable continuous improvements to the methods, derivation of maps for other time periods and geographic regions, and applications to new training data and for other forest species.

In **Chapter Two**, we demonstrate the application of an underexplored satellite proxy of fire intensity, fire radiative power (FRP), alongside satellite-derived burn severity to investigate the influence of aspen forest composition and structure on active fire behavior and subsequent ecosystem impacts. We introduce a novel index, FRPc, as a proxy for fire intensity and successfully harmonize this with satellite-derive Composite Burn Index (CBI), imputed wall-to-wall forest inventory data, and characteristics of topography and weather to elucidate the biotic and abiotic controls on fire intensity and post-fire ecosystem impacts. We found that aspen-dominated areas are characterized by relatively lower FRP and CBI compared to commonly co-occurring conifer forest species including ponderosa, Douglas-fir, spruce-fir (Engelmann spruce and subalpine fir), and especially lodgepole. For example, lodgepole pine forests exhibited 20.9% (95% CI: 18.3%, 23.6%) higher FRP compared to quaking aspen. In this forest type, and where lodgepole and aspen co-occur, every unit increase in proportional live basal area of aspen decreased FRPc by -3.5% and (-5.7% with VPD-mediation), highlighting the capacity for aspen to reduce fire intensity in lodgepole forests even under more extreme fire weather conditions. This also highlights the importance of aspen dominance and possibly an indication of the effects of aspen functional type on fire behavior. As aspen becomes more dominant, the reducing effect on both FRP and CBI is greater. This aligns with previous studies which highlight the difference in fire activity between seral aspen (greater fire activity) and stable or pure aspen, which is far less likely to burn with extreme fire behavior (Shinneman et al., 2013). This is further supported when assessing specific composition and structure within FRPc observations, with a -8.1% reduction FRPc for every unit increase in aspen percent cover. These findings are significant for both elucidating aspen's cooling influence on fire activity and demonstrating an effective application of satellite-derived fire radiative power as a proxy for fire intensity – a method that has wide applicability beyond this study (see *Methodological contributions*).

Chapter Three focused on identifying priority landscapes for aspen management in the Southern Rockies. We harmonized a suite of variables describing contemporary aspen canopy cover and patch dynamics, wildfire hazard, characteristics of the built environment, and existing vegetation type alongside projections of future aspen habitat suitability and wildfire activity under different climate scenarios. This effort represents a first-of-its-kind map and method for scenario-based planning of management activities in aspen forests. We identified 93 (5.4%) firesheds with the greatest expected trend in future fire occurrence and either low change or increasing aspen habitat suitability, representing regions where future conditions may favor aspen dominance. These regions likely also represent areas for potential establishment of new stands and where this type of activity is more likely to be successful under changing environmental conditions. Conversely, 405 (23%) firesheds make up regions where there is moderate to high increases in fire occurrence and yet *decreasing* aspen suitability. Using unsupervised clustering via SOM, we also mapped fireshed clusters with different archetypes of built environment characteristics, contemporary aspen cover, and risk to communities. For example, using this method, we identified three distinct clusters representing firesheds that include 588,951 building footprints and where aspen suitability is expected to remain relatively consistent or increase. These represent priority firesheds for aspen management in the context of fire hazard reduction (i.e., management for *living fire breaks*). While we present one scenario for priority landscapes in the results of Chapter Three, the interactive tool enables easy customization of model weights to emphasize different management goals. This database can be updated with additional data, especially given input from managers and community members. Combined with expanded maps of aspen's distribution following methods in Chapter One, this approach represents a significant step towards informed decision making for this aspen management now and into the future.

Methodological contributions

This dissertation provides at least three primary methodological advancements which may be widely useful for future research. First, the application of seasonal composite imagery from both synthetic aperture radar (SAR) and multispectral satellite imagery is a promising avenue for individual forest species classification. Overcoming challenges associated with large-area image classification tasks is no small feat – and the methods described herein provide advancements to that end. For example, the use of spatial block cross-validation for model training and assessment represents an effective method for model development and accuracy assessment. We demonstrate that this task can be completed in cloud-native environments (i.e., Google Earth Engine) with implications for future efforts. Furthermore, incorporating phenology of species to develop meaningful composite imagery is a useful approach, especially in areas with persistent cloud cover. Creating cloud-free satellite image mosaics which represent key stages in the phenological cycle helps minimize the number of input images required and improves classification accuracy. These methods are fully open-source, and all code is made publicly available, providing opportunities for others to use and improve these methods for aspen or other forest types.

Second, we demonstrate a novel application of satellite-derived FRP as a proxy for fire intensity and introduce a new metric; cumulative FRP (FRPc). This is significant, as assessments of forest species composition and landscape controls on emitted radiative energy during wildfire events is an underexplored area of research. Satellite-derive FRP has been generally applied to understand biomass burning rates or emissions but has yet been underutilized in the context of fire intensity and its relationship to biotic and abiotic controls. At the time of this dissertation, there have been no studies which assess the influence of forest species composition and structure alongside fire weather and topography to understand the spatial patterns and controls on fire intensity. Furthermore, few studies have directly linked FRP and satellite-derived burn severity metrics such as the composite burn index (CBI). We harmonize these two characteristics of fires using data from VIIRS and Landsat during recent (2017-2023) wildfires in the Southern Rockies – developing a first-of-its-kind database and method for aggregating active fire detections and FRP at the fire event scale. Beyond the interesting findings regarding aspen forests and controls on FRPc, including its capacity to reduce FRPc by -8.1% for every unit increase canopy cover, these methods facilitate a multitude of future studies. For example, FRPc can be leveraged to understand the relationship between bark beetle affected forests and radiative energy release, the influence of fuels treatments or suppression tactics, and the diurnal fluctuations in fire intensity. Efforts are already underway to expand this data product across western US forests, with clear implications for future research. Importantly, all code written to this end has been made publicly available enabling contributions from the community to improve on the methods.

Third, we demonstrate an application data harmonization and machine learning to identify landscape priorities for intentional aspen management in the Southern Rockies. Clustering regions for potential management priorities using self-organizing maps represents a novel application of this machine learning algorithm. Flexible weighting of variables enables both quantitative and manual adjustments to the clustering algorithm, a feature that we exploited by creating an R-Shiny application enabling interactive visualization of landscape factors relevant for management decision-making (*https://maxwellccook.shinyapps.io/aspen-firesheds-som/*). This approach is simple, efficient to build, and can handle complex data structures, making it particularly useful for ecological applications and landscape prioritization. A common issue with unsupervised clustering is the crosswalk to real-world applications. We assess the distribution of variables within each cluster in a way that elucidates the contributing factors and helps identify "archetypes" of management scenarios. We leverage landscape patch dynamics to help contextualize management goals in terms of not just the total area of aspen canopy cover, but also the distribution of patch sizes – an important consideration given the importance of aspen functional type in driving management goals and outcomes.

Management implications

There are several important management implications from this work. First, new high-resolution maps of aspen forest cover highlight the distribution of patch sizes across the Southern Rockies. This is significant, as small stands may respond readily to forest management activities such as coppice silviculture or prescribed burning, stimulating the suckering response of the root systems. In some cases, these might also be late-seral stands with little or no understory regeneration and greater proportions of conifer neighbors. Without active management or natural wildfire disturbance, these stands may be at-risk under rapidly changing environmental conditions. By leveraging higher-resolution satellite imagery, this work moves towards mapping aspen functional type, monitoring stand health and condition, and assessing changes in the distribution of aspen patches. These maps also providing finer detail for development of habitat suitability models describing the historic suitability and expected future suitability under different climate scenarios (Hart et al., *In review*). In tandem, these data and methods also facilitate mapping of stable aspen stands, which are more important from a fire-resistance perspective (Shinneman et al., 2013). These methods can and should be applied at annual or bi-annual timesteps to help monitor aspen forests over time. They can also assist land managers in making decisions about where to target management actions for positive benefits whether that be for fire hazard reduction, conservation, or improved forest resilience.

Second, there are clear signals of aspen's moderating influence on fire intensity and severity based on satellite-derived metrics, though these effects are likely mediated by fire weather (Chapter Two). During recent wildfires in the Southern Rockies (2017-2023), the effect of aspen dominance in lodgepole forests had a significant influence on both intensity and severity and VPD had less of a mediating influence than in other forest types. This suggests that targeted management of existing aspen in lodgepole-dominated forests may provide a buffer to extreme fire behavior, even under more severe fire weather scenarios. However, although greater aspen dominance significantly reduces radiative energy and burn severity under average weather conditions, this influence may be heavily mediated by vapor pressure deficit. This is significant from a management perspective, demonstrating the capacity for aspen to burn hot and severely when VPD is more extreme. From a management perspective, the expansion of aspen forests may reduce the risk of extreme fire behavior under certain conditions, although this influence is likely mediated by the specific forest structure and the fire weather conditions. The moderating influence of aspen forests is more stable in lodgepole-dominated areas and targeted management of aspen in these forests is likely to provide a larger benefit of wildfire risk reduction. Given this information, aspen management in lodgepole forests can be targeted to provide a potential buffer in regions near communities where wildfire risk and suppression difficulty are high. For example, high-elevation municipalities like Summit County, CO, may have more of an opportunity to leverage strategic aspen expansion as a way of buffering the fire hazard. More data and research are needed to refine our understanding of this dynamic and what this kind of management should look like.

Third, we contribute to improved understanding of the current and future conditions favorable for aspen forests. For management, this represents a significant advancement in our understanding of where targeted management actions may have benefits for aspen conservation, forest resilience, and potential fire hazard reduction. We contextualize the opportunities for aspen as a living fire break by identifying regions, defined using firesheds, where contemporary aspen cover exists adjacent to fire hazard for communities. This enables prioritization of landscape level management actions to maintain existing aspen, expanding aspen patch sizes, and improve stand condition. We also identify regions where the future conditions may be favorable for aspen establishment. These regions generally fall within high elevation forests of the Southern Rockies, although opportunities emerged in mid elevation areas which are also more densely populated, such as east of the continental divide along the Colorado Front Range. This exercise also had a focus on aspen patch size as a metric for understanding management opportunities. Where fire hazard to communities is greater, we generally see a lower-than-average patch size. This is important, as efforts to increase the average patch size in these regions may result in greater return on investment from a fire hazard reduction perspective. Overall, this extensive database provides a clearer picture regarding the opportunities and challenges for aspen management in the Southern Rockies now and into the future.

LITERACTURE CITED

Abatzoglou, J. T. (2013). Development of gridded surface meteorological data for ecological applications and modelling. *International Journal of Climatology*, *33*(1), Article 1. https://doi.org/10.1002/joc.3413

Abatzoglou, J. T., Battisti, D. S., Williams, A. P., Hansen, W. D., Harvey, B. J., & Kolden, C. A. (2021). Projected increases in western US forest fire despite growing fuel constraints. *Communications Earth & Environment*, *2*(1), Article 1. https://doi.org/10.1038/s43247-021-00299-0

Abatzoglou, J. T., & Williams, A. P. (2016). Impact of anthropogenic climate change on wildfire across western US forests. *Proceedings of the National Academy of Sciences*, *113*(42), 11770–11775. https://doi.org/10.1073/pnas.1607171113

Agee, J. K., & Skinner, C. N. (2005). Basic principles of forest fuel reduction treatments. *Forest Ecology and Management*, *211*(1), Article 1. https://doi.org/10.1016/j.foreco.2005.01.034

Alexander, M. E. (2010). Surface fire spread potential in trembling aspen during summer in the Boreal Forest Region of Canada. *The Forestry Chronicle*, *86*(2), 200–212. https://doi.org/10.5558/tfc86200-2

Andrus, R. A., Hart, S. J., Tutland, N., & Veblen, T. T. (2021). Future dominance by quaking aspen expected following short-interval, compounded disturbance interaction. *Ecosphere*, *12*(1), e03345. https://doi.org/10.1002/ecs2.3345

Balch, J. K., Bradley, B. A., Abatzoglou, J. T., Nagy, R. C., Fusco, E. J., & Mahood, A. L. (2017). Human-started wildfires expand the fire niche across the United States. *Proceedings of the National Academy of Sciences of the United States of America*, *114*(11), Article 11. https://doi.org/10.1073/pnas.1617394114

Balch, J. K., Iglesias, V., Mahood, A. L., Cook, M. C., Amaral, C., DeCastro, A., Leyk, S., McIntosh, T. L., Nagy, R. C., St. Denis, L., Tuff, T., Verleye, E., Williams, A. P., & Kolden, C. A. (2024). The fastest-growing and most destructive fires in the US (2001 to 2020). *Science*, *386*(6720), 425–431. https://doi.org/10.1126/science.adk5737

Balch, J. K., St. Denis, L. A., Mahood, A. L., Mietkiewicz, N. P., Williams, T. M., McGlinchy, J., & Cook, M. C. (2020). FIRED (Fire Events Delineation): An Open, Flexible Algorithm and Database of US Fire Events Derived from the MODIS Burned Area Product (2001–2019). *Remote Sensing*, *12*(21), Article 21. https://doi.org/10.3390/rs12213498

Barber, B. C. (1985). Review Article. Theory of digital imaging from orbital synthetic-aperture radar. *International Journal of Remote Sensing*, *6*(7), 1009–1057. https://doi.org/10.1080/01431168508948262

Barrett, A., Battisto, C., Bourbeau, J., Fisher, M., Kaufman, D., Kennedy, J., Lopez, L., Lowndes, J., Scheick, J., & Steiker, A. (2024). *Earthaccess* (Version v0.11.0) [Computer software]. Zenodo. https://doi.org/10.5281/zenodo.13871886

Barrett, K., & Quarles, S. L. (2024). Retrofitting Homes: Cost of Mitigation Strategies for Improved Wildfire Resistance. *Fire and Materials*, *n/a*(n/a). https://doi.org/10.1002/fam.3261

Bartos, D. L. (2001). Landscape dynamics of aspen and conifer forests. *In: Shepperd, Wayne D.; Binkley, Dan; Bartos, Dale L.; Stohlgren, Thomas J.; Eskew, Lane G., Comps. Sustaining Aspen in Western Landscapes: Symposium Proceedings; 13-15 June 2000; Grand Junction, CO. Proceedings RMRS-P-18. Fort Collins, CO: U.S. Department of Agriculture, Forest Service, Rocky Mountain Research Station. p. 5-14.*, *18*, 5–14.

Bayle, A., Carlson, B. Z., Thierion, V., Isenmann, M., & Choler, P. (2019). Improved Mapping of Mountain Shrublands Using the Sentinel-2 Red-Edge Band. *Remote Sensing*, *11*(23), Article 23. https://doi.org/10.3390/rs11232807

Bebi, P., Kulakowski, D., & Veblen, T. T. (2003). Interactions Between Fire and Spruce Beetles in a Subalpine Rocky Mountain Forest Landscape. *Ecology*, *84*(2), 362–371. https://doi.org/10.1890/0012-9658(2003)084[0362:IBFASB]2.0.CO;2

Beguin, J., Martino, S., Rue, H., & Cumming, S. G. (2012). Hierarchical analysis of spatially autocorrelated ecological data using integrated nested Laplace approximation. *Methods in Ecology and Evolution*, *3*(5), 921–929. https://doi.org/10.1111/j.2041-210X.2012.00211.x

Belgiu, M., & Drăguț, L. (2016). Random forest in remote sensing: A review of applications and future directions. *ISPRS Journal of Photogrammetry and Remote Sensing*, *114*, 24–31. https://doi.org/10.1016/j.isprsjprs.2016.01.011

Bosch, M. (2019). PyLandStats: An open-source Pythonic library to compute landscape metrics. *PLOS ONE*, *14*(12), e0225734. https://doi.org/10.1371/journal.pone.0225734

Bowman, D. M. J. S., Balch, J. K., Artaxo, P., Bond, W. J., Carlson, J. M., Cochrane, M. A., D'Antonio, C. M., DeFries, R. S., Doyle, J. C., Harrison, S. P., Johnston, F. H., Keeley, J. E., Krawchuk, M. A., Kull, C. A., Marston, J. B., Moritz, M. A., Prentice, I. C., Roos, C. I., Scott, A. C., … Pyne, S. J. (2009). Fire in the Earth System. *Science*, *324*(5926), Article 5926. https://doi.org/10.1126/science.1163886

Bowman, D. M. J. S., Kolden, C. A., Abatzoglou, J. T., Johnston, F. H., van der Werf, G. R., & Flannigan, M. (2020). Vegetation fires in the Anthropocene. *Nature Reviews Earth & Environment*, *1*(10), 500–515. https://doi.org/10.1038/s43017-020-0085-3

Bowman, D. M. J. S., Williamson, G. J., Abatzoglou, J. T., Kolden, C. A., Cochrane, M. A., & Smith, A. M. S. (2017). Human exposure and sensitivity to globally extreme wildfire events. *Nature Ecology & Evolution*, *1*(3), 1–6. https://doi.org/10.1038/s41559-016-0058

Buma, B., & Wessman, C. A. (2013). Forest resilience, climate change, and opportunities for adaptation: A specific case of a general problem. *Forest Ecology and Management*, *306*, 216–225. https://doi.org/10.1016/j.foreco.2013.06.044

Campbell, R. B., & Bartos, D. L. (2001). Aspen ecosystems: Objectives for sustaining biodiversity. *In: Shepperd, Wayne D.; Binkley, Dan; Bartos, Dale L.; Stohlgren, Thomas J.; Eskew, Lane G., Comps. Sustaining Aspen in Western Landscapes: Symposium Proceedings; 13-15 June 2000; Grand Junction, CO. Proceedings RMRS-P-18. Fort Collins, CO: U.S. Department of Agriculture, Forest Service, Rocky Mountain Research Station. p. 299-310.*, *18*, 299–310.

Chang, W., Cheng, J., Allaire, J. J., Sievert, C., Schloerke, B., Xie, Y., Allen, J., McPherson, J., Dipert, A., & Borges, B. (2025). *shiny: Web Application Framework for R*. https://shiny.posit.co/

Chapman, T. B., Schoennagel, T., Veblen, T. T., & Rodman, K. C. (2020). Still standing: Recent patterns of post-fire conifer refugia in ponderosa pine-dominated forests of the Colorado Front Range. *PLOS ONE*, *15*(1), e0226926. https://doi.org/10.1371/journal.pone.0226926

Clevers, J. G. P. W., & Gitelson, A. (2012). Using the red-edge bands on Sentinel-2 for retrieving canopy chlorophyll and nitrogen content. *European Space Agency, (Special Publication) ESA SP*, *707*.

Cook, M., Chapman, T., Hart, S., Paudel, A., & Balch, J. (2024). Mapping Quaking Aspen Using Seasonal Sentinel-1 and Sentinel-2 Composite Imagery across the Southern Rockies, USA. *Remote Sensing*, *16*(9), Article 9. https://doi.org/10.3390/rs16091619

Coop, J. D., Parks, S. A., Stevens-Rumann, C. S., Crausbay, S. D., Higuera, P. E., Hurteau, M. D., Tepley, A., Whitman, E., Assal, T., Collins, B. M., Davis, K. T., Dobrowski, S., Falk, D. A., Fornwalt, P. J., Fulé, P. Z., Harvey, B. J., Kane, V. R., Littlefield, C. E., Margolis, E. Q., … Rodman, K. C. (2020). Wildfire-Driven Forest Conversion in Western North American Landscapes. *BioScience*, *70*(8), 659–673. https://doi.org/10.1093/biosci/biaa061

Coop, J. D., Parks, S. A., Stevens-Rumann, C. S., Ritter, S. M., & Hoffman, C. M. (2022). Extreme fire spread events and area burned under recent and future climate in the western USA. *Global Ecology and Biogeography*, *31*(10), 1949–1959. https://doi.org/10.1111/geb.13496

Cova, T. J., Li, D., Siebeneck, L. K., & Drews, F. A. (2021). Toward Simulating Dire Wildfire Scenarios. *Natural Hazards Review*, *22*(3), 06021003. https://doi.org/10.1061/(ASCE)NH.1527-6996.0000474

Cumming, S. G. (2001). Forest Type and Wildfire in the Alberta Boreal Mixedwood: What Do Fires Burn? *Ecological Applications*, *11*(1), 97–110. https://doi.org/10.1890/1051-0761(2001)011[0097:FTAWIT]2.0.CO;2

Cunningham, C. X., Williamson, G. J., & Bowman, D. M. J. S. (2024). Increasing frequency and intensity of the most extreme wildfires on Earth. *Nature Ecology & Evolution*, *8*(8), 1420–1425. https://doi.org/10.1038/s41559-024-02452-2

Davis, D. (2011). *2017 NAIP information sheet.* US Department of Agriculture. https://www.fsa.usda.gov /Assets/USDA-FSA-Public/usdafiles/APFO/support-documents/pdfs/naip_infosheet_2017.pdf.

DeByle, N. V., Bevins, C. D., & Fischer, W. C. (1987). Wildfire Occurrence in Aspen in the Interior Western United States. *Western Journal of Applied Forestry*, *2*(3), 73–76. https://doi.org/10.1093/wjaf/2.3.73

DeByle, N. V., & Winokur, R. P. (1985). *Aspen: Ecology and management in the western United States*. http://www.fs.usda.gov/treesearch/pubs/24942

Deng, X., Li, W., Liu, X., Guo, Q., & Newsam, S. (2018). One-class remote sensing classification: One-class vs. Binary classifiers. *International Journal of Remote Sensing*, *39*, 1890–1910. https://doi.org/10.1080/01431161.2017.1416697

DeRose, R. J., & Leffler, A. J. (2014). Simulation of Quaking Aspen Potential Fire Behavior in Northern Utah, USA. *Forests*, *5*(12), Article 12. https://doi.org/10.3390/f5123241

Dillon, G., Menakis, J., & Fay, F. (2015). Wildland fire potential: A tool for assessing wildfire risk and fuels management needs. *In: Keane, Robert E.; Jolly, Matt; Parsons, Russell; Riley, Karin. Proceedings of the Large Wildland Fires Conference; May 19-23, 2014; Missoula, MT. Proc. RMRS-P-73. Fort Collins, CO: U.S. Department of Agriculture, Forest Service, Rocky Mountain Research Station. p. 60-76.*, *73*, 60–76.

Dobrinić, D., Gašparović, M., & Medak, D. (2021). Sentinel-1 and 2 Time-Series for Vegetation Mapping Using Random Forest Classification: A Case Study of Northern Croatia. *Remote Sensing*, *13*(2321), 2321. https://doi.org/10.3390/rs13122321

Dusseux, P., Corpetti, T., Hubert-Moy, L., & Corgne, S. (2014). Combined Use of Multi-Temporal Optical and Radar Satellite Images for Grassland Monitoring. *Remote Sensing*, *6*(7), Article 7. http://dx.doi.org.colorado.idm.oclc.org/10.3390/rs6076163

Eidenshink, J., Schwind, B., Brewer, K., Zhu, Z.-L., Quayle, B., & Howard, S. (2007). A Project for Monitoring Trends in Burn Severity. *Fire Ecology*, *3*(1), Article 1. https://doi.org/10.4996/fireecology.0301003

Ellenwood, J., Jr, F., & Romero, S. (2015). *National Individual Tree Species Atlas*.

Engel, M., Mette, T., & Falk, W. (2022). Spatial species distribution models: Using Bayes inference with INLA and SPDE to improve the tree species choice for important European tree species. *Forest Ecology and Management*, *507*, 119983. https://doi.org/10.1016/j.foreco.2021.119983

Evangelides, C., & Nobajas, A. (2020). Red-Edge Normalised Difference Vegetation Index (NDVI705) from Sentinel-2 imagery to assess post-fire regeneration. *Remote Sensing Applications: Society and Environment*, *17*, 100283. https://doi.org/10.1016/j.rsase.2019.100283

Evans, J. S., & Cushman, S. A. (2009). Gradient modeling of conifer species using random forests. *Landscape Ecology*, *24*(5), 673–683. https://doi.org/10.1007/s10980-009-9341-0

Evans, J. S., & Murphy, M. A. (2018). *rfUtilities*. https://cran.r-project.org/package=rfUtilities

Farwell, L. S., Gudex-Cross, D., Anise, I. E., Bosch, M. J., Olah, A. M., Radeloff, V. C., Razenkova, E., Rogova, N., Silveira, E. M. O., Smith, M. M., & Pidgeon, A. M. (2021). Satellite image texture captures vegetation heterogeneity and explains patterns of bird richness. *Remote Sensing of Environment*, *253*, 112175. https://doi.org/10.1016/j.rse.2020.112175

Fechner, G., & Barrows, J. (1976). Aspen stands as wildfire fuel breaks. *U.S Department of Agriculture. Forest Service, Rocky Mountain Forest and Range Experiment Station*, *Eisenhower Consortium Bulletin 4*. https://digitalcommons.usu.edu/aspen_bib/5029

Fechner, G. H. (1976). *Aspen stands as wildfire fuel breaks /*. [s.l.] : http://hdl.handle.net/2027/mdp.39015005797009

Frampton, W. J., Dash, J., Watmough, G., & Milton, E. J. (2013). Evaluating the capabilities of Sentinel-2 for quantitative estimation of biophysical variables in vegetation. *ISPRS Journal of Photogrammetry and Remote Sensing*, *82*, 83–92. https://doi.org/10.1016/j.isprsjprs.2013.04.007

Gill, N. S., Sangermano, F., Buma, B., & Kulakowski, D. (2017). Populus tremuloides seedling establishment: An underexplored vector for forest type conversion after multiple disturbances. *Forest Ecology and Management*, *404*, 156–164. https://doi.org/10.1016/j.foreco.2017.08.008

Girardin, M. P., & Terrier, A. (2015). Mitigating risks of future wildfires by management of the forest composition: An analysis of the offsetting potential through boreal Canada. *Climatic Change; Dordrecht*, *130*(4), Article 4. http://dx.doi.org.colorado.idm.oclc.org/10.1007/s10584-015-1373-7

Gitelson, A. A., Gritz †, Y., & Merzlyak, M. N. (2003). Relationships between leaf chlorophyll content and spectral reflectance and algorithms for non-destructive chlorophyll assessment in higher plant leaves. *Journal of Plant Physiology*, *160*(3), 271–282. https://doi.org/10.1078/0176-1617-00887

Gomez-Rubio, V. (2020). *Bayesian inference with INLA*. Chapman and Hall/CRC. https://doi.org/10.1201/9781315175584

Gorelick, N., Hancher, M., Dixon, M., Ilyushchenko, S., Thau, D., & Moore, R. (2017). Google Earth Engine: Planetary-scale geospatial analysis for everyone. *Remote Sensing of Environment*, *202*, 18–27. https://doi.org/10.1016/j.rse.2017.06.031

Gray, A., Brandeis, T., Shaw, J., McWilliams, W., & Miles, P. (2012). Forest Inventory and Analysis Database of the United States of America (FIA). *Biodiversity & Ecology*, *4*, 225–231. https://doi.org/10.7809/b-e.00079

Hagmann, R. K., Hessburg, P. F., Prichard, S. J., Povak, N. A., Brown, P. M., Fulé, P. Z., Keane, R. E., Knapp, E. E., Lydersen, J. M., Metlen, K. L., Reilly, M. J., Sánchez Meador, A. J., Stephens, S. L., Stevens, J. T., Taylor, A. H., Yocom, L. L., Battaglia, M. A., Churchill, D. J., Daniels, L. D., … Waltz, A. E. M. (2021). Evidence for widespread changes in the structure, composition, and fire regimes of western North American forests. *Ecological Applications*, *31*(8), e02431. https://doi.org/10.1002/eap.2431

Haralick, R. M., Shanmugam, K., & Dinstein, I. (1973). Textural Features for Image Classification. *IEEE Transactions on Systems, Man, and Cybernetics*, *SMC-3*(6), 610–621. IEEE Transactions on Systems, Man, and Cybernetics. https://doi.org/10.1109/TSMC.1973.4309314

Hermosilla, T., Wulder, M. A., White, J. C., & Coops, N. C. (2022). Land cover classification in an era of big and open data: Optimizing localized implementation and training data selection to improve mapping outcomes. *Remote Sensing of Environment*, *268*, 112780. https://doi.org/10.1016/j.rse.2021.112780

Hessburg, P. F., Miller, C. L., Parks, S. A., Povak, N. A., Taylor, A. H., Higuera, P. E., Prichard, S. J., North, M. P., Collins, B. M., Hurteau, M. D., Larson, A. J., Allen, C. D., Stephens, S. L., Rivera-Huerta, H., Stevens-Rumann, C. S., Daniels, L. D., Gedalof, Z., Gray, R. W., Kane, V. R., … Salter, R. B. (2019). Climate, Environment, and Disturbance History Govern Resilience of Western North American Forests. *Frontiers in Ecology and Evolution*, *7*. https://doi.org/10.3389/fevo.2019.00239

Hessburg, P. F., Prichard, S. J., Hagmann, R. K., Povak, N. A., & Lake, F. K. (2021). Wildfire and climate change adaptation of western North American forests: A case for intentional management. *Ecological Applications*, *31*(8), e02432. https://doi.org/10.1002/eap.2432

Higuera, P. E., & Abatzoglou, J. T. (2021). Record-setting climate enabled the extraordinary 2020 fire season in the western United States. *Global Change Biology*, *27*(1), 1–2. https://doi.org/10.1111/gcb.15388

Higuera, P. E., Cook, M. C., Balch, J. K., Stavros, E. N., Mahood, A. L., & St. Denis, L. A. (2023). Shifting social-ecological fire regimes explain increasing structure loss from Western wildfires. *PNAS Nexus*, *2*(3), pgad005. https://doi.org/10.1093/pnasnexus/pgad005

Iglesias, V., Balch, J. K., & Travis, W. R. (2022). U.S. fires became larger, more frequent, and more widespread in the 2000s. *Science Advances*, *8*(11), eabc0020. https://doi.org/10.1126/sciadv.abc0020

Iglesias, V., Braswell, A. E., Rossi, M. W., Joseph, M. B., McShane, C., Cattau, M., Koontz, M. J., McGlinchy, J., Nagy, R. C., Balch, J., Leyk, S., & Travis, W. R. (2021). Risky Development: Increasing Exposure to Natural Hazards in the United States. *Earth's Future*, *9*(7), e2020EF001795. https://doi.org/10.1029/2020EF001795

Immitzer, M., Link to external site, this link will open in a new window, Neuwirth, M., Böck, S., Brenner, H., Vuolo, F., Atzberger, C., & Link to external site, this link will open in a new window. (2019). Optimal Input Features for Tree Species Classification in Central Europe Based on Multi-Temporal Sentinel-2 Data. *Remote Sensing*, *11*(22), 2599. http://dx.doi.org.colorado.idm.oclc.org/10.3390/rs11222599

Jiang, W., Ni, Y., Pang, Z., He, G., Fu, J., Lu, J., Yang, K., Long, T., & Lei, T. (2020). A NEW INDEX FOR IDENTIFYING WATER BODY FROM SENTINEL-2 SATELLITE REMOTE SENSING IMAGERY. *ISPRS Annals of the*

Photogrammetry, Remote Sensing and Spatial Information Sciences, *V-3–2020*, 33–38. https://doi.org/10.5194/isprs-annals-V-3-2020-33-2020

Johnson, R. M. (2023). *Help build the Protected Areas Database of the United States (PAD-US)* (Report Nos. 2023–3013; Fact Sheet). USGS Publications Warehouse. https://doi.org/10.3133/fs20233013

Karasiak, N., Dejoux, J.-F., Monteil, C., & Sheeren, D. (2021). Spatial dependence between training and test sets: Another pitfall of classification accuracy assessment in remote sensing. *Machine Learning*. https://doi.org/10.1007/s10994-021-05972-1

Kaufman, Y. J., Justice, C. O., Flynn, L. P., Kendall, J. D., Prins, E. M., Giglio, L., Ward, D. E., Menzel, W. P., & Setzer, A. W. (1998). Potential global fire monitoring from EOS-MODIS. *Journal of Geophysical Research: Atmospheres*, *103*(D24), 32215–32238. https://doi.org/10.1029/98JD01644

Kaye, M. W. (2011). Mesoscale synchrony in quaking aspen establishment across the interior western US. *Forest Ecology and Management*, *262*(3), 389–397. https://doi.org/10.1016/j.foreco.2011.04.003

Keane, R. E. (2015). *Wildland Fuel Fundamentals and Applications*. Springer International Publishing. https://doi.org/10.1007/978-3-319-09015-3

Keeley, J. E. (2009). Fire intensity, fire severity and burn severity: A brief review and suggested usage. *International Journal of Wildland Fire*, *18*(1), 116–126. https://doi.org/10.1071/WF07049

Kimmerer, R. W., & Lake, F. K. (2001). The Role of Indigenous Burning in Land Management. *Journal of Forestry*, *99*(11), 36–41. https://doi.org/10.1093/jof/99.11.36

Kobayashi, N., Tani, H., Wang, X., & Sonobe, R. (2020). Crop classification using spectral indices derived from Sentinel-2A imagery. *Journal of Information and Telecommunication*, *4*(1), 67–90. https://doi.org/10.1080/24751839.2019.1694765

Kollert, A., Bremer, M., Löw, M., & Rutzinger, M. (2021). Exploring the potential of land surface phenology and seasonal cloud free composites of one year of Sentinel-2 imagery for tree species mapping in a mountainous region. *International Journal of Applied Earth Observation and Geoinformation*, *94*, 102208. https://doi.org/10.1016/j.jag.2020.102208

Krasnow, K. D., & Stephens, S. L. (2015). Evolving paradigms of aspen ecology and management: Impacts of stand condition and fire severity on vegetation dynamics. *Ecosphere; Washington*, *6*(1), Article 1. http://dx.doi.org.colorado.idm.oclc.org/10.1890/ES14-00354.1

Krawchuk, M. A., Cumming, S. G., Flannigan, M. D., & Wein, R. W. (2006). Biotic and Abiotic Regulation of Lightning Fire Initiation in the Mixedwood Boreal Forest. *Ecology*, *87*(2), 458–468. https://doi.org/10.1890/05-1021

Kulakowski, D., Kaye, M. W., & Kashian, D. M. (2013). Long-term aspen cover change in the western US. *Forest Ecology and Management*, *299*, 52–59. https://doi.org/10.1016/j.foreco.2013.01.004

Kulakowski, D., Veblen, T. T., & Drinkwater, S. (2004). The Persistence of Quaking Aspen (populus Tremuloides) in the Grand Mesa Area, Colorado. *Ecological Applications*, *14*(5), 1603–1614. https://doi.org/10.1890/03-5160

Lake, F. K., Wright, V., Morgan, P., McFadzen, M., McWethy, D., & Stevens-Rumann, C. (2017). Returning Fire to the Land: Celebrating Traditional Knowledge and Fire. *Journal of Forestry*, *115*(5), 343–353. https://doi.org/10.5849/jof.2016-043R2

Landhäusser, S. M., Deshaies, D., & Lieffers, V. J. (2010). Disturbance facilitates rapid range expansion of aspen into higher elevations of the Rocky Mountains under a warming climate. *Journal of Biogeography*, *37*(1), Article 1. https://doi.org/10.1111/j.1365-2699.2009.02182.x

Landhäusser, S. M., Pinno, B. D., & Mock, K. E. (2019). Tamm Review: Seedling-based ecology, management, and restoration in aspen (Populus tremuloides). *Forest Ecology and Management*, *432*, 231–245. https://doi.org/10.1016/j.foreco.2018.09.024

Laurent, P., Mouillot, F., Moreno, M. V., Yue, C., & Ciais, P. (2019). Varying relationships between fire radiative power and fire size at a global scale. *Biogeosciences*, *16*(2), 275–288. https://doi.org/10.5194/bg-16-275-2019

Lechner, M., Dostálová, A., Hollaus, M., Atzberger, C., & Immitzer, M. (2022). Combination of Sentinel-1 and Sentinel-2 Data for Tree Species Classification in a Central European Biosphere Reserve. *Remote Sensing*, *14*(2687), 2687. https://doi.org/10.3390/rs14112687

Li, F., Zhang, X., & Kondragunta, S. (2020). Biomass Burning in Africa: An Investigation of Fire Radiative Power Missed by MODIS Using the 375 m VIIRS Active Fire Product. *Remote Sensing*, *12*(10), Article 10. https://doi.org/10.3390/rs12101561

Li, F., Zhang, X., Kondragunta, S., & Csiszar, I. (2018). Comparison of Fire Radiative Power Estimates From VIIRS and MODIS Observations. *Journal of Geophysical Research: Atmospheres*, *123*(9), 4545–4563. https://doi.org/10.1029/2017JD027823

Li, F., Zhang, X., Roy, D. P., & Kondragunta, S. (2019). Estimation of biomass-burning emissions by fusing the fire radiative power retrievals from polar-orbiting and geostationary satellites across the conterminous United States. *Atmospheric Environment*, *211*, 274–287. https://doi.org/10.1016/j.atmosenv.2019.05.017

Li, H., Shi, Q., Wan, Y., Shi, H., & Imin, B. (2021). Using Sentinel-2 Images to Map the Populus euphratica Distribution Based on the Spectral Difference Acquired at the Key Phenological Stage. *Forests*, *12*(2), Article 2. https://doi.org/10.3390/f12020147

Lin, S., Li, J., Liu, Q., Li, L., Zhao, J., & Yu, W. (2019). Evaluating the Effectiveness of Using Vegetation Indices Based on Red-Edge Reflectance from Sentinel-2 to Estimate Gross Primary Productivity. *Remote Sensing*, *11*(11), Article 11. https://doi.org/10.3390/rs11111303

Liu, Y., Gong, W., Hu, X., & Gong, J. (2018). Forest Type Identification with Random Forest Using Sentinel-1A, Sentinel-2A, Multi-Temporal Landsat-8 and DEM Data. *Remote Sensing*, *10*(6), Article 6. https://doi.org/10.3390/rs10060946

Long, J. N., & Mock, K. (2012). Changing perspectives on regeneration ecology and genetic diversity in western quaking aspen: Implications for silviculture. *Canadian Journal of Forest Research*, *42*(12), 2011–2021. https://doi.org/10.1139/x2012-143

Macintyre, P., van Niekerk, A., & Mucina, L. (2020). Efficacy of multi-season Sentinel-2 imagery for compositional vegetation classification. *International Journal of Applied Earth Observation and Geoinformation*, *85*, 101980. https://doi.org/10.1016/j.jag.2019.101980

Mahmoud, H. (2024). Reimagining a pathway to reduce built-environment loss during wildfires. *Cell Reports Sustainability*, *1*(6). https://doi.org/10.1016/j.crsus.2024.100121

Marlon, J. R., Bartlein, P. J., Gavin, D. G., Long, C. J., Anderson, R. S., Briles, C. E., Brown, K. J., Colombaroli, D., Hallett, D. J., Power, M. J., Scharf, E. A., & Walsh, M. K. (2012). Long-term perspective on wildfires in the western USA. *Proceedings of the National Academy of Sciences*, *109*(9), E535–E543. https://doi.org/10.1073/pnas.1112839109

McFarland, J. R., Coop, J. D., Balik, J. A., Rodman, K. C., Parks, S. A., & Stevens-Rumann, C. S. (2025). Extreme Fire Spread Events Burn More Severely and Homogenize Postfire Landscapes in the Southwestern United States. *Global Change Biology*, *31*(2), e70106. https://doi.org/10.1111/gcb.70106

Meier, G. A., Brown, J. F., Evelsizer, R. J., & Vogelmann, J. E. (2015). Phenology and climate relationships in aspen (Populus tremuloides Michx.) forest and woodland communities of southwestern Colorado. *Ecological Indicators*, *48*, 189–197. https://doi.org/10.1016/j.ecolind.2014.05.033

Meigs, G. W., & Krawchuk, M. A. (2018). Composition and Structure of Forest Fire Refugia: What Are the Ecosystem Legacies across Burned Landscapes? *Forests*, *9*(5), Article 5. https://doi.org/10.3390/f9050243

Morris, J. L., DeRose, R. J., Brussel, T., Brewer, S., Brunelle, A., & Long, J. N. (2019). Stable or seral? Fire-driven alternative states in aspen forests of western North America. *Biology Letters*, *15*(6), 20190011. https://doi.org/10.1098/rsbl.2019.0011

Mullissa, A., Vollrath, A., Odongo-Braun, C., Slagter, B., Balling, J., Gou, Y., Gorelick, N., & Reiche, J. (2021). Sentinel-1 SAR Backscatter Analysis Ready Data Preparation in Google Earth Engine. *Remote Sensing*, *13*(1954), 1954. https://doi.org/10.3390/rs13101954

Nagy, R. C., Fusco, E., Bradley, B., Abatzoglou, J. T., & Balch, J. (2018). Human-Related Ignitions Increase the Number of Large Wildfires across U.S. Ecoregions. *Fire*, *1*(1), Article 1. https://doi.org/10.3390/fire1010004

Nembrini, S., König, I. R., & Wright, M. N. (2018). The revival of the Gini importance? *Bioinformatics*, *34*(21), 3711–3718. https://doi.org/10.1093/bioinformatics/bty373

Nesbit, K. A., Yocom, L. L., Trudgeon, A. M., DeRose, R. J., & Rogers, P. C. (2023). Tamm review: Quaking aspen's influence on fire occurrence, behavior, and severity. *Forest Ecology and Management*, *531*, 120752. https://doi.org/10.1016/j.foreco.2022.120752

Niekerk, J. van, Bakka, H., Rue, H., & Schenk, O. (2019). *New frontiers in Bayesian modeling using the INLA package in R* (No. arXiv:1907.10426). arXiv. https://doi.org/10.48550/arXiv.1907.10426

Nigro, K. M., Rocca, M. E., Battaglia, M. A., Coop, J. D., & Redmond, M. D. (2022). Wildfire catalyzes upward range expansion of trembling aspen in southern Rocky Mountain beetle-killed forests. *Journal of Biogeography*, *49*(1), 201–214. https://doi.org/10.1111/jbi.14302

Numbisi, F. N., Numbisi, F. N., Coillie, F. V., & Wulf, R. D. (2018). MULTI-DATE SENTINEL1 SAR IMAGE TEXTURES DISCRIMINATE PERENNIAL AGROFORESTS IN A TROPICAL FOREST-SAVANNAH TRANSITION LANDSCAPE. *The International Archives of the Photogrammetry, Remote Sensing and Spatial Information Sciences*, *XLII–1*, 339–346. https://doi.org/10.5194/isprs-archives-XLII-1-339-2018

Parks, S. A., & Abatzoglou, J. T. (2020). Warmer and Drier Fire Seasons Contribute to Increases in Area Burned at High Severity in Western US Forests From 1985 to 2017. *Geophysical Research Letters*, *47*(22), e2020GL089858. https://doi.org/10.1029/2020GL089858

Parks, S. A., Guiterman, C. H., Margolis, E. Q., Lonergan, M., Whitman, E., Abatzoglou, J. T., Falk, D. A., Johnston, J. D., Daniels, L. D., Lafon, C. W., Loehman, R. A., Kipfmueller, K. F., Naficy, C. E., Parisien, M.-A., Portier, J., Stambaugh, M. C., Williams, A. P., Wion, A. P., & Yocom, L. L. (2025). A fire deficit persists across diverse North American forests despite recent increases in area burned. *Nature Communications*, *16*(1), 1493. https://doi.org/10.1038/s41467-025-56333-8

Parks, S. A., Holsinger, L. M., Blankenship, K., Dillon, G. K., Goeking, S. A., & Swaty, R. (2023). Contemporary wildfires are more severe compared to the historical reference period in western US dry conifer forests. *Forest Ecology and Management*, *544*, 121232. https://doi.org/10.1016/j.foreco.2023.121232

Parks, S. A., Holsinger, L. M., Koontz, M. J., Collins, L., Whitman, E., Parisien, M.-A., Loehman, R. A., Barnes, J. L., Bourdon, J.-F., Boucher, J., Boucher, Y., Caprio, A. C., Collingwood, A., Hall, R. J., Park, J., Saperstein, L. B., Smetanka, C., Smith, R. J., & Soverel, N. (2019). Giving Ecological Meaning to Satellite-Derived Fire Severity Metrics across North American Forests. *Remote Sensing*, *11*(14), Article 14. https://doi.org/10.3390/rs11141735

Pasquarella, V. J., Brown, C. F., Czerwinski, W., & Rucklidge, W. J. (2023). Comprehensive quality assessment of optical satellite imagery using weakly supervised video learning. *2023 IEEE/CVF Conference on Computer Vision* *and Pattern Recognition Workshops (CVPRW)*, 2125–2135. https://doi.org/10.1109/CVPRW59228.2023.00206

Penman, T. D., Collins, L., Syphard, A. D., Keeley, J. E., & Bradstock, R. A. (2014). Influence of Fuels, Weather and the Built Environment on the Exposure of Property to Wildfire. *PLOS ONE*, *9*(10), e111414. https://doi.org/10.1371/journal.pone.0111414

Persson, M., Lindberg, E., & Reese, H. (2018). Tree Species Classification with Multi-Temporal Sentinel-2 Data. *Remote Sensing*, *10*(11), Article 11. https://doi.org/10.3390/rs10111794

Phiri, D., Simwanda, M., Salekin, S., Nyirenda, V. R., Murayama, Y., & Ranagalage, M. (2020). Sentinel-2 Data for Land Cover/Use Mapping: A Review. *Remote Sensing*, *12*(14), Article 14. https://doi.org/10.3390/rs12142291

Picotte, J. J., Dockter, D., Long, J., Tolk, B., Davidson, A., & Peterson, B. (2019). LANDFIRE Remap Prototype Mapping Effort: Developing a New Framework for Mapping Vegetation Classification, Change, and Structure. *Fire*, *2*(2), 35. https://doi.org/10.3390/fire2020035

Prichard, S. J., Hessburg, P. F., Hagmann, R. K., Povak, N. A., Dobrowski, S. Z., Hurteau, M. D., Kane, V. R., Keane, R. E., Kobziar, L. N., Kolden, C. A., North, M., Parks, S. A., Safford, H. D., Stevens, J. T., Yocom, L. L., Churchill, D. J., Gray, R. W., Huffman, D. W., Lake, F. K., & Khatri-Chhetri, P. (2021). Adapting western North American forests to climate change and wildfires: 10 common questions. *Ecological Applications*, *31*(8), e02433. https://doi.org/10.1002/eap.2433

R Core Team. (2022). *R: A Language and Environment for Statistical Computing*. R Foundation for Statistical Computing. https://www.R-project.org/

R Core Team. (2024). *R: A Language and Environment for Statistical Computing*. R Foundation for Statistical Computing. https://www.R-project.org/

R. K. Peete. (1988). Forest and Meadows of the Rocky Mountains. In *North American terrestrial vegetation* (M.G. Barbour&W.D. Billings (editors), pp. 63–102). Cambridge University Press, New York, NY.

Radeloff, V. C., Helmers, D. P., Kramer, H. A., Mockrin, M. H., Alexandre, P. M., Bar-Massada, A., Butsic, V., Hawbaker, T. J., Martinuzzi, S., Syphard, A. D., & Stewart, S. I. (2018). Rapid growth of the US wildland-urban interface raises wildfire risk. *Proceedings of the National Academy of Sciences*, *115*(13), 3314–3319. https://doi.org/10.1073/pnas.1718850115

Radeloff, V. C., Mockrin, M. H., Helmers, D., Carlson, A., Hawbaker, T. J., Martinuzzi, S., Schug, F., Alexandre, P. M., Kramer, H. A., & Pidgeon, A. M. (2023). Rising wildfire risk to houses in the United States, especially in grasslands and shrublands. *Science*, *382*(6671), 702–707. https://doi.org/10.1126/science.ade9223

Rehfeldt, G. E., Ferguson, D. E., & Crookston, N. L. (2009). Aspen, climate, and sudden decline in western USA. *Forest Ecology and Management*, *258*(11), Article 11. https://doi.org/10.1016/j.foreco.2009.06.005

Riley, K. L., Grenfell, I. C., Finney, M. A., & Wiener, J. M. (2021). TreeMap, a tree-level model of conterminous US forests circa 2014 produced by imputation of FIA plot data. *Scientific Data*, *8*(1), Article 1. https://doi.org/10.1038/s41597-020-00782-x

Riley, K. L., Grenfell, I. C., Shaw, J. D., & Finney, M. A. (2022). TreeMap 2016 Dataset Generates CONUS-Wide Maps of Forest Characteristics Including Live Basal Area, Aboveground Carbon, and Number of Trees per Acre. *JOURNAL OF FORESTRY*. Science Citation Index Expanded. https://doi.org/10.1093/jofore/fvac022

Roberts, G., Wooster, M. J., Lauret, N., Gastellu-Etchegorry, J.-P., Lynham, T., & McRae, D. (2018). Investigating the impact of overlying vegetation canopy structures on fire radiative power (FRP) retrieval through simulation and measurement. *Remote Sensing of Environment*, *217*, 158–171. https://doi.org/10.1016/j.rse.2018.08.015

Rogers, P. C., Landhäusser, S. M., Pinno, B. D., & Ryel, R. J. (2014). A Functional Framework for Improved Management of Western North American Aspen (Populus tremuloides Michx.). *Forest Science; Bethesda*, *60*(2), Article 2.

Rogers, P. C., Leffler, A. J., & Ryel, R. J. (2010). Landscape assessment of a stable aspen community in southern Utah, USA. *Forest Ecology and Management*, *259*(3), 487–495. https://doi.org/10.1016/j.foreco.2009.11.005

Rogers, P. C., Pinno, B. D., Šebesta, J., Albrectsen, B. R., Li, G., Ivanova, N., Kusbach, A., Kuuluvainen, T., Landhäusser, S. M., Liu, H., Myking, T., Pulkkinen, P., Wen, Z., & Kulakowski, D. (2020). A global view of aspen: Conservation science for widespread keystone systems. *Global Ecology and Conservation*, *21*, e00828. https://doi.org/10.1016/j.gecco.2019.e00828

Roos, C. I., Guiterman, C. H., Margolis, E. Q., Swetnam, T. W., Laluk, N. C., Thompson, K. F., Toya, C., Farris, C. A., Fulé, P. Z., Iniguez, J. M., Kaib, J. M., O'Connor, C. D., & Whitehair, L. (2022). Indigenous fire management and cross-scale fire-climate relationships in the Southwest United States from 1500 to 1900 CE. *Science Advances*, *8*(49), eabq3221. https://doi.org/10.1126/sciadv.abq3221

Rosenblum, A. (2015). Altered Fire Regimes and the Persistence of Quaking Aspen in the Rocky Mountains: A Literature Review. *Open Journal of Forestry*, *5*(5), Article 5. https://doi.org/10.4236/ojf.2015.55050

Roy, D. P., Boschetti, L., & Trigg, S. N. (2006). Remote sensing of fire severity: Assessing the performance of the normalized burn ratio. *IEEE Geoscience and Remote Sensing Letters*, *3*(1), 112–116. IEEE Geoscience and Remote Sensing Letters. https://doi.org/10.1109/LGRS.2005.858485

Rue, H., Martino, S., & Chopin, N. (2009). Approximate Bayesian Inference for Latent Gaussian Models by Using Integrated Nested Laplace Approximations. *Journal of the Royal Statistical Society. Series B (Statistical Methodology)*, *71*(2), 319–392.

Sadykova, D., Scott, B. E., De Dominicis, M., Wakelin, S. L., Sadykov, A., & Wolf, J. (2017). Bayesian joint models with INLA exploring marine mobile predator–

prey and competitor species habitat overlap. *Ecology and Evolution*, *7*(14), 5212–5226. https://doi.org/10.1002/ece3.3081

Scholten, R. C., Veraverbeke, S., Chen, Y., & Randerson, J. T. (2024). Spatial variability in Arctic–boreal fire regimes influenced by environmental and human factors. *Nature Geoscience*, *17*(9), 866–873. https://doi.org/10.1038/s41561-024-01505-2

Schroeder, W., Csiszar, I., Giglio, L., & Schmidt, C. C. (2010). On the use of fire radiative power, area, and temperature estimates to characterize biomass burning via moderate to coarse spatial resolution remote sensing data in the Brazilian Amazon. *Journal of Geophysical Research: Atmospheres*, *115*(D21). https://doi.org/10.1029/2009JD013769

Schroeder, W., Oliva, P., Giglio, L., & Csiszar, I. A. (2014). The New VIIRS 375m active fire detection data product: Algorithm description and initial assessment. *Remote Sensing of Environment*, *143*, 85–96. https://doi.org/10.1016/j.rse.2013.12.008

Schug, F., Bar-Massada, A., Carlson, A. R., Cox, H., Hawbaker, T. J., Helmers, D., Hostert, P., Kaim, D., Kasraee, N. K., Martinuzzi, S., Mockrin, M. H., Pfoch, K. A., & Radeloff, V. C. (2023). The global wildland–urban interface. *Nature*, *621*(7977), 94–99. https://doi.org/10.1038/s41586-023-06320-0

Schultz, C. A., McCaffrey, S. M., & Huber-Stearns, H. R. (2019). Policy barriers and opportunities for prescribed fire application in the western United States. *International Journal of Wildland Fire*, *28*(11), 874–884. https://doi.org/10.1071/WF19040

Shepperd, W. (1990). A Classification of Quaking Aspen in the Central Rocky Mountains Based on Growth and Stand Characteristics. *Western Journal of Applied Forestry*, *5*, 69–75. https://doi.org/10.1093/wjaf/5.3.69

Shepperd, W. D., Smith, F. W., & Pelz, K. A. (2015). Group Clearfell Harvest Can Promote Regeneration of Aspen Forests Affected by Sudden Aspen Decline in Western Colorado. *Forest Science*, *61*(5), 932–937.

Shinneman, D. J., Baker, W. L., Rogers, P. C., & Kulakowski, D. (2013). Fire regimes of quaking aspen in the Mountain West. *Forest Ecology and Management*, *299*, 22–34. https://doi.org/10.1016/j.foreco.2012.11.032

Shinneman, D. J., & McIlroy, S. K. (2019). Climate and disturbance influence self-sustaining stand dynamics of aspen (Populus tremuloides) near its range margin. *Ecological Applications*, *29*(6), e01948. https://doi.org/10.1002/eap.1948

St. Denis, L. A., Short, K. C., McConnell, K., Cook, M. C., Mietkiewicz, N. P., Buckland, M., & Balch, J. K. (2023). All-hazards dataset mined from the US National Incident Management System 1999–2020. *Scientific Data*, *10*(1), Article 1. https://doi.org/10.1038/s41597-023-01955-0

Stavros, E. N., Gezon, C., St. Denis, L., Iglesias, V., Zapata, C., Byrne, M., Cooper, L., Cook, M., Doyle, E., Stephens, J., Tapia, M., Tuff, T., Thomas, E., Maxted, S. J., Sen, R., & Balch, J. K. (2023). Environmental Resilience Technology:

Sustainable Solutions Using Value-Added Analytics in a Changing World. *Applied Sciences*, *13*(19), Article 19. https://doi.org/10.3390/app131911034
Steinhausen, M. J., Wagner, P. D., Narasimhan, B., & Waske, B. (2018). Combining Sentinel-1 and Sentinel-2 data for improved land use and land cover mapping of monsoon regions. *International Journal of Applied Earth Observation and Geoinformation*, *73*, 595–604. https://doi.org/10.1016/j.jag.2018.08.011
Stephens, J. J., Joseph, M. B., Iglesias, V., Tuff, T. A., Mahood, A. L., Rangwala, I., Wolken, J., & Balch, J. K. (n.d.). *"Fires of Unusual Size: Future of Extreme and Emerging Wildfires in a Warming United States (2020-2060)."* Retrieved February 21, 2025, from https://www.authorea.com/users/705887/articles/691394--fires-of-unusual-size-future-of-extreme-and-emerging-wildfires-in-a-warming-united-states-2020-2060
Stephens, S. L., Moghaddas, J. J., Edminster, C., Fiedler, C. E., Haase, S., Harrington, M., Keeley, J. E., Knapp, E. E., McIver, J. D., Metlen, K., Skinner, C. N., & Youngblood, A. (2009). Fire treatment effects on vegetation structure, fuels, and potential fire severity in western U.S. forests. *Ecological Applications*, *19*(2), 305–320. https://doi.org/10.1890/07-1755.1
Stevens-Rumann, C. S., Kemp, K. B., Higuera, P. E., Harvey, B. J., Rother, M. T., Donato, D. C., Morgan, P., & Veblen, T. T. (2018). Evidence for declining forest resilience to wildfires under climate change. *Ecology Letters*, *21*(2), 243–252. https://doi.org/10.1111/ele.12889
Swain, D. L., Abatzoglou, J. T., Kolden, C., Shive, K., Kalashnikov, D. A., Singh, D., & Smith, E. (2023). Climate change is narrowing and shifting prescribed fire windows in western United States. *Communications Earth & Environment*, *4*(1), 1–14. https://doi.org/10.1038/s43247-023-00993-1
Syphard, A. D., Rustigian-Romsos, H., Mann, M., Conlisk, E., Moritz, M. A., & Ackerly, D. (2019). The relative influence of climate and housing development on current and projected future fire patterns and structure loss across three California landscapes. *Global Environmental Change*, *56*(C). https://doi.org/10.1016/j.gloenvcha.2019.03.007
Szpakowski, D. M., & Jensen, J. L. R. (2019). A Review of the Applications of Remote Sensing in Fire Ecology. *Remote Sensing*, *11*(22), Article 22. https://doi.org/10.3390/rs11222638
Tepley, A. J., & Veblen, T. T. (2015). Spatiotemporal fire dynamics in mixed-conifer and aspen forests in the San Juan Mountains of southwestern Colorado, USA. *Ecological Monographs*, *85*(4), 583–603. https://doi.org/10.1890/14-1496.1
The Fireshed Registry: Fireshed and subfireshed boundaries for the continental United States and Alaska (3rd Edition). (n.d.). Retrieved March 2, 2025, from https://www.fs.usda.gov/rds/archive/catalog/RDS-2020-0054-3
Theobald, D. M., Harrison-Atlas, D., Monahan, W. B., & Albano, C. M. (2015). Ecologically-Relevant Maps of Landforms and Physiographic Diversity for

Climate Adaptation Planning. *PLOS ONE*, *10*(12), e0143619. https://doi.org/10.1371/journal.pone.0143619
Thompson, M. P., Liu, Z., Wei, Y., Caggiano, M. D., Thompson, M. P., Liu, Z., Wei, Y., & Caggiano, M. D. (2018). Analyzing Wildfire Suppression Difficulty in Relation to Protection Demand. In *Environmental Risks*. IntechOpen. https://doi.org/10.5772/intechopen.76937
Udali, A., Lingua, E., & Persson, H. J. (2021). Assessing Forest Type and Tree Species Classification Using Sentinel-1 C-Band SAR Data in Southern Sweden. *Remote Sensing*, *13*(16), Article 16. https://doi.org/10.3390/rs13163237
Uhl, J. H., & Leyk, S. (2022). A framework for scale-sensitive, spatially explicit accuracy assessment of binary built-up surface layers. *Remote Sensing of Environment*, *279*, 113117. https://doi.org/10.1016/j.rse.2022.113117
Wang, H.-H., Finney, M. A., Song, Z.-L., Wang, Z.-S., & Li, X.-C. (2021). Ecological techniques for wildfire mitigation: Two distinct fuelbreak approaches and their fusion. *Forest Ecology and Management*, *495*, 119376. https://doi.org/10.1016/j.foreco.2021.119376
Wehrens, R., & Buydens, L. M. C. (2007). Self- and Super-organizing Maps in R: The kohonen Package. *Journal of Statistical Software*, *21*, 1–19. https://doi.org/10.18637/jss.v021.i05
Wildfire Risk to Communities: Spatial datasets of landscape-wide wildfire risk components for the United States (2nd Edition). (n.d.). Retrieved March 2, 2025, from https://www.fs.usda.gov/rds/archive/catalog/RDS-2020-0016-2
Wong, C. Y. S., D'Odorico, P., Bhathena, Y., Arain, M. A., & Ensminger, I. (2019). Carotenoid based vegetation indices for accurate monitoring of the phenology of photosynthesis at the leaf-scale in deciduous and evergreen trees. *Remote Sensing of Environment*, *233*, 111407. https://doi.org/10.1016/j.rse.2019.111407
Wooster, M. J., Roberts, G. J., Giglio, L., Roy, D. P., Freeborn, P. H., Boschetti, L., Justice, C., Ichoku, C., Schroeder, W., Davies, D., Smith, A. M. S., Setzer, A., Csiszar, I., Strydom, T., Frost, P., Zhang, T., Xu, W., de Jong, M. C., Johnston, J. M., … San-Miguel-Ayanz, J. (2021). Satellite remote sensing of active fires: History and current status, applications and future requirements. *Remote Sensing of Environment*, *267*, 112694. https://doi.org/10.1016/j.rse.2021.112694
Wooster, M. J., Zhukov, B., & Oertel, D. (2003). Fire radiative energy for quantitative study of biomass burning: Derivation from the BIRD experimental satellite and comparison to MODIS fire products. *Remote Sensing of Environment*, *86*(1), 83–107. https://doi.org/10.1016/S0034-4257(03)00070-1
Worrall, J. J., Marchetti, S. B., Egeland, L., Mask, R. A., Eager, T., & Howell, B. (2010). Effects and etiology of sudden aspen decline in southwestern Colorado, USA. *Forest Ecology and Management*, *260*(5), 638–648. https://doi.org/10.1016/j.foreco.2010.05.020

Worrall, J. J., Rehfeldt, G. E., Hamann, A., Hogg, E. H., Marchetti, S. B., Michaelian, M., & Gray, L. K. (2013). Recent declines of Populus tremuloides in North America linked to climate. *Forest Ecology and Management*, *299*, 35–51. https://doi.org/10.1016/j.foreco.2012.12.033

Zhang, X., Liu, L., Liu, Y., Jayavelu, S., Wang, J., Moon, M., Henebry, G. M., Friedl, M. A., & Schaaf, C. B. (2018). Generation and evaluation of the VIIRS land surface phenology product. *Remote Sensing of Environment*, *216*, 212–229. https://doi.org/10.1016/j.rse.2018.06.047

APPENDIX A: CHAPTER ONE

Phenology of Quaking Aspen across the Southern Rockies

The Southern Rockies study region is an ecologically diverse landscape with complex topography. In complex systems, exploring the phenological patterns of vegetation development is useful when generating seasonal satellite image composites (Kollert et al., 2021). For quaking aspen forests in particular, the timing of canopy growth differs by elevation, slope, and climate (Meier et al., 2015). These differences across a large and diverse region can influence the generation of satellite image composites which are representative of specific phenological stages for this deciduous forest species.

To examine the seasonal variation of canopy development within aspen forests across the Southern Rockies, we summarized phenological metrics from the Visible Infrared Imaging Radiometer Suite (VIIRS) Land Cover Dynamics data product (VNP22Q2), which provides global land surface phenology metrics at yearly intervals since 2013 (Zhang et al., 2018). These include day-of-year (DOY) for the onset of greenness increase, mid-greenup phase, onset of greenness maximum, onset of greenness decrease, mid-senescence phase, and the onset of greenness minimum. For each spatial block, we calculated the median day-of-year for each metric within aspen forest area based on the USFS TreeMap product (see Section 2.3.1 of the main text). Analysis was carried out in the Google Earth Engine (GEE) Code Editor (Gorelick et al., 2017). We examined the variation in the average DOY across spatial blocks (Figure A1) for each metric and calculated the average and standard deviation across blocks and years for the Southern Rockies. The variation in quaking aspen phenology is well-explained by elevation as demonstrated by the inset plots in Figure A1. To capture this variation when selecting temporal windows for creating seasonal image composites, we subtracted the standard deviation (in days) from the metric average (day-of-year) and used these values as start and end dates. Specifically, we defined two temporal windows: summer, or the mid-greenup phase to the onset of greenness decrease; and autumn, or the mid-senescence phase to the onset of greenness minimum.

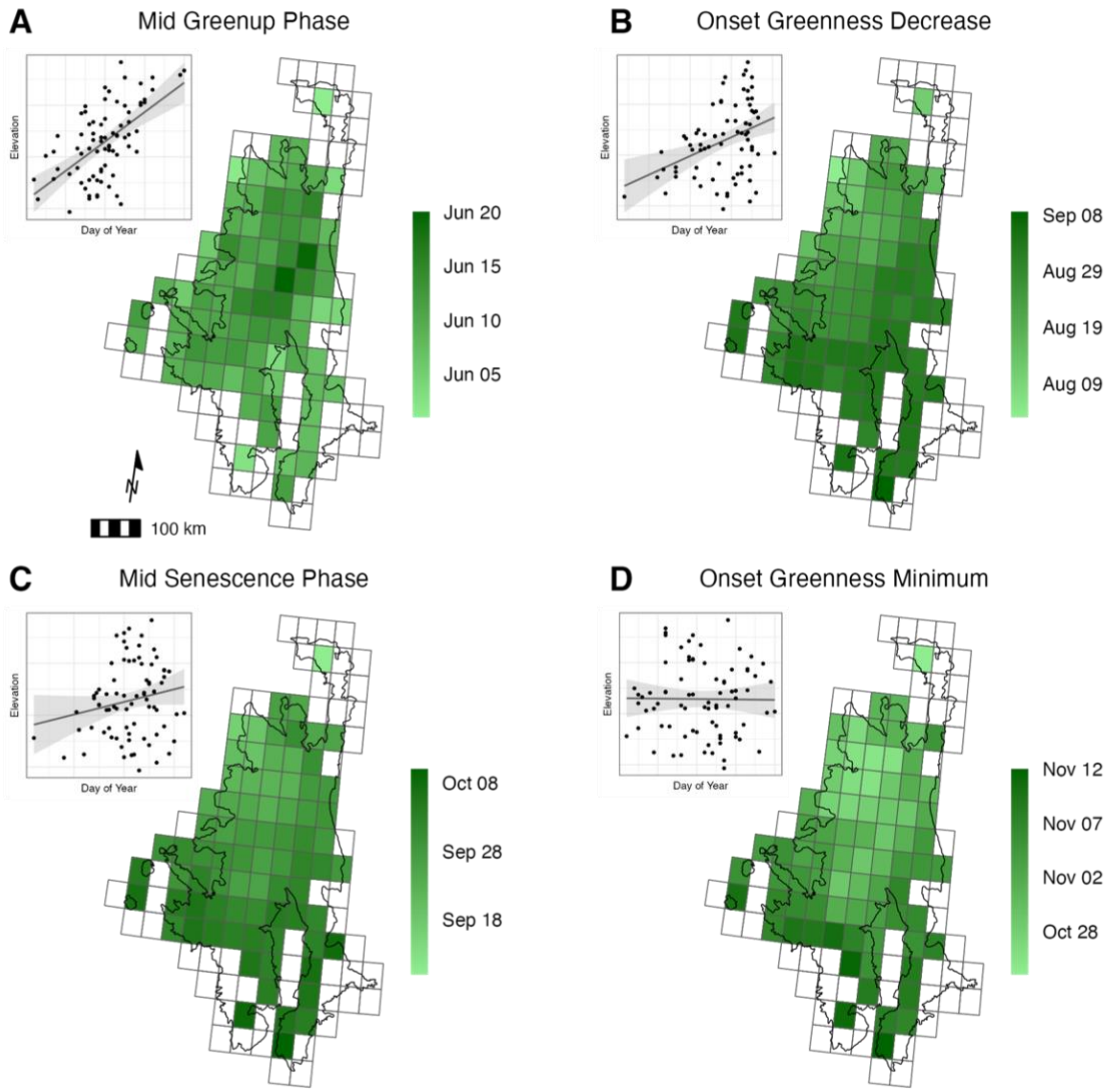

Figure A1. *Quaking aspen phenology derived from the VNP22Q1 in the Southern Rockies and relationship with elevation. Day-of-year estimates represent the median across all years (2013-2022). (**A**) Mid-greenup phase (late May to late June) and (**B**) the onset of greenness decrease (early August to early September) defines the summer temporal window, and both show a strong positive linear relationship with elevation. (**C**) Mid-senescence phase (mid-September to early October) and (**D**) the onset of greenness minimum (late October to mid-November) defines the autumn temporal window. Senescence phase indicates a strong relationship with elevation while the onset of greenness minimum is less influenced by elevation.*

Accuracy Assessment and Optimal Threshold for Classification

To assess model performance and to calculate the optimum threshold for classification based on the probability grids from the random forest classifier, we calculated a confusion matrix for 100 different classification threshold values between 0-1 based on the training data in each of the 10 model iterations. From this, we calculated an AUC-ROC curve which represents the true positive rate against the false positive rate (Figure B1A). To calculate the optimum threshold, we found the maximum F1 score of the average across all 10 model iterations (Figure B1B). We used this optimum threshold on the average probability of aspen forest grid to calculate the binary output (aspen and no aspen).

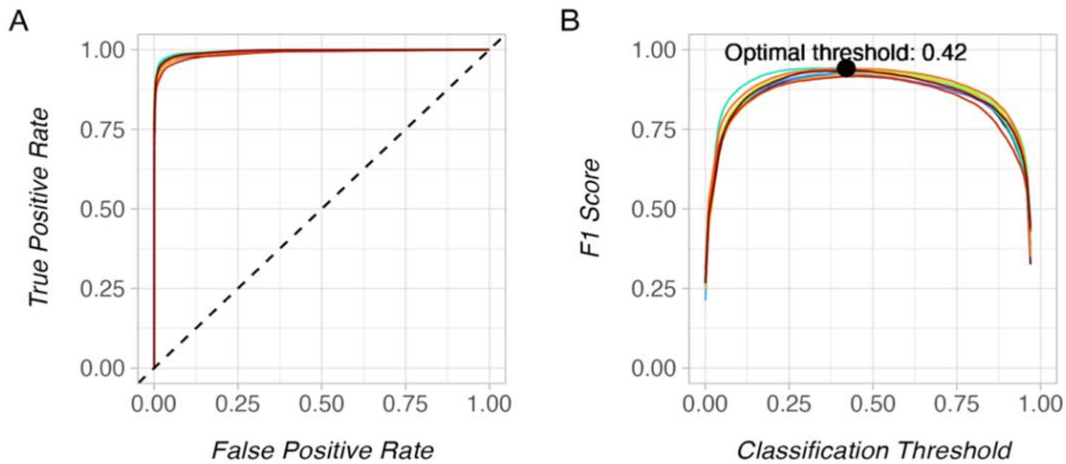

Figure A2. *Model performance metrics from the final classification. (A) AUC-ROC or the true-positive rate against the false-positive rate with colors representing the 10 model iterations; (B) The F1 score across threshold values. The black line is the average across model iterations and the black point represents the location of the maximum F1 from the average across folds. At this point is our optimum threshold for classification (0.42).*

Data associated with this paper are available as public Google Earth Engine assets. An interactive web viewing application provides access to the results and input satellite data (https://maco.users.earthengine.app/view/aspen-viewer). All analyses and code used in this paper are available in a public GitHub repository (https://github.com/maxwellCcook/aspen-fire) and a public Google Earth Engine repository (https://code.earthengine.google.com/?accept_repo=users/maco/aspen-fire).

APPENDIX B: CHAPTER TWO

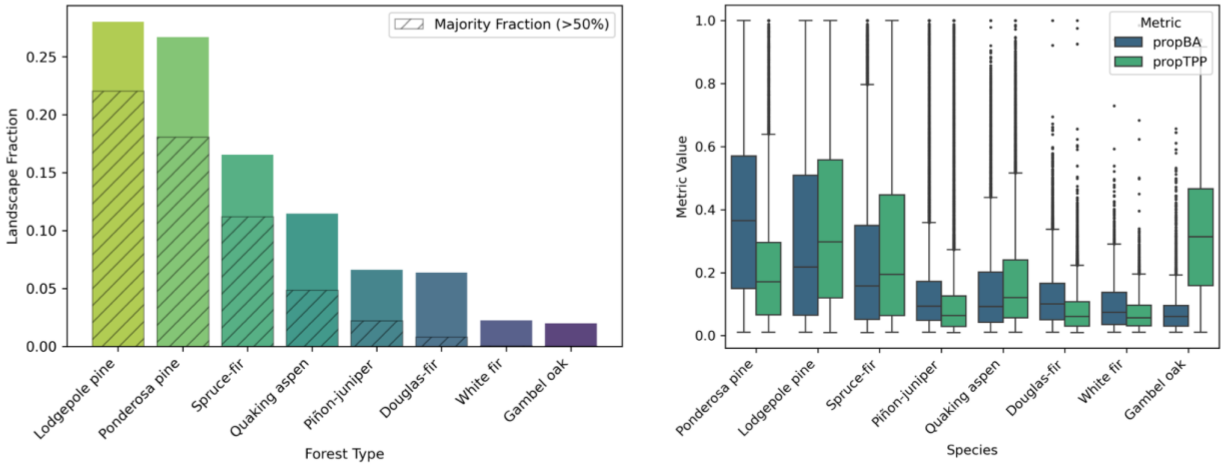

***Figure B1**. (**A**) Predominant forest species groups making up 97% of forested area. Hatching represents the fraction of gridcells where that species is the majority (>50% gridcell forested area). (**B**) Distribution of species structural metrics from the TreeMap Tree Table including the proportion of live basal area (BA) and trees/pixel (TPP).*

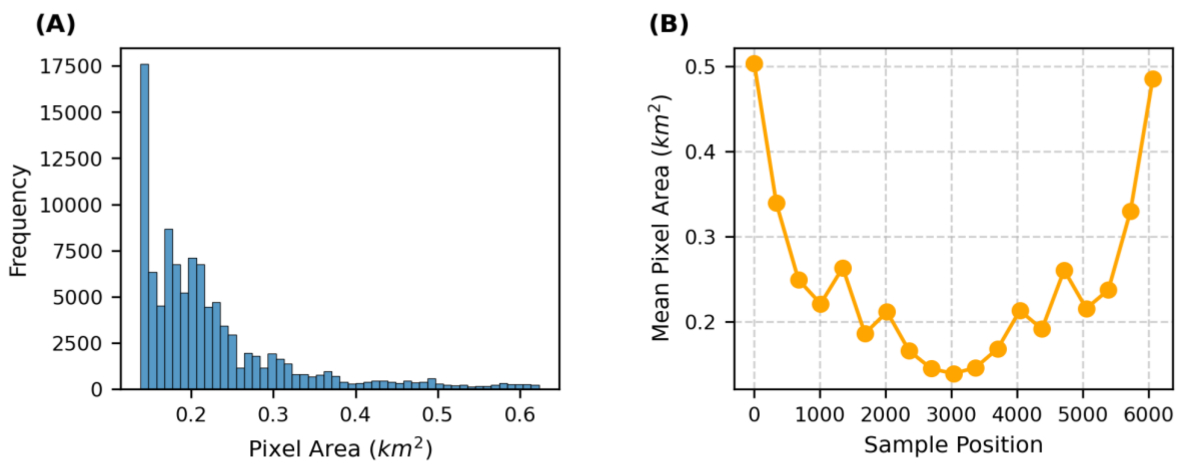

***Figure B2.** (A) Distribution of pixel ground area in square kilometers from VIIRS active fire detections. (B) The mean pixel ground area at each swath sample location. The further off-nadir a pixel is, the greater its ground area.*

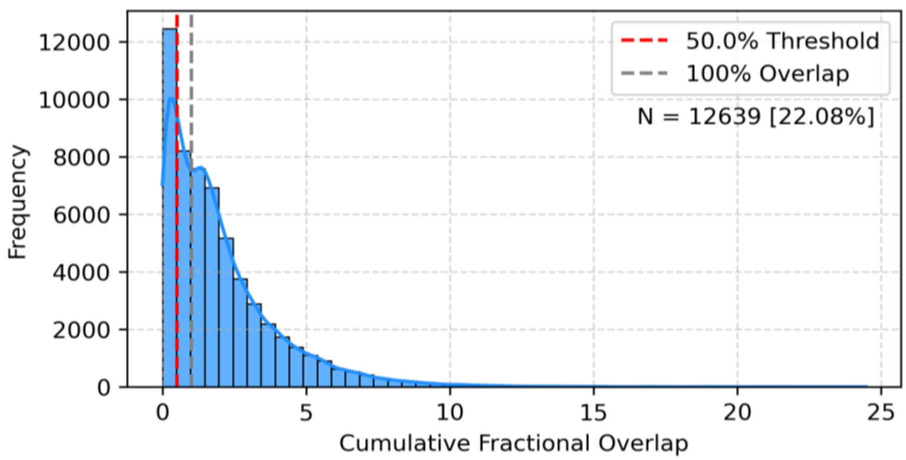

Figure B3. *Distribution of VIIRS pixel area overlaps with the regular 375 m² grid of the Southern Rockies showing the cutoff value (>50% gridcell overlap) as a red dashed line and the 100% overlap threshold as a dashed grey line. Only gridcells with at least 50% overlap with VIIRS detections were retained for the analysis to limit the contributions of gridcells with very small fractional overlap. 12,639 gridcells were removed from the analysis.*

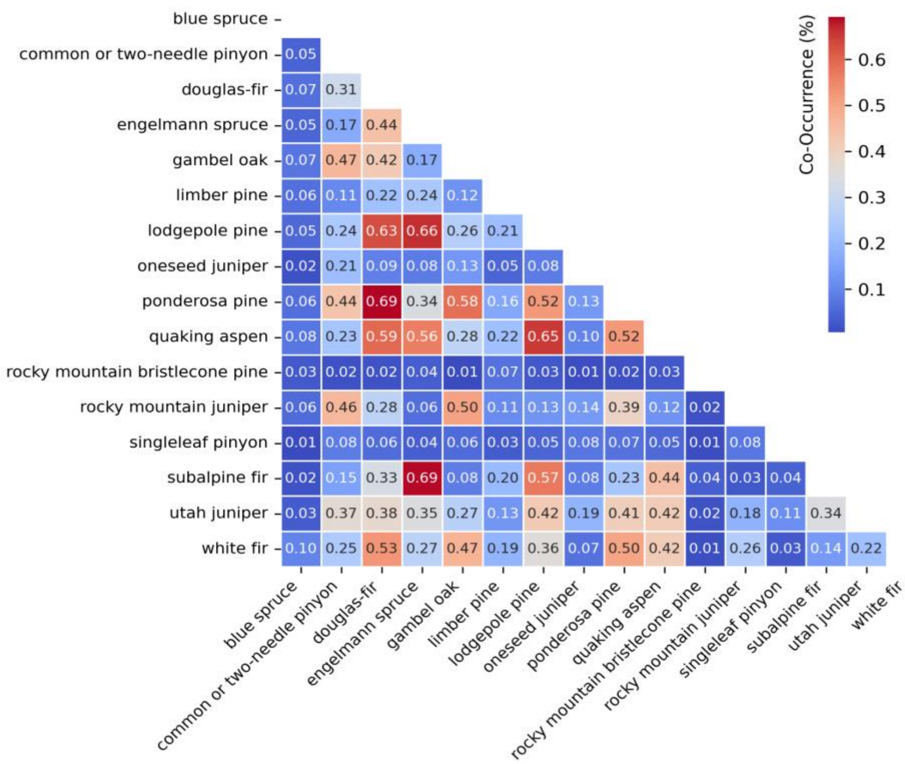

Figure B4*. Observed species co-occurrence matrix from the TreeMap Tree Table for all forest species considered to be common in the Southern Rockies.*

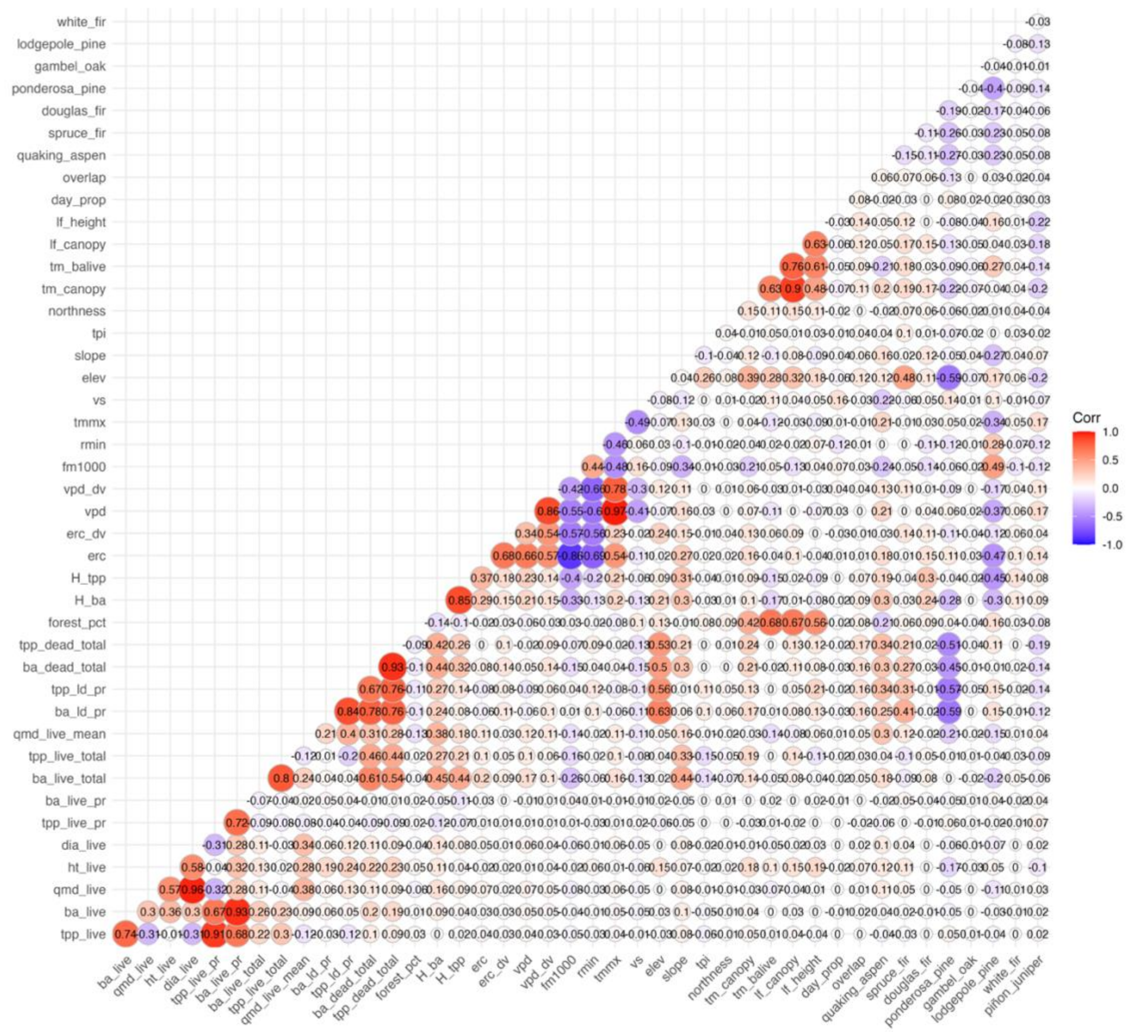

Figure B5. *Correlation matrix for all variables explored for the modeling procedure. Variables which were included in the models were assessed for collinearity.*

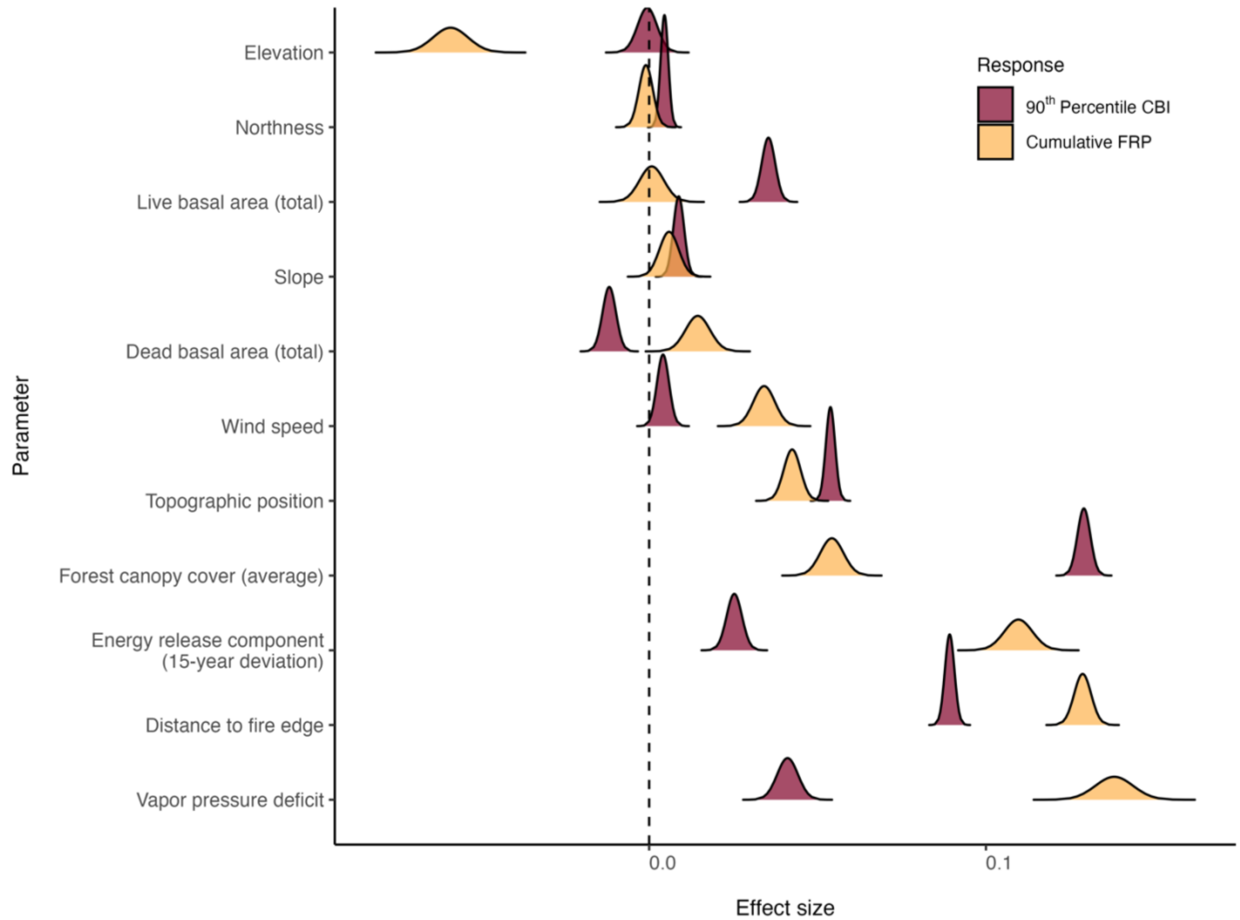

Figure B6. *Posterior distribution of effects for all non-forest type fixed effects.*

Table B1. *Model results for FRPc models including the mean effects and credible intervals, exponentiated effects, and random effects.*

Model Parameter	Mean Effect	SD	0.025 Q	0.975 Q	Exponentiated Mean Effect
(Intercept)	2.095	0.036	2.025	2.165	7.129
fortypnm_gpdouglas_fir	0.094	0.017	0.062	0.127	0.099
fortypnm_gpgambel_oak	-0.082	0.06	-0.2	0.035	-0.079
fortypnm_gplodgepole_pine	0.19	0.011	0.168	0.212	0.209
fortypnm_gppinon_juniper	-0.047	0.017	-0.081	-0.013	-0.046
fortypnm_gpponderosa_pine	0.087	0.012	0.064	0.109	0.09
fortypnm_gpspruce_fir	0.039	0.011	0.016	0.061	0.039
fortypnm_gpwhite_fir	0.163	0.039	0.087	0.238	0.177
fortypnm_gpquaking_aspen:fortyp_pct	-0.084	0.008	-0.099	-0.069	-0.081
fortypnm_gpdouglas_fir:fortyp_pct	0.06	0.015	0.031	0.089	0.062
fortypnm_gpgambel_oak:fortyp_pct	0.03	0.04	-0.05	0.109	0.03

fortypnm_gplodgepole_pine:fortyp_pct	0.055	0.006	0.044	0.067	0.057
fortypnm_gppinon_juniper:fortyp_pct	-0.012	0.011	-0.034	0.009	-0.012
fortypnm_gpponderosa_pine:fortyp_pct	0.017	0.005	0.007	0.026	0.017
fortypnm_gpspruce_fir:fortyp_pct	-0.013	0.008	-0.028	0.002	-0.013
fortypnm_gpwhite_fir:fortyp_pct	0.072	0.037	-0.002	0.145	0.074
species_gp_nquaking_aspen:sdi_live	-0.026	0.007	-0.041	-0.012	-0.026
species_gp_ndouglas_fir:sdi_live	-0.01	0.012	-0.033	0.012	-0.01
species_gp_ngambel_oak:sdi_live	0.047	0.017	0.014	0.081	0.049
species_gp_nlodgepole_pine:sdi_live	-0.021	0.004	-0.029	-0.012	-0.02
species_gp_npinon_juniper:sdi_live	-0.004	0.01	-0.023	0.016	-0.004
species_gp_nponderosa_pine:sdi_live	0.003	0.004	-0.006	0.012	0.003
species_gp_nspruce_fir:sdi_live	-0.013	0.006	-0.024	-0.002	-0.013
species_gp_nwhite_fir:sdi_live	-0.001	0.015	-0.03	0.027	-0.001
species_gp_nquaking_aspen:hdr_live	-0.008	0.007	-0.021	0.005	-0.008
species_gp_ndouglas_fir:hdr_live	0.005	0.02	-0.035	0.045	0.005
species_gp_ngambel_oak:hdr_live	-0.021	0.015	-0.05	0.008	-0.021
species_gp_nlodgepole_pine:hdr_live	0.004	0.007	-0.01	0.018	0.004
species_gp_npinon_juniper:hdr_live	0.013	0.005	0.004	0.023	0.013
species_gp_nponderosa_pine:hdr_live	0.049	0.016	0.017	0.081	0.05
species_gp_nspruce_fir:hdr_live	-0.096	0.012	-0.119	-0.072	-0.091
species_gp_nwhite_fir:hdr_live	-0.042	0.024	-0.09	0.006	-0.041
species_gp_nquaking_aspen:ba_per	-0.003	0.01	-0.022	0.017	-0.003
species_gp_ndouglas_fir:ba_per	0.013	0.006	0.002	0.024	0.013
species_gp_ngambel_oak:ba_per	-0.016	0.013	-0.04	0.009	-0.015
species_gp_nlodgepole_pine:ba_per	0.022	0.011	0.001	0.042	0.022
species_gp_npinon_juniper:ba_per	0.006	0.007	-0.008	0.02	0.006
species_gp_nponderosa_pine:ba_per	0.011	0.005	0.002	0.02	0.011
species_gp_nspruce_fir:ba_per	-0.077	0.014	-0.104	-0.049	-0.074
species_gp_nwhite_fir:ba_per	-0.009	0.008	-0.024	0.006	-0.009
lf_canopy	0.061	0.004	0.054	0.069	0.063
ba_live_total	-0.002	0.004	-0.01	0.005	-0.002
ba_dead_total	0.019	0.004	0.012	0.027	0.019
erc_dv	0.106	0.004	0.097	0.115	0.112
vpd	0.141	0.006	0.129	0.152	0.151
vs	0.039	0.003	0.032	0.046	0.04
elev	-0.054	0.006	-0.065	-0.043	-0.053
slope	0.006	0.003	0	0.012	0.006
northness	0	0.002	-0.004	0.005	0
tpi	0.046	0.003	0.041	0.051	0.047
overlap	0.688	0.003	0.683	0.693	0.989

day_prop	0.6	0.003	0.595	0.605	0.823
dist_to_perim	0.115	0.003	0.11	0.12	0.122

***Table B2**. Model results for CBIbc models including the mean effects and credible intervals, exponentiated effects, and random effects.*

Model Parameter	Mean Effect	SD	0.025 Q	0.975 Q	Exponentiated Mean Effect
(Intercept)	0.117	0.025	0.068	0.166	0.124
fortypnm_gpdouglas_fir	0.209	0.016	0.179	0.24	0.233
fortypnm_gpgambel_oak	-0.244	0.059	-0.359	-0.128	-0.216
fortypnm_gplodgepole_pine	0.095	0.011	0.075	0.116	0.1
fortypnm_gppinon_juniper	0.124	0.016	0.092	0.156	0.132
fortypnm_gpponderosa_pine	0.144	0.011	0.123	0.166	0.155
fortypnm_gpspruce_fir	0.082	0.011	0.061	0.103	0.085
fortypnm_gpwhite_fir	0.201	0.036	0.13	0.272	0.223
fortypnm_gpquaking_aspen:fortyp_pct	-0.14	0.007	-0.155	-0.126	-0.131
fortypnm_gpdouglas_fir:fortyp_pct	0.022	0.014	-0.005	0.049	0.022
fortypnm_gpgambel_oak:fortyp_pct	-0.031	0.04	-0.11	0.048	-0.03
fortypnm_gplodgepole_pine:fortyp_pct	-0.035	0.005	-0.046	-0.025	-0.035
fortypnm_gppinon_juniper:fortyp_pct	0.03	0.011	0.009	0.051	0.03
fortypnm_gpponderosa_pine:fortyp_pct	0.014	0.005	0.005	0.023	0.014
fortypnm_gpspruce_fir:fortyp_pct	-0.018	0.007	-0.032	-0.004	-0.018
fortypnm_gpwhite_fir:fortyp_pct	-0.02	0.035	-0.089	0.049	-0.02
species_gp_nquaking_aspen:sdi_live	-0.016	0.007	-0.03	-0.001	-0.016
species_gp_ndouglas_fir:sdi_live	0.001	0.011	-0.022	0.023	0.001
species_gp_ngambel_oak:sdi_live	0.047	0.017	0.014	0.08	0.048
species_gp_nlodgepole_pine:sdi_live	-0.005	0.004	-0.013	0.003	-0.005
species_gp_npinon_juniper:sdi_live	0.003	0.01	-0.017	0.023	0.003
species_gp_nponderosa_pine:sdi_live	0.002	0.004	-0.007	0.01	0.002
species_gp_nspruce_fir:sdi_live	-0.012	0.005	-0.022	-0.001	-0.011
species_gp_nwhite_fir:sdi_live	-0.001	0.014	-0.029	0.027	-0.001
species_gp_nquaking_aspen:hdr_live	-0.015	0.007	-0.028	-0.002	-0.015
species_gp_ndouglas_fir:hdr_live	-0.029	0.02	-0.069	0.011	-0.029
species_gp_ngambel_oak:hdr_live	0.02	0.015	-0.008	0.049	0.02
species_gp_nlodgepole_pine:hdr_live	-0.007	0.007	-0.021	0.007	-0.007
species_gp_npinon_juniper:hdr_live	0.014	0.005	0.004	0.023	0.014
species_gp_nponderosa_pine:hdr_live	0.097	0.016	0.064	0.129	0.102
species_gp_nspruce_fir:hdr_live	-0.03	0.012	-0.053	-0.006	-0.029

species_gp_nwhite_fir:hdr_live	-0.047	0.024	-0.094	0.001	-0.046
species_gp_nquaking_aspen:ba_per	-0.005	0.01	-0.025	0.014	-0.005
species_gp_ndouglas_fir:ba_per	-0.001	0.006	-0.012	0.01	-0.001
species_gp_ngambel_oak:ba_per	-0.017	0.013	-0.041	0.008	-0.016
species_gp_nlodgepole_pine:ba_per	0.016	0.011	-0.005	0.037	0.016
species_gp_npinon_juniper:ba_per	0.014	0.007	0	0.028	0.014
species_gp_nponderosa_pine:ba_per	0.019	0.005	0.009	0.028	0.019
species_gp_nspruce_fir:ba_per	0.003	0.014	-0.024	0.031	0.003
species_gp_nwhite_fir:ba_per	-0.008	0.008	-0.023	0.008	-0.008
lf_canopy	0.136	0.004	0.129	0.143	0.145
ba_live_total	0.048	0.004	0.041	0.055	0.049
ba_dead_total	-0.011	0.004	-0.018	-0.004	-0.011
erc_dv	0.017	0.004	0.009	0.025	0.018
vpd	0.044	0.005	0.033	0.054	0.045
vs	0.004	0.003	-0.002	0.011	0.004
elev	0.015	0.005	0.005	0.025	0.016
slope	0.003	0.003	-0.002	0.009	0.003
northness	0.006	0.002	0.002	0.01	0.006
tpi	0.051	0.002	0.046	0.056	0.053
overlap	0.062	0.003	0.057	0.067	0.064
day_prop	0.003	0.002	-0.002	0.007	0.003
dist_to_perim	0.093	0.002	0.088	0.098	0.097